TESTS OF PREDICTIONS MADE BY THE EQUILIBRIUM MODEL FOR THE EFFECT OF TEMPERATURE ON ENZYME ACTIVITY

A thesis
submitted in partial fulfilment
of the requirements for the degree
of
Master in Science in Biological Sciences
at
The University of Waikato
by
Matthew Oudshoorn

THE UNIVERSITY OF
WAIKATO
Te Whare Wānanga o Waikato

The University of Waikato

2008

Abstract

The Classical Model describing the effects of temperature on enzyme activity consists of two processes: the catalytic reaction defined by $\Delta G^{\ddagger}_{cat}$ and irreversible inactivation defined by $\Delta G^{\ddagger}_{inact}$, this model however, does not account for the observed temperature- dependant behaviour of enzymes. The recent development of the Equilibrium Model is governed not only by $\Delta G^{\ddagger}_{cat}$ and $\Delta G^{\ddagger}_{inact}$ but also by two new intrinsic parameters ΔH_{eq} and T_{eq}, which describe the enthalpy and the temperature of the midpoint, respectively, of a active and reversibly inactive enzyme transition. T_{eq} is central to the physiological adaptation of an enzyme to its environmental temperature and links the molecular, physiological and environmental aspects of life to temperature in a way that has not been previously possible. The Equilibrium Model is therefore a more complete and accurate description of the effects of temperature on enzymes, it has provided new tools for describing and investigating enzyme thermal adaptation and possibly new biotechnological tools.

The effects of the incorporating in the new Model of the parameters T_{eq} and $\Delta H^{\ddagger}_{eq}$ yield major differences from the Classical Model, with simulated data calculated according to the Equilibrium Model fitting well to experimental data and showing an initial rate temperature optimum that is independent of assay duration. Simulated data simulated according to the Classical Model can not be fitted to experimental data. All enzymes so far studied (>30) display behaviour predicted by the Equilibrium Model.

The research described here has set out to: experimentally test observations made by Eisenthal et al., on the basis of enzyme reactor data simulated according to the Equilibrium Model; to test the Equilibrium Model using an unusual (rapidly renaturable) enzyme, RNAase; and to test the proposed molecular basis of the Equilibrium Model by examining the effect of a change at the enzymes active site.

The experimental results gathered here on the effect of time and temperature on enzyme reactor output confirm the predictions made by Eisenthal et al. (2006) and indicate that the Equilibrium Model can be a useful aid in predicting reactor performance. The Equilibrium Model depends upon the acquisition of data on the variation of the V_{max} of an enzyme with time and temperature, and the non-ideal behaviour of RNase A made it impossible to collect such data for this enzyme, as a result the Equilibrium Model could not be applied. The disulfide bond within the active site cleft of A.k 1 protease was cleaved as a probe of the mechanism of the Equilibrium Model, which is proposed to arise from molecular changes at the enzymes active site.Support for the proposed mechanism was gained through the comparison of experimentally determined temperature dependence of the native and reduced forms of the enzyme and application of this data to the Equilibrium Model.

Acknowledgements

Firstly I would like to thank my supervisor Professor Roy Daniel for the guidance and encouragement he has shown me throughout my masters, especially when I have been writing this thesis. Many thanks go to Colin Monk, Charlie Lee and Michelle Peterson who have helped me greatly in understanding theory behind my experimental work and with technical assistance. I would also like to thank the Marsden Fund, under the contract UOW0501, "T_{eq} – A new and fundamental enzyme property controlling activity" for providing a Scholarship to carry out this work and making my masters possible. I would also like to acknowledge all my other lab mates and colleagues (past and present!) at the Thermophile Research Unit who have made my time inside and outside of work hours entertaining.

And thanks Mum and Dad!!

Table of Contents

ABSTRACT ii

ACKNOWLEDGEMENTS iv

TABLE OF CONTENTS v

LIST OF FIGURES ix

LIST OF TABLES xii

ABBREVIATIONS xiv

CHAPTER ONE- INTRODUCTION 1

1.1 Introduction 1

1.2 Enzyme Functionality 2

1.3 Effect of Temperature on Enzyme Functionality 6

1.3.1 Effect of Temperature on Catalysis 6

1.3.2 Effect of Temperature on Enzyme Denaturation 9

1.4 Apparent Enzyme Temperature Optima 10

1.5 The Classical Model 12

1.6 The Equilibrium Model 14

1.7 Enzymes in Industry: Immobilized Enzymes 18

1.8 Enzyme Reactors 18

1.9 A Test of the Equilibrium Model on an unusual enzyme 22

1.10 Test of the Equilibrium Model using a change at the active site of Ak1 protease 22

1.11 Thesis Objectives 23

CHAPTER TWO- MATERIALS AND METHODS 24

2.1 The Temperature Dependence of Enzyme Activity and Application to the Equilibrium Model: Experimental Considerations, Methods and Data Analysis 24

2.1.1 Introduction 24

2.1.2 Experimental Considerations 25

2.1.2.1 Assay Selection 25

2.1.2.2 Assay Component Stability 26

2.1.2.3 pH Control 26

2.1.3 Assay Method and Technique 28

2.1.3.1 Substrate and Enzyme Solution Preparation 28

2.1.3.2 Temperature Control 29

2.1.3.3 Assays 29

2.1.3.4 Protein Concentration Determination 30

2.1.4 Data Analysis 31

2.1.4.1 Construction of 3D Plots from Experimental Data 31

2.1.4.2 Determination of Equilibrium Model Parameters 33

2.1.4.3 Construction of 3D Plots from Simulated Data 35

2.1.4.4 Comparing the 3D Plots 35

2.1.4.5 K_M Adjustment for Deviations from V_{max} 36

2.2 The Development of a Stirred Tank Batch Reactor 36

2.2.1 Introduction 36

2.2.2 Instrumentation and Reaction Issues Associated with the Development of a Stirred Tank Batch Reactor 37

2.2.3 Penicillin Amidase: Characteristics

and use in my Research 38

2.2.4 Alkaline Phosphatase: Characteristics

and use in my Research 40

2.2.5 Stirred Tank Batch Reactor: Model One 41

2.2.6 Stirred Tank Batch Reactor: Model Two 42

2.2.7 Stirred Tank Batch Reactor: Model Three 43

2.2.8 Stirred Tank Batch Reactor: Model Four 47

2.2.9 Penicillin Amidase: Enzyme Reactor Procedure 48

2.2.10 Alkaline Phosphatase: Enzyme Reactor Procedure 49

2.2.11 Data Analysis 50

2.3 RNase A 51

2.4 Ak. 1 Protease; Native and DTT Treated 53

CHAPTER THREE- THE IMPLICATIONS OF THE EQUILIBRIUM MODEL FOR THE PREDICTION OF ENZYME REACTOR PERFORMANCE 56

Preface 56

Abstract 56

1. Introduction 57

2. Materials and Methods 61

2.1. Materials 61

2.2. Enzyme Reactor Conditions 62

2.3. Enzyme Reactor Operation 63

2.4. Instrumentation 63

2.5. Temperature Control 64

2.6. Protein Determination 64

2.7. Data Treatment 65

3. Results and Discussion 67

3.1 Penicillin Amidase Results 70

3.2 Alkaline Phosphatase Results 81

4. Conclusion 92

5. References 95

CHAPTER FOUR- RNASE RESULTS AND DISCUSSION 100

CHAPTER FIVE- A.k 1 PROTEASE RESULTS AND DISCUSSION 113

CHAPTER FOUR- RNASE RESULTS AND DISCUSSION 119

APPENDICIES

A. Simulated time course of enzyme reactor product formation with varying temperature; calculated from 3 minute parameters 124

REFERENCES 129

List of Figures

CHAPTER ONE

Figure 1.1: Changes in free energy with reaction progress. 3

Figure 1.2: The apparent enzyme temperature optimum. 11

Figure 1.3: The temperature dependence of enzyme activity, according to simulated data calculated from the Classical Model using experimental phenylalanine ammonia lyase data. 14

Figure 1.4: The temperature dependence of enzyme activity according to A) Simulated data calculated by the Equilibrium Model using experimental phenylalanine ammonia lyase data. B) Experimental phenylalanine ammonia lyase data. 17

Figure 1.5: Common enzyme reactor types. 19

Figure 1.6: The effect of T_{eq} on time courses of product concentration simulated at various temperatures. 21

CHAPTER TWO

Figure 2.1: Reaction catalysed by penicillin amidase (EC 3.5.1.11). 39

Figure 2.2: Reaction catalysed by alkaline phosphatase (EC 3.1.3.1). 40

Figure 2.3: Basic diagram of stirred tank batch reactor: Model One. 41

Figure 2.4: Basic diagram of my stirred tank batch reactor: Model Three. 44

Figure 2.5: Average trial results of enzyme reactor model three using acid phosphatase. 45

Figure 2.6: Average trial results of enzyme reactor model three

using immobilized penicillin amidase. 46

Figure 2.7: Average trial results of enzyme reactor model four using immobilized penicillin amidase. 48

Figure 2.8: Hydrolysis reaction catalyzed by pancreatic ribonuclease (3.1.27.5). 52

CHAPTER THREE

Figure 1: The temperature dependence of enzyme activity. 60

Figure 2: The effect of T_{eq} on time courses of product concentration simulated at various temperatures. 69

Figure 3: Free penicillin amidase enzyme reactor results. 70

Figure 4: Immobilized penicillin amidase enzyme reactor results. 71

Figure 5: Free penicillin amidase simulated product formation, calculated from 1 hour parameters. 76

Figure 6: Free penicillin amidase experimental product formation. 77

Figure 7: Immobilized penicillin amidase simulated product formation, calculated from 1 hour parameters. 79

Figure 8: Immobilized penicillin amidase experimental product formation. 80

Figure 9: Free alkaline phosphatase enzyme reactor results. 82

Figure 10: Immobilized alkaline phosphatase enzyme reactor results. 83

Figure 11: Free alkaline phosphatase simulated product formation, calculated from 1 hour parameters. 87

Figure 12: Free alkaline phosphatase experimental product formation. 88

Figure 13: Immobilized alkaline phosphatase simulated product formation, calculated from 1 hour parameters. 90

Figure 14: Immobilized alkaline phosphatase experimental product formation. 91

CHAPTER FOUR

Figure 4.1: RNase A assay trial results performed at 25°C using the Rabin, Blackburn and Bencina method, with a substrate concentration of 6.2mM; ten times the K_M at 25°C. 101

Figure 4.2: RNase A assay trial results performed at 25°C using the Rabin, Blackburn and Bencina method, with a substrate concentration of 1.24mM; two times the K_M at 25°C. 102

Figure 4.3: RNase A assay trial results performed using the Fujii, Tanimizu and Moussaoui method with a substrate concentration of 6.2mM; ten times the K_M at 25°C. 103

Figure 4.4: RNase A results with the K_M adjustment not made. 105

Figure 4.5: RNase A results with the K_M adjustments made. 106

Figure 4.6: Initial rate analysis of RNase A activity. 109

CHAPTER FIVE

Figure 5.1: Native A.k 1 results. 114

Figure 5.2: DTT treated A.k 1 results. 115

List of Tables

CHAPTER ONE

Table 1.1: Equations of the Classical Model. 12

Table 1.2: Equations of the Equilibrium Model. 15

CHAPTER THREE

Table 1: Thermodynamical parameters of penicillin amidase from *Escherichia Coli;* calculated by the Equilibrium Model from experimental data. 73

Table 2: Thermodynamical parameters of alkaline phosphatase from calf intestinal mucosa; calculated by the Equilibrium Model from experimental data. 84

Table 3: Comparison of T_{eq} to the temperatures of observed experimental maximum rate and observed experimental maximum product formation. 93

CHAPTER FOUR

Table 4.1: K_M values calculated at different temperatures. 108

Table 4.2: Thermodynamical parameters of RNase A from bovine pancrease; calculated by the Equilibrium Model from experimental data. 110

CHAPTER FIVE

Table 5.1: Thermodynamical parameters of native and DTT treated A.k 1 calculated by the Equilibrium Model from experimental data. 116

Abbreviations

6-APA	6-aminopenicillanic acid
$[E_0]$	total concentration of enzyme
A	the pre-exponential factor or the Arrhenius constant
BSA	Bovine Serum Albumin
C>p	Cytidine 2':3'-cyclic monophosphate
$\Delta G^{\ddagger}$	the change in free energy of activation
$\Delta G_{cat}{}^{\ddagger}$	the change in free energy of activation for the catalysed reaction
$\Delta G^{\ddagger}_{inact}$	the change in free energy of activation for thermal inactivation
$\Delta H^{\ddagger}$	the change in enthalpy for the activation
$\Delta H^{\ddagger}_{eq}$	the change in enthalpy for the equilibrium
$\Delta S^{\ddagger}$	the change in entropy for the activation
DTT	Dithiothreitol
ε	the molar extinction coefficient
E	enzyme
E_a	the Arrhenius activation energy
E_{act}	active form of the enzyme
EC	Enzyme Commission Number
EDTA	ethylenediaminetetraacetic acid
E_{inact}	inactive form of the enzyme
ES	the enzyme-substrate complex
$EX^{\ddagger}$	the enzyme-transition state complex
h	the Planck's constant

HEPES	4-(2-hydroxyethyl)-1-piperazineethanesulfonic acid
κ	the transition coefficient
$K^{\ddagger}$	the equilibrium constant for the equilibrium between the activated complex and the un-activated molecules
k_B	the Boltzmann constant (th gas constant per molecule)
k_{cat}	the enzymes catalytic rate constant
K_{eq}	equilibrium constant between active and inactive forms of the enzyme
k_{inact}	thermal inactivation rate constant
K_M	Michaelis-Menten constant
k_r	rate constant of the reaction
$MgCl_2$	Magnesium chloride
NaOH	Sodium hydroxide
NIPAB	6-nitro-3-phenylacetamido benzoic
P	product
PA	Penicillin Amidase
pH	negative logarithm of the hydrogen ion activity
pNA	p-nitroanilide
p-NPP	*p*-nitrophenylphosphate
R.M.D	Roy M. Daniel
R	universal gas constant
S	substrate
t	assay duration
T	absolute temperature
T_{eq}	the temperature at which E_{act} and E_{inact}
Tris	tris(hydroxymethyl) aminomethane

v	reaction velocity
V_{max}	maximum velocity of the enzyme
$X^{‡}$	the transition state
X	thermally denatured state

Chapter One

Introduction

1.1 Introduction

Life depends on a complex network of biochemical reactions which are mediated by catalytic proteins known as enzymes. Enzyme structure and the rate of the reactions catalysed are affected by variations in temperature: in order to understand the molecular functioning of enzymes and the great catalytic power they posses, it is important that the effect of temperature on enzymes be understood.

As the temperature is raised chemical reactions proceed at a faster velocity due to the reactant molecules possessing increased kinetic energy, resulting in more productive collisions per unit time (Chang, 1994). However the increasing rate of enzyme catalysed reactions with increasing temperature is offset by the increasing rate of thermal denaturation (since enzymes, like all proteins have limited thermal stability), resulting in a decrease in catalytic rate. All enzymes readily denature or loose conformation above certain temperatures due to the thermal energy becoming too great for the chemical bonds involved. The conflicting influences of thermal denaturation and thermal acceleration of catalytic activity generate a point on the temperature profile at which the enzyme displays maximum reaction velocity that is known as the optimum temperature and was at one time thought to be characteristic of the enzyme. However temperature optimum arises from an unknown mixture of thermal stability and temperature coefficient and is also dependant on assay duration. Therefore temperature optimum became regarded as an ill- defined quality of limited value. Recent evidence, however, suggests that in fact some enzymes may have a

genuine temperature optima (Thomas and Scopes, 1998; Buchanan et al., 1999; Gerike et al., 1997).

Enzymes are required to be both flexible and stable molecules in order to function, with the balance between enzyme rigidity and stability being paramount in terms of enzyme activity (e.g., Fraunfelder et al., 1979; Brooks et al., 1988; and Gerstein et al., 1994). Enzyme flexibility is implied by the Induced Fit Model which is a widely accepted model used to explain the high specificity that enzymes have for the particular reactions which they catalyse (Koshland, 1958; Yankeelov and Koshland, 1965). The three dimensional structure of an enzyme is hugely important in relation to temperature as this determines the stability (or flexibility), and therefore activity of a particular enzyme at a certain temperature, this can then be related back to living organisms which can only tolerate a defined temperature range, above and below which their cells and proteins are adversely affected (Daniel and Cowan, 2000).

The effects of temperature on enzymes can be analysed experimentally and is routinely used as a diagnostic tool of individual enzymes. The effects of temperature can also be described mathematically using thermodynamic parameters which mathematically describe the effects of temperature on factors such as catalytic rate and thermal inactivation.

1.2 Enzyme Functionality

Enzymes have great catalytic power and substrate specificity allowing them to rapidly catalyse very specific reactions. Enzyme catalysis can produce rate accelerations as large as a factor of 10^{19} and demonstrate exquisite molecular recognition at the highest level of development (Garcia-Viloca et al., 2004).

Enzymes catalyse reactions by lowering the free energy of activation or Arrhenius activation energy (E_a) of a reaction as shown in Figure 1.1 and by effectively stabilising Transition States which are intermediates of product formation. $\Delta G^{\ddagger}$ is the energy barrier that must be overcome in order for a reaction to occur and describes the effect of temperature on the enzymes catalytic rate constant. The enzymes catalytic rate constant is known as k_{cat} and is the rate constant of the chemical step corresponding to the formation of the product, the value of k_{cat} varies with temperature, as does the value of $\Delta G^{\ddagger}$.

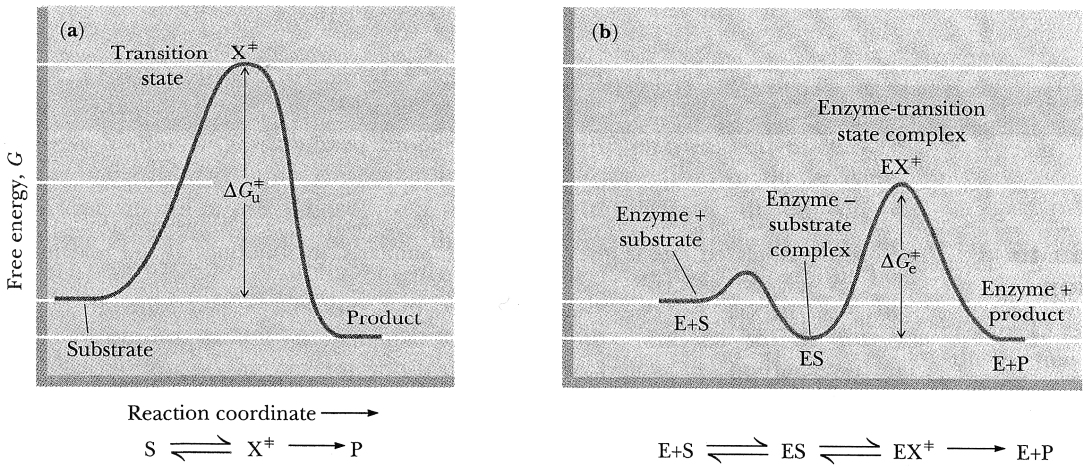

Figure 1.1: Changes in free energy with reaction progress. (a) The uncatalysed reaction. (b) The enzyme catalysed reaction (Garrett and Grisham, 1999).

In figure 1.1 S is the substrate, $X^{\ddagger}$ is the transition state, P is the product, E is enzyme, ES is the enzyme-substrate complex and $EX^{\ddagger}$ is the enzyme-transition state complex.

The Transition State Stabilisation Theory

The current hypothesis used to explain the phenomenal reaction rate increase exhibited by enzymes is the Transition State Stabilisation Theory, proposed by Pauling in 1978. This theory suggests that the catalytic power of enzymes results from their highly specific binding to the transition state, increasing its stabilisation and lowering the free energy of activation, effectively promoting catalysis. The transition state for a chemical reaction is the most unstable species on the reaction pathway, generally, the transition state is considered to be a species in which chemical bonds or interactions are in the process of being formed or broken. Central to the transition state theory is that the rate of any reaction at a given temperature depends only on the concentration of the transition state which is in equilibrium with the un-activated reactants (Kraut, 1988; Palmer, 1981). The concentration of the transition state is governed by the laws of thermodynamics, applying standard thermodynamic equations to this equilibrium gives:

$$\Delta G^{\ddagger} = \Delta H^{\ddagger} - T\Delta S^{\ddagger} = -RT \ln K^{\ddagger} \qquad \textbf{Equation 1.1}$$

Where T is the absolute temperature (Kelvin), R is the universal gas constant and $K^{\ddagger}$ is the equilibrium constant for the equilibrium between the activated complex and the un-activated molecules. $\Delta G^{\ddagger}$, $\Delta H^{\ddagger}$ and $\Delta S^{\ddagger}$ represent the changes in free energy, enthalpy and entropy for the reaction respectively. These thermodynamical parameters provide valuable information on the nature of the transition state and the reaction mechanism.

The Lock and Key Hypothesis

The specificity of an enzyme for a particular substrate lies within the specificity of binding ligands at the enzymes active site (Benkovic and Hammes-Schiffer, 2003). Among the first hypotheses offered to explain the high specificity of enzymes was the 'Lock and Key' hypothesis proposed by Emil Fischer as early as 1890. This proposed that the structure of the active site was complimentary to that of the substrate and that the substrate fitted into the active site like a key does into a lock; binding of the substrate into the enzymes active site was proposed to result in activation of the substrate. According to the lock and key hypothesis all structures remain rigid throughout the binding process (Palmer, 1981).

The Induced Fit Hypothesis

Enzyme activity is widely regarded as being dependant on protein flexibility. The structural pliancy of enzymes implies the induced fit hypothesis, which was proposed by Koshland in 1958. The induced fit hypothesis assumes that an exact substrate complementary binding site as proposed by the 'lock and key' model does not exist, alternatively it proposes that a flexible enzyme molecule wraps itself around a rigid ligand. The binding of a ligand to an enzyme is thought to cause a change in three dimensional structure of the enzyme; ligand binding could result in enzyme groups becoming exposed or protected from the solvent, promoting further ligand binding and therefore catalysis (Palmer, 1981; Daniel et al., 2003). Such conformational changes in enzyme structure can be detected and measured by various physical techniques such as X-ray diffraction and circular dichromism (Creighton, 1993). Electron density maps provide direct evidence for flexibility in protein molecules, by the extent to which the electron density is smeared out (Creighton, 1993). The

induced fit model is the current hypothesis used to explain the exquisite molecular recognition displayed by enzyme substrate specificity.

1.3 Effect of Temperature on Enzyme Functionality

1.3.1 Effect of Temperature on Catalysis

Generally an increase in temperature causes a corresponding increase in the rate of a reaction (although increasing the temperature also leads to denaturation of the enzyme).

An Arrhenius plot is a plot of log v (log of velocity of the catalysed reaction) against $1/T$ (1/absolute temperature), graphically displays the effect of temperature on enzyme catalysis. The Arrhenius plot originates from reaction rate theories, which first must be understood in order for the Arrhenius plot to be understood.

According to the van't Hoff equation (equation 1.2) the equilibrium constant for a reaction increases with temperature (Walmsley, 1996).

$$\frac{d \ln K^{\ddagger}}{dT} = \frac{\Delta H^{\ddagger}}{RT^2} \qquad \textbf{Equation 1.2}$$

Where $K^{\ddagger}$ is the equilibrium constant, T is the absolute temperature (Kelvin), $\Delta H^{\ddagger}$ is the standard enthalpy change for the reaction (kJ) and R is the gas constant. This led to Svante Arrhenius in 1889 proposing that the effect of temperature on a rate constant, k_r, could be described by equation 1.3 (Arrhenius, 1889).

$$\frac{d \ln k_r}{dT} = \frac{E_a}{RT^2} \qquad \textbf{Equation 1.3}$$

Where E_a is the activation energy for the reaction (kJ), according to equations 1.2 and 1.3 the equilibrium constant increases exponentially with increasing temperature. The integration and rearrangement of the above equations and the assumption that *Ea* does not vary with temperature leads to what is known as the Arrhenius Equation:

$$k_r = A \bullet e^{-Ea/RT} \qquad \textbf{Equation 1.4}$$

Where A is the pre-exponential factor or the Arrhenius constant, determined experimentally for a given reaction under given conditions.

The Arrhenius Equation has been shown experimentally to be a close estimation of the effect of temperature on rate constants. According to the Arrhenius Equation molecules must achieve a certain critical energy of E_a before they can react, the Boltzmann constant (a weighting factor determining the relative probability of a system in thermodynamic equilibrium (Kittel and Kroemer, 1980)), defined by $e^{-Ea/RT}$ gives the fraction of molecules which achieve the critical energy.

This theory is essentially correct; however the Arrhenius Equation does have its short comings. Since it is empirically derived, there is no way of calculating E_a and A from reacting molecules, it is valid only if the temperature range is not too large and it assumes that the properties of the reaction medium do not change with temperature: therefore a more detailed theory is necessary to completely describe the temperature dependence of reaction rates, in terms of physical properties of the reacting molecules.

According to the Transition State Stabilisation theory all activated complexes break down at a rate of

$$k_r = \kappa \bullet \frac{k_B T}{h} \bullet K^{\ddagger} \qquad \textbf{Equation 1.5}$$

where k_r is the rate constant of the reaction, κ is the transition coefficient (which describes the probability that the breakdown of the activated complex will be in the direction of product formation, assumed to be unity (Garcia-Viloca et al., 2004)), k_B is the Boltzmann constant, h is the Planck's constant, T is the absolute temperature and $K^{\ddagger}$ is the equilibrium constant for the equilibrium between the activated complex and the un-activated molecules.

The Eyring Equation (equation 1.6) is generated by substituting the thermodynamic equation (equation 1.1) (Eyring, 1935).

$$k_r = \frac{k_B T}{h} \bullet e^{-\Delta G\ddagger/RT} = \frac{k_B T}{h} \bullet e^{-\Delta H\ddagger/RT} \bullet e^{-\Delta S\ddagger/RT} \qquad \textbf{Equation 1.6}$$

Where $\Delta G^{\ddagger}$, $\Delta H^{\ddagger}$, $\Delta S^{\ddagger}$ represent the change in free energy, enthalpy and entropy respectively.

Assuming that $\Delta S^{\ddagger}$ does not vary with temperature the following relationship is given

$$\frac{d \ln k_r}{dT} = \frac{1}{T} + \frac{\Delta H^{\ddagger}}{RT^2} = \frac{\Delta H^{\ddagger} + RT}{RT^2} \qquad \textbf{Equation 1.7}$$

When equation 1.7 is compared to the Arrhenius Equation (equation 1.3) it can be seen that they are very similar, suggesting that the energy of activation defined by the Arrhenius Equation and the change in the enthalpy of activation as defined by the Transition State Theory can be related as:

$$E_a = \Delta H^{\ddagger} + RT \qquad \textbf{Equation 1.8}$$

According to the activation energy, E_a, and the above equations the rate constant, k_r, will decrease at low temperatures. An Arrhenius plot can be expected to give a linear slope, with the slope of the line yielding E_a or the energy of activation (Dixon and Webb, 1979), which can be used with equation 1.8 to estimate $\Delta H^{\ddagger}$. However enzyme catalysed reactions do not always result in linear Arrhenius plots, departures from linearity are generally due to changes in experimental conditions with changes in temperature (Dixon and Webb, 1979; Laidler and Peterman, 1979), assuming that the concentration of the active enzyme remains constant. Arrhenius plot linearity depends on the enzyme acting optimally, therefore the enzyme must be appropriately ionised, be saturated with substrate, not inhibited and the reaction mix maintained at an appropriate pH.

1.3.2 Effect of Temperature on Enzyme Denaturation

The increase in catalytic rate with increasing temperature is offset by the increasing rate of the thermal inactivation of the enzyme, resulting in less functional enzyme present (Illanes et al., 2000; Engel, 1981). Thermal denaturation can be considered a two step process, the first step is a reversible conformational change to an unfolded

state and the second step is to an irreversibly unfolded state. The process of thermal denaturation can be represented by:

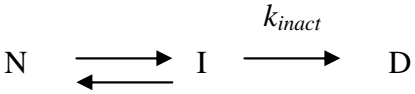

Equation 1.9

Where N represents the native, catalytically active enzyme, I represents the intermediate form which is potentially rapidly interchanging with the native form and D represents the inactive, and possibly aggregated, thermally denatured polypeptide. The native catalytically active enzyme is only marginally stable, as the difference between the sum of stabilising forces and destabilising forces of the enzyme molecule is usually very small. Therefore small changes in the structure of the protein can have major effects in the overall stability of the molecule (Matthews, 1993). An increase in temperature will instigate such small changes, resulting in the molecule beginning to unfold and adopt a less ordered conformation. The conversion of the native enzyme to the intermediate form is manifested as increases in protein flexibility and localised conformational alterations, however the overall structure of the protein is unchanged (Creighton, 1993).

$\Delta G^{\ddagger}_{\text{inact}}$ is the change in free energy of activation for the irreversible thermal inactivation reaction and describes the effect of temperature on k_{inact}, the irreversible thermal inactivation rate constant (e.g., Daniel et al., 2008).

1.4 Apparent Enzyme Temperature Optima

The combination of the effects of temperature on catalytic rate and denaturation allows enzymes to exhibit an apparent temperature optima, which is the point on an

enzymes temperature profile at which the enzyme displays maximum reaction velocity. However temperature optimum arises from an unknown mixture of thermal stability and temperature coefficient and is dependant on assay duration (Peterson et al., 2007; Daniel et al., 2008), as the shorter the assay the higher the temperature optima. Therefore the concept of enzyme temperature optimum was discredited (Cornish-Bowden, 1995; Daniel and Danson, 2001). Figure 1.2 displays a graph of enzyme activity versus temperature showing the "temperature optimum" of an enzyme catalysed reaction (Daniel et al., 2008).

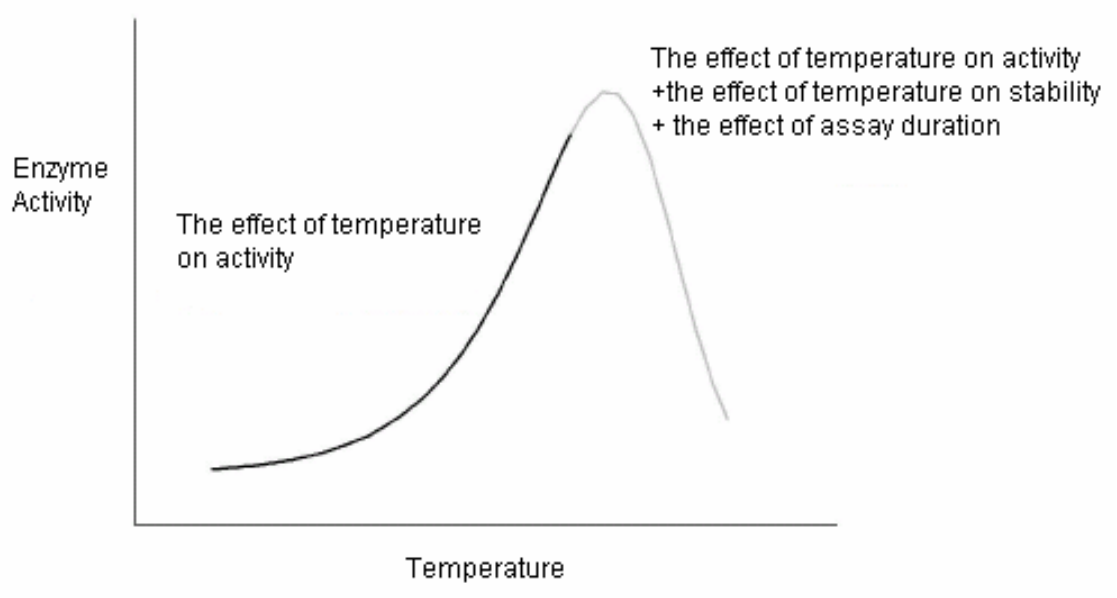

Figure 1.2: The apparent enzyme temperature optimum (Daniel et al., 2008).

Recent evidence, however, suggests that some enzymes show lower activity at high temperatures that can be accounted for by thermal denaturation (Thomas and Scopes, 1998; Gerike et al., 1997; Buchanan et al., 1999). This has prompted a reappraisal of the two-state "Classical Model" and resulted in a new model termed the "Equilibrium Model"(Daniel et al., 2001).

1.5 The Classical Model

The effects of temperature on enzymes have traditionally been understood in terms of two well established thermal parameters $\Delta G^{\ddagger}_{cat}$ and $\Delta G^{\ddagger}_{inact}$, which define the Classical Model (Peterson et al., 2004; Daniel et al., 2001). The Classical Model is based on a two state reaction mechanism where the enzyme is proposed to exist in two species, an active enzyme form and a thermally denatured form, as shown in equation 1.10 (Peterson et al. 2004). As previously stated $\Delta G^{\ddagger}_{cat}$ describes the effect of temperature on the enzymes catalytic rate constant and $\Delta G^{\ddagger}_{inact}$ describes the effect of temperature on the enzymes thermal inactivation rate constant (Peterson et al., 2007).

$E_{act} \rightarrow X$	The reaction mechanism	**Equation 1.10**
$V_{max} = k_{cat} \bullet [E]_0 \, e^{-k_{inact} \bullet t}$	The variation of enzyme activity with temperature and time of assay	**Equation 1.11**
$k_{cat} = \frac{k_B T}{h} \bullet e^{-(\Delta G^{*}_{cat}/RT)}$	The variation of k_{cat} with temperature	**Equation 1.12**
$k_{inact} = \frac{k_B T}{h} \bullet e^{-(\Delta G^{*}_{inact}/RT)}$	The variation of k_{inact} with temperature	**Equation 1.13**

Table 1.1: Equations of the Classical Model.

Where: V_{max} = maximum velocity of the enzyme; k_{inact} = thermal inactivation rate constant; h = planck's constant; k_{cat} = the catalytic rate constant; t = assay duration; R = gas constant; $[E_0]$ = total concentration of enzyme; T = absolute temperature and k_B = Boltzmann's constant (Daniel et al, 2001; Peterson et al., 2004).

As both rate constants, k_{cat} and k_{inact} are temperature dependant, 3-dimensional temperature, time and activity graphs can be constructed showing the variation in enzyme activity with varying time and temperature. Figure 1.3 displays simulated temperature, time and activity data, over the range of 300- 350 K and 0- 180 s, calculated using the Classical Model from experimental phenylalanine ammonia lyase data (Lee et al., 2007). The simulated data shows that the apparent temperature optimum of the assay decreases with increasing time and at zero assay duration, the Classical Model has no temperature optimum. Experimental phenylalanine ammonia lyase data is shown in figure 1.4B.

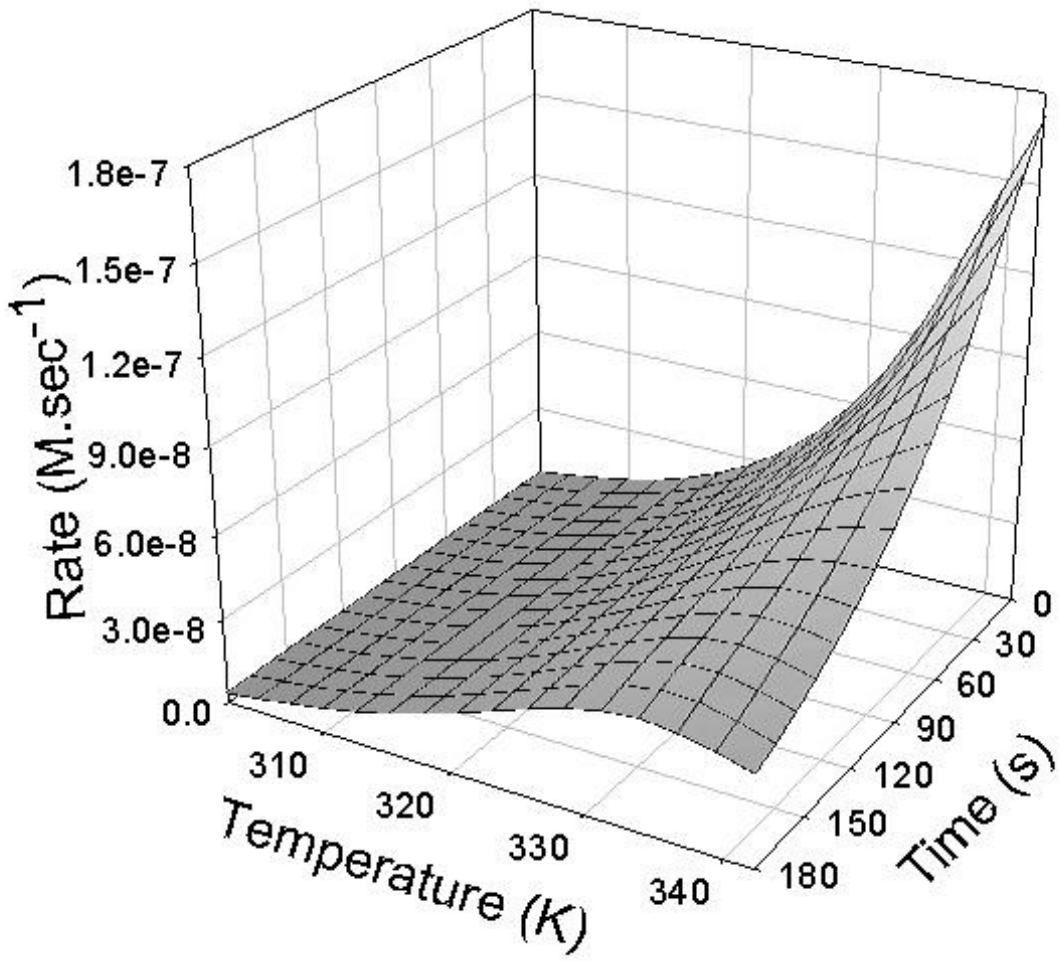

Figure 1.3: The temperature dependence of enzyme activity, according to simulated data calculated from the Classical Model using experimental phenylalanine ammonia lyase data. ($\Delta G^{\ddagger}_{cat}$ = 80 kJ mol^{-1} and $\Delta G^{\ddagger}_{inact}$ = 97 kJ mol^{-1}) (Lee et al., 2007).

1.6 The Equilibrium Model

The Equilibrium Model proposes that the enzyme exists in three species, one active enzyme form, one inactive enzyme form and one thermally denatured form. The active form of the enzyme is in rapid reversible equilibrium with an inactive form which undergoes an irreversible conversion to the thermally denatured state (Daniel et al., 2001), as shown in Equation 1.14. This 3 state reaction mechanism provides a

thermal buffer that protects the enzyme from thermal inactivation. K_{eq} is the equilibrium constant between active and inactive forms of the enzyme ($K_{eq} = (E_{inact})/(E_{act})$), with the position of this equilibrium being affected by temperature. K_{eq} is therefore a new temperature dependant property of the enzyme, introduced by proposed reaction mechanism, with its variation with temperature given by equation 1.17. The Equilibrium Model is defined by four thermal parameters $\Delta G^{\ddagger}_{cat}$, $\Delta G^{\ddagger}_{inact}$, T_{eq} and $\Delta H^{\ddagger}_{eq}$, the two new thermal parameters T_{eq} and $\Delta H^{\ddagger}_{eq}$ describe the reversible equilibrium between the active and inactive enzyme forms, allowing a complete description of the temperature effects on enzymes (Daniel et al., 2007). T_{eq} is the temperature at which the concentrations of the active and inactive forms of the enzyme are equal and $\Delta H^{\ddagger}_{eq}$ is the enthalpic change associated with the conversion of the active enzyme to the inactive form.

$E_{act} \rightleftarrows E_{inact} \xrightarrow{K_{eq}} X$	The reaction mechanism	**Equation 1.14**
$V_{max} = k_{cat} \bullet [E_{act}]$	The variation of enzyme activity with temperature	**Equation 1.15**
k_{cat} (same as Classical Model)	The variation of k_{cat} with temperature	**Equation 1.12**
k_{inact} (same as Classical Model)	The variation of k_{inact} with temperature	**Equation 1.13**
$[E_{act}] = \frac{[E_0] - [X]}{1 + K_{eq}}$	The concentration of the active enzyme at any point	**Equation 1.16**
$K_{eq} = e^{\frac{\Delta H_{eq}}{R}\left(\frac{1}{T_{eq}} - \frac{1}{T}\right)}$	The variation of K_{eq} with temperature	**Equation 1.17**
$\frac{d[X]}{dt} = k_{inact}\{[E_0] - [E_{act}] - [X]\}$	The rate of the appearance of X	**Equation 1.18**

Table 1.2: Equations of the Equilibrium Model (Daniel et al., 2001; Peterson et al., 2004).

The overall dependence of the velocity of an enzyme catalysed reaction on temperature with time can be described by the Equilibrium Model by the relationship shown in equation 1.19.

$$V_{max} = \frac{k_B T e^{-\left(\frac{\Delta G^{\ddagger}_{cat}}{RT}\right)} E_0 e^{\left(\frac{-k_B T e^{-\left(\frac{\Delta G^{\ddagger}_{inact}}{RT}\right)} e^{\left(\frac{\Delta H_{eq}\left(\frac{1}{T_{eq}}-\frac{1}{T}\right)}{R}\right)} t}{h\left(1+e^{\left(\frac{\Delta H_{eq}\left(\frac{1}{T_{eq}}-\frac{1}{T}\right)}{R}\right)}\right)}\right)}}{h\left(1+e^{\left(\frac{\Delta H_{eq}\left(\frac{1}{T_{eq}}-\frac{1}{T}\right)}{R}\right)}\right)} \quad \textbf{Equation 1.19}$$

Where k_B is Boltzmann's constant, h is Planck's constant, $\Delta G^{\ddagger}_{cat}$ is the free energy of activation of the catalytic reaction, $\Delta G^{\ddagger}_{inact}$ is the free energy of activation of the thermal denaturation process, T is the absolute temperature, t is time, E_0 is the total concentration of the enzyme and R is the gas constant (Daniel et al., 2001; Peterson et al., 2004).

The effects of incorporating the parameters T_{eq} and $\Delta H^{\ddagger}_{eq}$ yields major differences from the Classical Model. The simulated data according to the Equilibrium Model in figure 1.4A, using the same values for $\Delta G^{\ddagger}_{cat}$ and $\Delta G^{\ddagger}_{inact}$ as for the Classical Model in figure 1.3, shows an initial rate temperature optimum that is independent of assay duration, enabling an experimental distinction between the two models (Eisenthal et al., 2006). Data simulated using the Equilibrium Model fits well to experimental data, while data simulated using the Classical Model can not be fitted to experimental data.

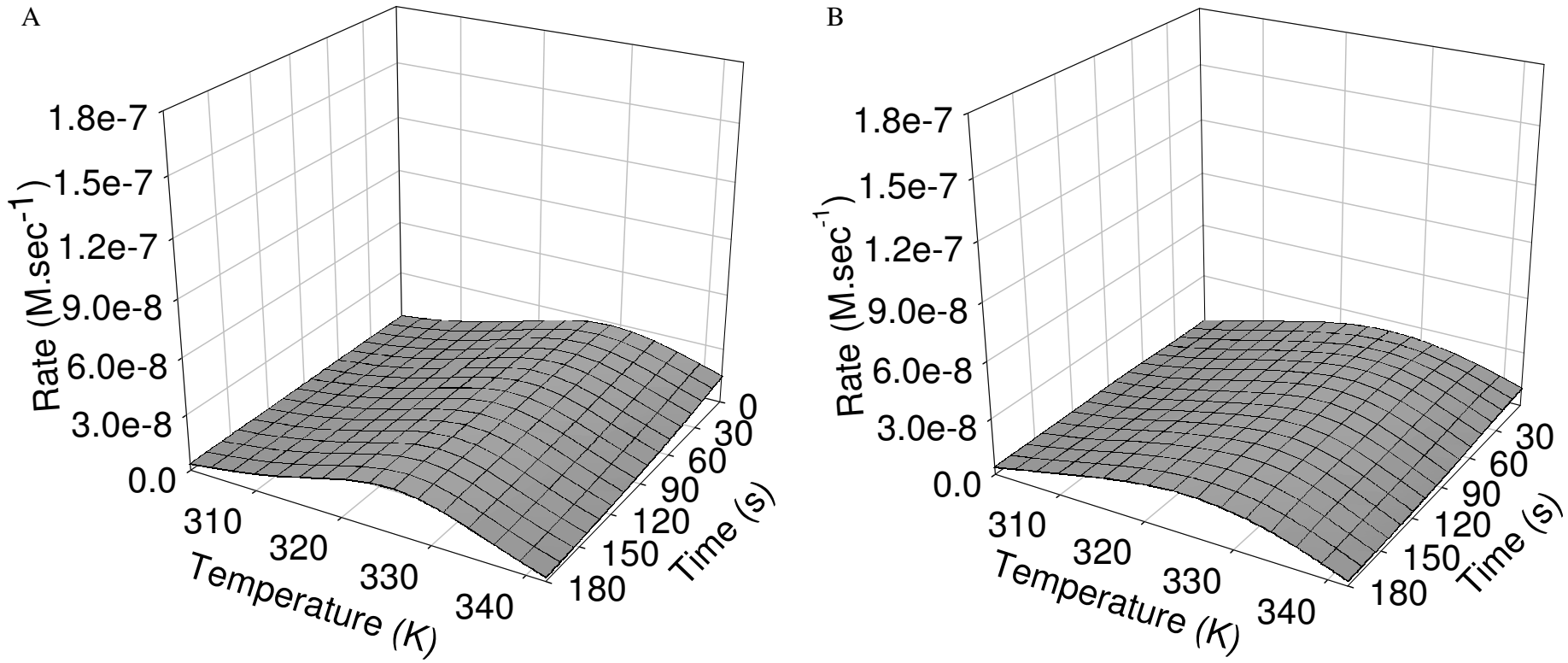

Figure 1.4: The temperature dependence of enzyme activity, according to A) Simulated data calculated by the Equilibrium Model using experimental phenylalanine ammonia lyase data. B) Experimental phenylalanine ammonia lyase data. ($\Delta G^{\ddagger}_{cat}$ = 80 kJmol^{-1} $\Delta G^{\ddagger}_{inact=}$ 97 kJmol^{-1}, T_{eq} = 330 K and $\Delta H^{\ddagger}_{eq}$ = 181 kJmol^{-1}) (Lee et al., 2007).

The Equilibrium Model has been experimentally validated (Peterson et al., 2004) and so far every enzyme that has been studied has followed the Equilibrium Model (Lee et al., 2007, Daniel et al., 2008).

1.7 Enzymes in Industry: Immobilized Enzymes

Biotechnology is very basically defined as the practice of using biological materials and practices to create goods and services. The catalytic power and specificity of enzymes is commonly utilised within the biotechnology industry, which has in recent years hugely increased. Dissolved enzyme molecules behave as solute, in that they are readily dispersed in the solution and have complete freedom of movement. Enzyme immobilization is the irreversible covalent immobilization to an inert, insoluble support material, a technique specifically designed to restrict the free movement of an enzyme. Immobilization prevents the release of the enzyme into the reaction media (Bickerstaff, 1997). The immobilization of enzymes may increase enzyme stability (Mozhaev, 1993; Blanco and Guisan, 1989) and allows the enzyme to be recovered and reused if it is still active (Van Langen et al., 2002). The fact that immobilized enzymes can easily be recycled makes them attractive and widely used in the biotechnology industry, with one of the major applications of immobilized enzymes in the biotechnology industry being their use within enzyme reactors (eg. Illanes et al., 2000).

1.8 Enzyme Reactors

Enzyme reactors consist of a vessel or series of vessels which are used to perform desired conversions by enzymic means; they play an important role in

biotechnological applications and in the biotechnology industry, for example through their use in antibiotic production as demonstrated by Alkema et al. (2003) and Giordano et al. (2006). Optimum enzyme reactor performance and accurate predictions of this performance have large potential biotechnological benefits as maximising the output of enzyme reactors requires a very careful balance of temperature and its effects upon enzyme stability and activity (Bartholomew and Tansey 2006). Enzyme Reactor operation is very cost sensitive as they operate on a large scale with expensive products and reactants, small changes in operation can result in large potential benefits or loss (Giordano et al., 2006).

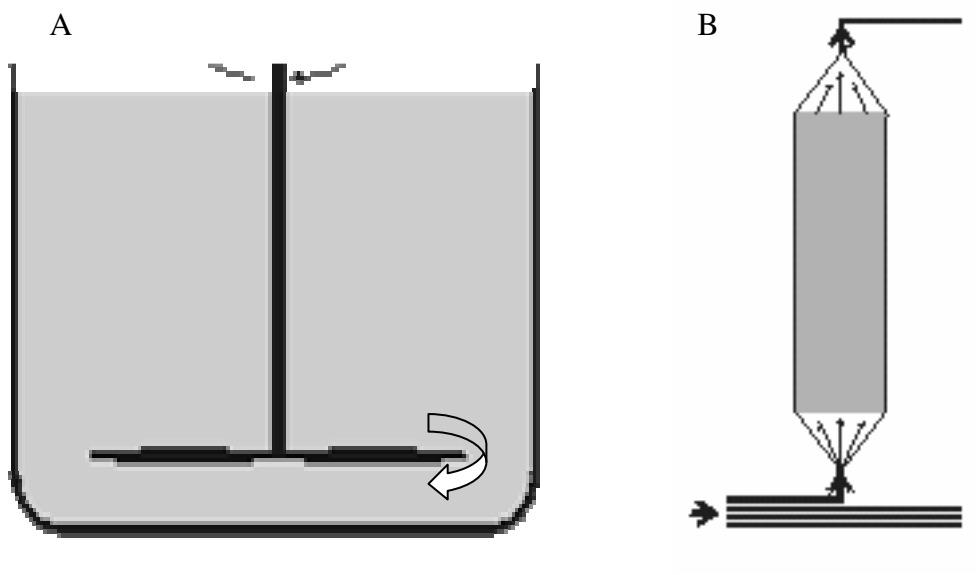

Figure 1.5: Common enzyme reactor types. A) Stirred Tank Batch Reactor. B) Packed bed or plug flow reactor.

(http://www.lsbu.ac.uk/biology/enztech/reactors.html).

Figure 1.5 shows basic diagrams of the most common types of enzyme reactors. A stirred tank batch reactor is simply a stirred vessel containing all reagents required for conversion to the desired product. A packed bed reactor contains a bed of packed beads on which the enzyme is immobilized, substrates flows through, conversions take place and then the product flows out the other side. The advantages of using a Stirred Tank Batch Reactor are: operation and set up is simple using common lab equipment and can be used with both immobilized and free enzymes. The disadvantages of using a Stirred Tank Batch Reactor are: They suffer batch-to-batch variations and it can be hard to recycle immobilized enzyme if used.

Preliminary calculations of enzyme reactor product output with time and temperature based upon the Equilibrium Model are quite different from those found using the Classical Model, as shown in the figure 1.6. When using a batch reactor for chemical synthesis, intuition would predict that the higher the operating temperature, the faster the catalysed reaction, but also the less stable the enzyme. Simulated data fitted to the Equilibrium Model has shown that this is only generally true if T_{eq} exceeds the operating temperature of the reactor. If T_{eq} is less than the working temperature the reverse is seen (compare 1.6 (a) with 1.6 (b) (Eisenthal et al., 2006) where increases in temperature result in decreases in reaction rate. Figure 1.6 (c) shows the typical time courses of product formation at various temperatures, as predicted by the Classical Model; the behaviour seen with the Equilibrium Model simulations is not seen here.

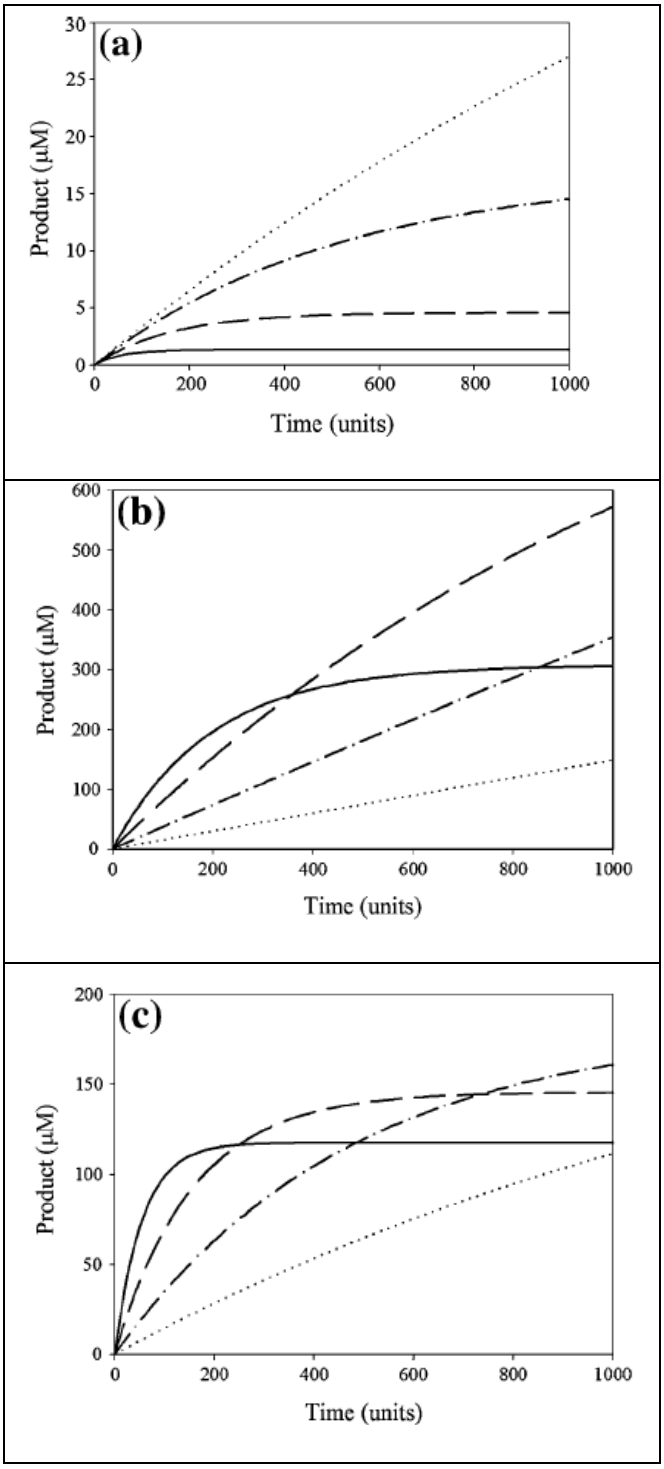

Figure 1.6: The effect of T_{eq} on time courses of product concentration simulated at various temperatures: 310 K (·····); 320 K (– · – · -); 330 K (– – –); 340 K (——). a) Equilibrium Model (T_{eq} = 300 K) b) Equilibrium Model (T_{eq} = 350 K) c) Classical Model. (other parameter values: $\Delta G^{\ddagger}_{cat}$ = 75 kJ mol^{-1}, $\Delta G^{\ddagger}_{inact}$ = 95 kJ mol^{-1} $\Delta H^{\ddagger}_{eq}$ = 95 kJ mol^{-1}) (Eisenthal, et al., 2006).

1.9 A test of the Equilibrium Model on an unusual enzyme

Bovine pancreatic ribonuclease A (RNase A, EC 3.1.27.5) catalyses the depolymerization of RNA, it is an enzyme that has been studied extensively (eg., D'Alessio and Riordan, 1997; Raines, 1998). Bovine pancreatic RNase A was the first enzyme to be chemically sequenced, and been used as a model for protein structure/ function studies (Blackburn and Moore, (1982). RNase A is one of the hardiest enzymes in common laboratory usage, as fully denatured and reduced RNase A (after treatment with 8M Urea and a reducing agent) is regenerated after exposure to air, with the structure and activity of the renatured enzyme being identical to that of the native enzyme (Blackburn, 1979). The fact that RNase so readily renatures makes it a very unusual enzyme, which may not obey typical variations in activity with temperature and as a result may not follow predictions made by the Equilibrium Model.

1.10 Test of the Equilibrium Model using a change at the active site of Ak1 protease

Ak. 1 protease is a highly thermostable serine protease active against substrates containing neutral or hydrophobic branched- chain amino acids at the P_1 site (Toogood et al., 2000). Originally isolated from *Bacillus* st. Ak. 1 and partially characterised by Peek et al. (1993), this protease is a member of the subtilisin superfamily (subtilases), which are widely distributed enzymes through many living species, performing a variety of processing functions and also used extensively in industry (Smith et al., 1999; Wells and Estell, 1988). Like many Subtilases Ak. 1 protease is strongly stabilised by calcium, with calcium ions playing a large role in

protecting protease's against autolysis and thermal denaturation (Briedigkeit and Frommel, 1989).

Structural analyses have revealed the unusual presence of a disulfide bond within the active- site cleft of Ak. 1 protease. This bond has a dual role of maintaining substrate binding cleft integrity and of increasing thermostability of the protease (Smith et al., 1998).

The molecular basis of the Equilibrium Model is suspected to be conformational changes at the active site, so that cleavage of the active site disulfide bond may be a useful probe of the Equilibrium Model mechanism (Daniel et al., 2008).

1.11 Thesis Objectives

My research is part of a larger project into new and fundamental hypotheses involving the Equilibrium Model. My research has several objectives. The main one seeks to experimentally investigate a proposal made by Eisenthal et al. (2006), that the Equilibrium Model and the knowledge of T_{eq} might be essential to the optimum use of enzyme reactors. The results of my proposed research may have far reaching implications within the biotechnology industry due to the widespread use of enzyme reactors (Illanes and Wilson, 2003; Abu-Reesh, 2005).

Subsidiary objectives are to test the Equilibrium Model in different ways. RNase A may deviate from the Equilibrium Model due to its unusual ability to very rapidly renature. Cleavage of the disulfide bond at the A.k 1 protease active site may be a useful probe of the Equilibrium Model mechanism which seems to be located at the active site.

Chapter Two

Materials and Methods

2.1 The Temperature Dependence of Enzyme Activity and Application to the Equilibrium Model: Experimental Considerations, Methods and Data Analysis

2.1.1 Introduction

The temperature dependence of enzyme activity can be determined experimentally by performing appropriate enzyme assays at different temperatures. The Equilibrium Model allows mathematical modeling of the temperature dependant behaviour of enzymes, and hence the calculation of thermodynamical parameters. From enzyme assay results performed at varying temperatures a three dimensional graph showing the variation in reaction rate, temperature and time can be constructed, such graphs display the time and temperature dependence of activity of the enzyme assayed. This data can then be fitted to the Equilibrium Model and Thermodynamical parameter values calculated according to the Equilibrium Model (equation 1.19). These can then be used in the calculation of simulated data. By comparing the experimental 3D graph of reaction rate, temperature and time to the simulated 3D graph it can be seen how well the experimental data follows the Equilibrium Model.

The use of appropriate assays is hugely important in order to get valid and reliable data, and it particularly should be noted that the Equilibrium Model depends upon V_{max} data. All assays must be performed under identical conditions with time and temperature being the only variables. Certain experimental considerations which will

be outlined in section 2.1.2 must be considered in order to ensure that any decrease in the measured enzyme activity at higher temperatures is due solely to reversible or irreversible thermal inactivation.

2.1.2 Experimental Considerations

When experimentally determining the temperature dependence of enzyme activity certain assay criteria and complicating factors associated with increases in temperature must be taken into account, the following experimental considerations were considered to ensure the data obtained is for the relevant V_{max}.

2.1.2.1 Assay Selection

Ideally all enzyme assays used will be continuous, spectroscopic assays, as these assays are convenient, accurate and allow a large number of data points to be collected at precisely timed intervals. By monitoring the colorimetric end signal of such assays reaction progress curves of product produced versus time (as calculated from absorbance change) were constructed, which provide a wealth of information unique to the enzyme being analysed (Cornish-Bowden, 1972). The catalysed reaction should follow normal Michaelis-Menten kinetics where enzyme activity is the rate limiting factor, the enzyme should not be allosteric or product inhibited under the assay conditions used. It is important that all assay data be collected when the enzyme is operating at V_{max}, i.e., behaving in an ideal fashion and be fully saturated with substrate, as this ensures that any decrease in enzyme velocity is due to thermal inactivation of the enzyme and not substrate depletion (Daniel et al., 2001). Substrate concentrations were maintained at not less than ten times K_M, at all temperatures used, to ensure that the enzyme remained saturated with substrate for the duration of

the assay (Lee et al., 2007; Peterson et al., 2004; Peterson et al., 2007). If it was not possible to maintain substrate concentrations at ten times K_M a correction was applied to the data, as outlined in section 2.1.4.5, compensating for deviations from V_{max}. The reaction should be essentially irreversible or largely in favor of product formation and therefore far from reaction equilibrium, as the approach to reaction equilibrium is a common factor in the decrease in enzyme reaction velocity with time due to the increasing contribution of the reverse reaction.

2.1.2.2 Assay Component Stability

The temperature and pH of the assay may affect the stability of certain assay components such as the substrate or cofactor, affecting the obtained results. Non-enzymic catalysis can result from thermal degradation of the substrate, which commonly occurs when colorimetric substrates are used. Thermal substrate degradation was counteracted by performing blank assays at all temperatures used, with enzyme catalysed reaction rates corrected if necessary (Lee et al., 2007). Blank assays were run in the same way as enzyme catalysed assays, however the enzyme was substituted with buffer or irreversibly denatured enzyme. The resulting change in absorbance (if any) was then subtracted from the change in absorbance resulting from the enzyme catalysed assay at the same temperature. This ensures that any product evolved is due to enzyme catalysis.

2.1.2.3 pH Control

Of particular importance when analysing the effects of temperature on enzyme activity is the maintenance of assay pH, which is required to remain constant throughout the assay and at all temperatures used. This is because many enzymes are

sensitive to changes in pH, especially when it is combined with changes in temperature. Extinction coefficient's of substrates (required for the calculation of product concentration from absorbance values) change in response to pH and/or temperature changes, as is the case with assays based on the release of *p*-nitrophenol or *p*-nitroaniline where the extinction coefficient changes dramatically with small changes in pH (John, 1992). Care must be taken to select a buffer that is appropriate for the enzyme reaction being analysed and appropriate for use over the temperature range required.

Buffers should be chosen on the basis that the buffer:

a) Preferably has a low or no temperature coefficient (or needs to be reformulated for each temperature);

b) Is stable with regards to temperature and time;

c) Does not react with the enzyme and reaction components;

d) Does not inhibit the enzyme reaction in any way, either by removing or lowering the availability of essential reaction constituents or by containing inhibitors to the enzyme.

Often the most ideal buffer to use does not have a low temperature coefficient, in such cases it is necessary that the pH be adjusted for use at different temperatures. This requires the use of a $\Delta pH/\ \Delta t$ (pH units per °C) value which is specific for different buffers and allows the change in pH as a result of temperature to be calculated. The buffer pH was adjusted at room temperature, allowing the buffer pH to be constant for all temperatures used.

2.1.3 Assay Method and Technique

The following experimental considerations and methods were considered and followed to ensure good assay practice and the collection of reliable and reproducible results.

2.1.3.1 Substrate and Enzyme Solution Preparation

Substrate and enzyme were dissolved and diluted in the buffer used for the assay with the pH checked and adjusted if necessary. As previously stated the substrate concentration within the assay was maintained at, at least ten times K_M (Lee et al., 2007; Peterson et al., 2004; Peterson et al., 2007). Concentrated stock substrate and enzyme solutions were made up fresh daily, kept on ice and diluted with buffer to give the appropriate final concentration within the cuvette, minimising assay to assay variations in substrate and enzyme concentration. Degradation of the substrate or enzyme was identified through the use of a standard assay performed at a particular temperature, where any decrease in activity indicated degradation had occurred, and at regular intervals during the days work. Appropriate enzyme concentrations were obtained from trial assays at several temperatures, with enzyme stock solutions being diluted until the resulting change in absorbance did not go over 0.7, since above this absorbance errors become larger. Triton X-100 is a non-ionic detergent which is commonly added to enzyme solutions of low concentration to prevent loss of the enzyme onto walls of the cuvette, all stock enzyme solutions contained 0.1% Triton X-100, this was important to prevent changes in enzyme concentration that are not as a result of thermal inactivation.

2.1.3.2 Temperature Control

The control of temperature is a very important factor which can introduce error when experimentally analysing the temperature dependence of enzyme activity. A Peltier was used to control the temperature of cuvette contents; temperature was directly monitored for accurate temperature control by placing a temperature probe within the cuvette adjacent to the light path during temperature equilibration. Temperature equilibration at relatively low assay temperatures (up to 40ºC) is a quick process, however temperature equilibration takes longer as the temperature increases, therefore it was essential to check the temperature of the cuvette prior to the initiation of the reaction to ensure temperature equilibration was complete. If temperature measurements taken before the initiation of the reaction and immediately after reaction completion differed by more than 0.1°C the reaction was repeated (Peterson et al., 2007; Peterson et al., 2004). At high temperatures (above 60ºC), temperature gradients within cuvettes can be significant; these were identified by taking temperature measurements from the top and bottom of the cuvette; if significant a stirred cuvette was used. Evaporation of cuvette contents and heat loss during circulation may also be significant at higher assay temperatures; these problems were overcome by using a cap to seal the cuvette (Peterson et al., 2007) and an insulation block around the cuvette holder. Quartz cuvettes were used for their relatively quick temperature equilibration and their heat retaining capacity (Peterson et al., 2007).

2.1.3.3 Assays

For each enzyme, progress curves (absorbance versus time) were collected in triplicate for at least eight temperatures, with at least 3 temperature points above T_{eq}. The reaction was initiated by the addition of microlitre amounts of enzyme (less than

2% of the total assay volume) to prevent any significant temperature changes within the cuvette (Lee et al., 2007; Peterson et al., 2004; Peterson et al., 2007). The evolution of product was monitored at an appropriate wavelength (wavelength at which the substrates extinction coefficient is calculated) with the time interval set so that an absorbance reading was collected every second.

Instrumentation

All enzyme activities were measured using a Thermospectronic™ Helios γ-spectrophotometer equipped with a Thermospectronic™ single cell peltier-effect cuvette holder. This system was networked to a computer installed with Vision32™ (Version 1.25, Unicam Ltd) software including the Vision Enhanced Rate Programme capable of recording absorbance changes over time intervals down to 0.125 seconds. The temperature of each assay was recorded using a Cole-Parmer Digi-Sense® thermocouple thermometer accurate to ± 0.1% of the reading and calibrated using a Cole-Parmer NIST (National Institute of Standards and Technology)-traceable high-resolution glass thermometer.

2.1.3.4 Protein Concentration Determination

The concentration of protein used within assays was determined since the amount of enzyme present in the assay is an essential input required for the calculation of thermodynamical parameters by the Equilibrium Model. The Bradford method was used which colorimetrically determines the concentration of protein in solution. This method incorporates the use of Coomasie Blue dye (Bradford Reagent), the metachromatic response and the use of protein standards (Sapan et al., 1999). The dye-protein complex absorbs at 595nm, therefore measuring the absorbance at 595nm

quantitates the amount of protein bound (Bradford, 1976). Bovine Serum Albumin (BSA) standards were used in the construction of the standard curve; standards were diluted from a 1mg/mL BSA standard which has an absorbance of 0.66 at 280nm (Bradford, 1976). Plastic cuvettes were used for all absorbance readings carried out at 595nm and the final unknown protein concentration was calculated from the average of several different protein dilutions. A modified Bradford assay was used for the determination of the concentration of immobilized enzymes, this was necessary as the Bradford Reagent bound both to the protein and the immobilization support, which then settled at the bottom of the cuvette preventing any change in absorbance from being detected. The modified Bradford method involved dissociation of the protein and standards by incubation with 1M NaOH overnight at room temperature, effectively removing the protein from the immobilization support and allowing the concentration of the dissociated protein to be determined.

2.1.4 Data Analysis

2.1.4.1 Construction of 3D Plots from Experimental Data

For each enzyme 3D plots showing the variation in reaction rate with time and temperature were constructed from experimental data for the purpose of comparison to 3D plots constructed from simulated data calculated by the Equilibrium Model. First each reaction progress curve were exported out of the data collection program Vision32™ in the form of “data points of rates” and saved as a text file. When opened using Microsoft® Office Excel the data was within two columns: time and absolute absorbance. All assay data for each enzyme was compiled into a single Microsoft® Office Excel file where product concentration and catalytic rates were

calculated; assay data was inserted into worksheets labeled with the appropriate temperature.

The first data point collected may have deviated from an absorbance value of zero due to slight absorbance changes related to addition of the enzyme and the approximate two second time delay between addition of the enzyme and the start of the collection of data (Peterson et al., 2004). The first adjustment made to the data was a correction to all absorbance points accounting for this initial deviation from zero, if necessary.

Next, substrate degradation as a result of temperature was accounted for by subtracting the blank absorbance values from that of the enzyme catalysed reaction. Product concentration was then calculated according to the Beer-Lambert Law (Palmer, 1981), from the corrected absorbance values and the substrates extinction coefficient. It is important that the extinction coefficient used has been calculated at the same temperature, pH, wavelength and path length as that used for the collection of experimental data. Equation 2.1 was used to calculate reaction rates in terms of product formation from the calculated product concentrations.

$$\text{Rate} = \frac{\Delta[\text{product}]}{\Delta\text{time}} \qquad \textbf{Equation 2.1}$$

3D plots showing the variation in reaction rate with time and temperature were constructed using the computer program SigmaPlot® 2001 for Windows™, Version 7.101, SPSS. Data within the Microsoft® Office Excel file was first rearranged and prepared into a format that was compatible with SigmaPlot and the function of 3D plot generation. All data which was input into SigmaPlot was required to be in three columns of Time (seconds), Temperature (Kelvin) and Rate (M^{-1}•second). A Loess

algorithm was used to smooth the data which is a curve fitting technique used to elicit trends from noisy data (Peterson et al., 2004).

2.1.4.2 Determination of Equilibrium Model Parameters

The Equilibrium Model is defined by four thermodynamic parameters: $\Delta G^{\ddagger}_{cat}$, $\Delta G^{\ddagger}_{inact}$, ΔH_{eq} and T_{eq}, as outlined in section 1.6. A stand-alone Matlab® [version 7.1.0.246 (R14) Service Pack 3; Mathworks] application (*available on CD from R.M.D.), enables the fitting of the experimental data to the Equilibrium Model equation (equation 1.19) to derive the Equilibrium Model parameters: this application is only suitable for computers running Microsoft® XP (Lee et al., 2007; Peterson et al., 2007).

A Microsoft® Office Excel file containing experimental progress curves of product concentration against time was prepared as per the Microsoft® Office Excel file labeled “template.xls” (available on Matlab Progress Curve Fitting CD within “fitting files” folder), with enzyme concentration input as mol • l^{-1} (cell labeled E_0) and starting parameter values of 80 kJ • mol^{-1} ($\Delta G^{\ddagger}_{cat}$), 95 kJ • mol^{-1} ($\Delta G^{\ddagger}_{inact}$), 100 kJ • mol^{-1} (ΔH_{eq}) and 320 K (T_{eq}). The starting parameter values are deemed to be plausible parameter estimates and therefore can be adjusted to slightly alter calculated parameter values if required (Peterson et al., 2007). This is useful when the experimental data plot appears not to match the simulated plots; if this is caused by an "artificial minima" in the programme, then changing the starting parameters may lead to parameters that generate a match with experimental data.

(*available on request from Charles Lee (cklee@waikato.ac.nz) or Roy Daniel (r.daniel@waikato.ac.nz)).

It should be noted that when data gives a good match with the model, varying the starting parameters does not significantly affect the final parameter values. By opening the prepared Microsoft® Office Excel file using the fitting file (within "program files" folder) the data was analysed, initially by a low resolution fit and then by a high resolution fit which calculated standard deviations and confidence intervals. Within the Microsoft® Office Excel file used for the fit an extra worksheet named "Rate Data Actual" containing simulated or fitted reaction rates (according to the calculated parameters) against temperature and time was automatically generated.

By setting *t* in equation 1.19 at zero, equation 2.2 is generated, allowing parameters to be determined under initial conditions with the exception of the time dependant parameter $\Delta G^{\ddagger}_{\text{inact}}$. Initial reaction rates (M/second) instead of product concentration were applied to the Matlab application when the time zero equation (equation 2.2) was used. The zero time Equilibrium Model was only used when enzymes were not operating under "non-ideal" conditions and a good match of simulated data to experimental data was not seen, derived parameters using the zero time model have larger statistical errors due to the small size of the data set (Peterson et al., 2007).

$$V_{\max} = \frac{k_B T \cdot e^{\left(-\frac{\Delta G^{\ddagger}_{\text{cat}}}{RT}\right)} \cdot E_0}{h\left(1 + e^{\left(-\frac{\Delta H_{\text{eq}}\left(\frac{1}{T_{\text{eq}}} - \frac{1}{T}\right)}{R}\right)}\right)}$$

Equation 2.2

2.1.4.3 Construction of 3D Plots from Simulated Data

The comparison of 3D plots generated from experimental data to 3D plots generated from simulated data is the key to confirming whether the experimental data follows the Equilibrium Model and whether the calculated parameters are valid. A 3D plot of simulated data was generated by plotting and smoothing the calculated data within the "Rate Data Actual" worksheet using SigmaPlot, this data is present within three columns titled Temperature, Time and Rate. When plotting the simulated data it is important to make sure that the same type of data is plotted on the same axis as used for the experimental data.

2.1.4.4 Comparing the 3D Plots

When comparing the 3D plots of the experimental and simulated data it is important to check the following features:

a) The activity axis- the peak activity level should be within one order of magnitude of each other.
b) The temperature axis- the width of the activity peaks should be roughly similar.
c) The temperature axis- the rates of irreversible denaturation (the rate of the downward slope) should be similar.
d) The overall shape of the plots should be similar.

(available on CD from R.M.D.)

2.1.4.5 K_M Adjustment for Deviations from V_{max}

When reactions were performed at substrate concentrations of less than ten times K_M adjustments were made to the raw data, according to equation 2.3, to compensate for deviations from V_{max}. These adjustments were essential as the Equilibrium Model assumes that the enzyme operates at V_{max} at all times.

$$v = \frac{V_{max} \bullet [S]}{K_M + [S]} \qquad \textbf{Equation 2.3}$$

This procedure potentially introduces errors and was only be used when all other methods for increasing [S] have been exhausted.

2.2 The Development, Operation and Data Analysis of a Stirred Tank Batch Reactor

2.2.1 Introduction

A stirred tank batch reactor is simply a stirred tank or vessel in which a desired chemical conversion takes place, with the product usually being recovered and utilised within the lab or sold. Maximising the output of enzyme reactors requires a very careful balance of temperature and its effects upon enzyme stability and activity (Illanes et al., 2000), therefore accurate prediction of optimum enzyme reactor operation is beneficial (Eisenthal et al., 2006). Stirred tank batch reactors differ from enzyme assays as they operate on a larger scale, are stirred, run for a much longer time period and the product is usually recovered. Other type of enzyme reactors are also used, but are not dealt with here.

This section will first address instrumentation and reaction issues associated with the development of a stirred tank batch reactor, document development to a final reactor design and finally give the materials and methods used in its operation and data collection. The purpose of the developed enzyme reactor is to gather experimental data from biotechnologically important enzymes which will be fitted to the Equilibrium Model as per section 2.1.

2.2.2 Instrumentation and Reaction Issues Associated with the Development of a Stirred Tank Batch Reactor

Stirred tank batch reactors can be constructed using common lab equipment; however the simultaneous need for temperature control, stirring and monitoring of the reaction can pose a problem. There are several important factors which must be taken into account when developing a stirred tank batch reactor; these have been divided into instrumental and reaction factors.

Instrumental factors:

a) Scale of operation

b) Temperature control

c) Mixing method and efficiency

d) Reaction monitoring

Reaction factors:

a) pH control

b) Stability of reactor contents

c) Length of run

d) Cost of operation

The enzyme reactor developed is required to be small scale (maximum 50mL's) for reasons of cost, be temperature controlled from 25ºC- 80ºC, be uniformly yet sufficiently mixed (keeping immobilized enzyme particles suspended for example) and allow the reaction progress to be easily monitored.

The reactions performed in the reactor will be selected according to section 2.1.2 and catalysed by biotechnologically important enzymes, both in the free and immobilized form, with the length of the reactor run being from 1 to 1.5 hours.

Acid Phosphatase: Characteristics and use in my research

Acid Phosphatase [EC 3.1.3.3, orthophosphoric-monoester phosphohydrolase (acid optimum)] from wheat germ was purchased from Serva Electrophoresis Gmbh (Heidelberg, Germany) and used only for the development of a stirred tank enzyme reactor. Acid Phosphatase is a well characterised enzyme with the ability to hydrolyse *p*-nitrophenylphosphate (*p*-NPP) to *p*-nitrophenyl, this is a colorimetric reaction which can be monitored spectroscopically at 410nm (Hollander, 1971). 0.1M Acetic Acid, Sodium Acetate buffer pH 5.0 is a suitable buffer for use with this reaction. *p*-NPP, was purchased from Sigma-Aldrich, all other chemicals used were of analytical grade.

2.2.3 Penicillin Amidase: Characteristics and use in my Research

Penicillin G Amidase's (PA, EC 3.5.1.11) from different sources have been widely studied and used within the biotechnology industry in the production of 6-aminopenicillanic acid (6-APA). 6-APA is used in the production of some semi

synthetic penicillins (ampicillin), and cephalosporins, with this biosynthetic route being one of the major applications of immobilized enzymes and enzyme reactors (Alkema et al., 2003; Giordano et al., 2006; Torres et al., 2005). Spectrophotometric determination of Penicillin Amidase activity is widely carried out using the colorimetric reference substrate 6-nitro-3-phenylacetamido benzoic acid (NIPAB) (Galunsky et al., 1994). An assay widely available in literature describes the enzyme assay of Penicillin Amidase with NIPAB in sodium phosphate buffer pH 7.4, *I*=0.2M, with the hydrolysis of NIPAB being measured at a wavelength of 380nm (Alkema et al., 2003; Kasche et al., 1987; Guncheva et al., 2004).

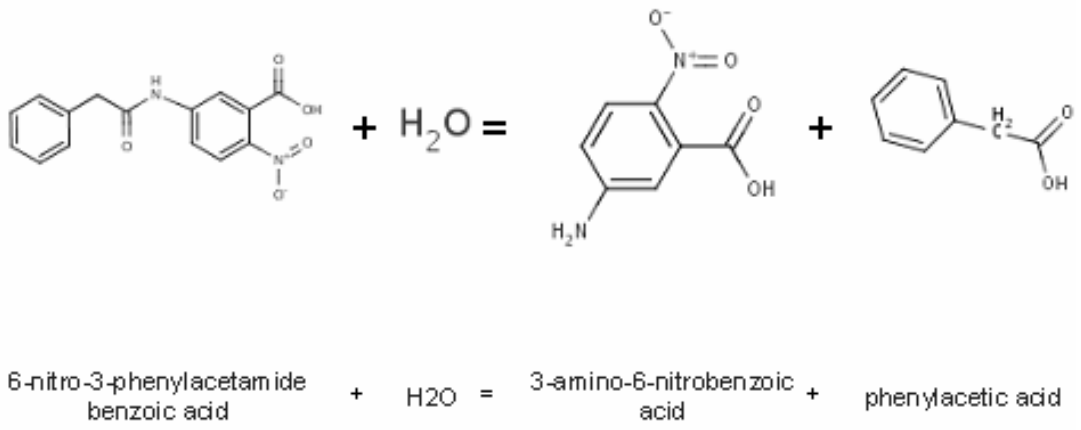

Figure 2.1: Reaction catalysed by penicillin amidase (EC 3.5.1.11). (http://www.brenda-enzymes.info)

Specific methods used for penicillin amidase and its use within a stirred tank enzyme reactor will be given after the development of my enzyme reactor has been described, in section 2.2.9.

2.2.4 Alkaline Phosphatase: Characteristics and use in my Research

Alkaline Phosphatase (EC 3.1.3.1) is used primarily in the biotechnology industry for the dephosphorylation of 5' phosphorylated DNA or RNA ends, giving this enzyme applications in DNA and RNA sequencing, mapping and fingerprinting studies and DNA recombination (Gerhartz, 1990). Standard and widely published assays of Alkaline Phosphatase employ the colorimetric substrate *p*-nitrophenyl phosphate (*p*-NPP), with the phenol released being determined spectroscopically at 405nm (Hoylaerts et al., 1992) (extinction coefficient= $0.0182M^{-1}\bullet cm^{-1}$). 1M Diethanolamine buffer pH 9.8 containing 0.5mM $MgCl_2$ is commonly used for Alkaline Phosphatase assays (Hoylaerts et al., 1992), this buffer however has a large temperature coefficient (-0.0250 ApKa/ºC). For the pH to remain constant at all temperatures used a series of buffers must be prepared with the pH corrected using the temperature coefficient. The buffer contains Mg^{2+} as this is required for maximum activity of the enzyme (Fernley, 1971).

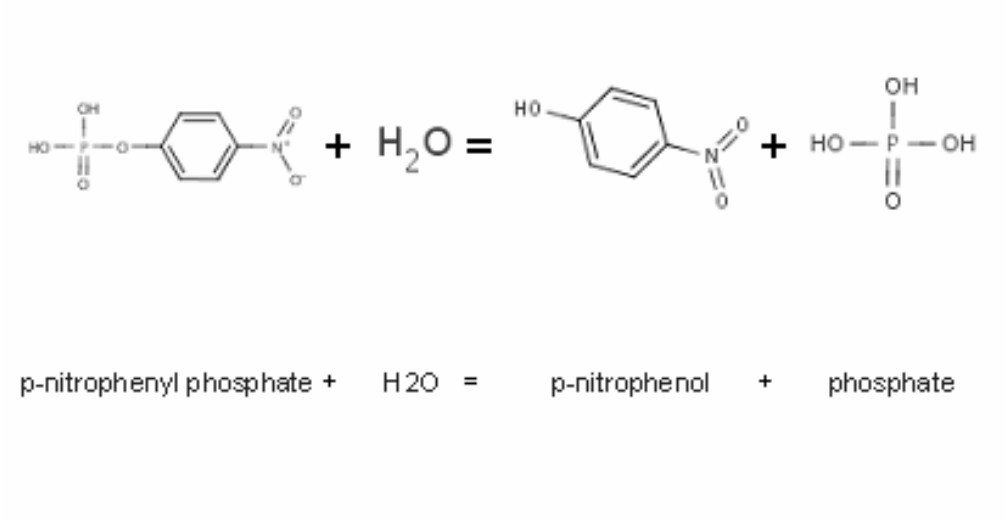

Figure 2.2: Reaction catalysed by alkaline phosphatase (EC 3.1.3.1). (http://www.brenda-enzymes.info).

Specific methods used for alkaline phosphatase and its use within a stirred tank enzyme reactor will be given after the development of my enzyme reactor has been described, in section 2.2.10.

2.2.5 Stirred Tank Batch Reactor: Model One

Figure 2.3 shows a basic diagram of this enzyme reactor. The reaction vessel used was a 100mL schott bottle, a water bath with a circulating thermostat (HETO, Birkerod, Denmark) was used to control the temperature and a Cole-Parmer® Stir-Pak® heavy duty mixer head controlled by a Cole-Parmer® Stir-Pak® speed controller was used to mix the reaction, the stirrer entered the reaction vessel through a hole in the schott bottle lid.

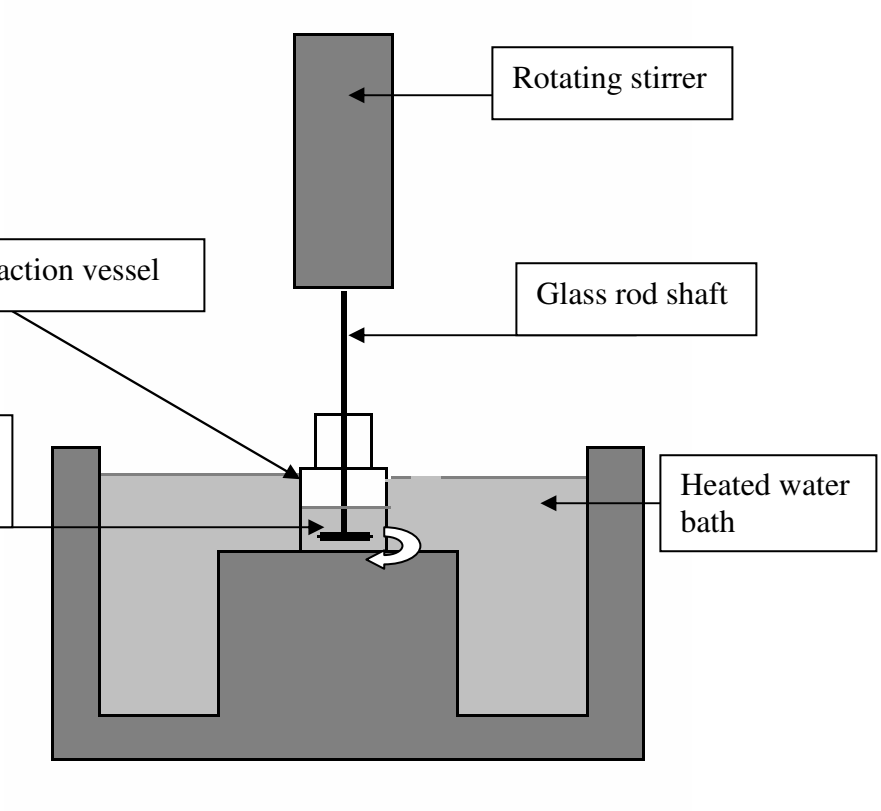

Figure 2.3: Basic diagram of stirred tank batch reactor: Model One.

This reactor was developed and trialled using Acid Phosphatase and *p*-NPP, the reaction mix was a total of 30mL's with 1mL being removed at 10 minute intervals and used to monitor the reaction at 410nm for a total length of 1.5 hours. 23.7mL of 0.1M Acetic Acid, Sodium Acetate buffer and 6.0mL of 0.1M *p*-NPP were equilibrated at the desired temperature within the reaction vessel within the water bath and the temperature checked using a Cole-Parmer Digi-Sense® thermocouple thermometer, the reaction was initiated by the addition of 300µL Acid Phosphatase enzyme (10mg/mL). This enzyme reactor was rejected as the 30mL volume of the reaction mix was too large, making operation too expensive. Monitoring the reaction was not easy or accurate as removing samples from the reactor was awkward with the stirrer operating and prone to experimental error due to the approximate 10 second time delay between removal of the sample and the measurement of absorbance. The temperature profile is made up from a relatively low number of data points which is not ideal if the data is to be applied to the Equilibrium Model. Results from this reactor are not presented in this work.

2.2.6 Stirred Tank Batch Reactor: Model Two

This enzyme reactor was developed from problems observed with the method of operation and design of enzyme reactor model one. In an attempt to reduce operation cost and to increase accuracy of reaction monitoring the size of the reaction mix was reduced and the use of a stopped enzyme reaction was employed. The reaction vessel used was a 5mL screw cap vial fitted with a rubber bung with a hole in the top allowing the stirrer to enter. The reaction mix was a total of 5mL with the constituents in the same ratio as previously used. The method of operation was the same as model one, however 50µL samples were removed at ten minute intervals,

added to 250μL 0.5M NaOH to stop the reaction and put on ice, absorbance at 410nm was then measured for all samples once the enzyme reactor run was complete. This reactor was improved in terms of ease of operation; the equilibration time of the reaction mix to the desired temperature was a lot quicker, sampling was less awkward by the use of the rubber bung to stopper the reaction vessel. The smaller reaction mix greatly reduced the cost of operation, however the reaction volume of 5mL is still large and cost could be saved by reducing it further. The use of the discontinuous reaction minimised experimental error due to the time delay between sampling and taking the absorbance reading, however it does have the disadvantage that not all enzymes intended for use will have an appropriate stopping reagent. This method does not improve on the low number of data points collected; as a result this enzyme reactor was rejected, and no collected data is presented here.

2.2.7 Stirred Tank Batch Reactor: Model Three

This enzyme reactor utilised the water bath and the water bath shaker to both control the temperature and mix the reactor contents, the reactor vessel was a glass test tube stoppered by a rubber bung. The reaction mix was a total volume of 5mL, with the constituents in the same ratio as previous used. Again a stopped reaction was used, using the same method as used previously.

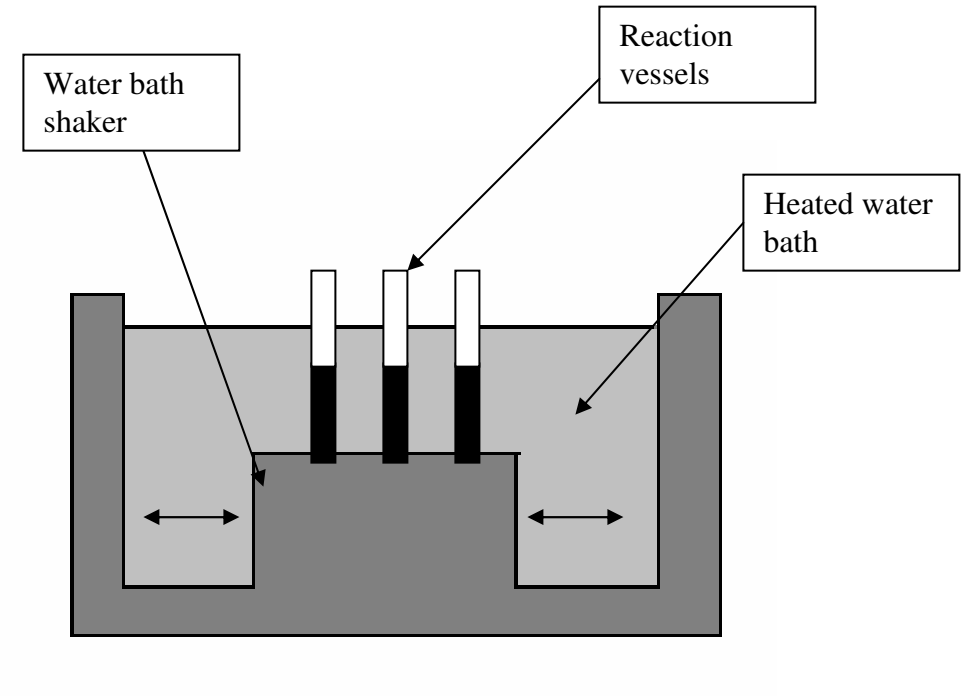

Figure 2.4: Basic diagram of my stirred tank batch reactor: Model Three.

This reactor was improved in terms of sampling, as access to the reaction vessel was not obstructed by the shaft and propeller as the previous designs were. By using the water bath shaker to mix the reaction, multiple enzyme reactor runs could be performed at the same time, allowing triplicate runs at the same temperature to be run simultaneously. Figure 2.5 shows that the average absorbance changes from triplicate runs obtained smooth reaction progress curves displaying the expected effects of temperature on enzyme activity.

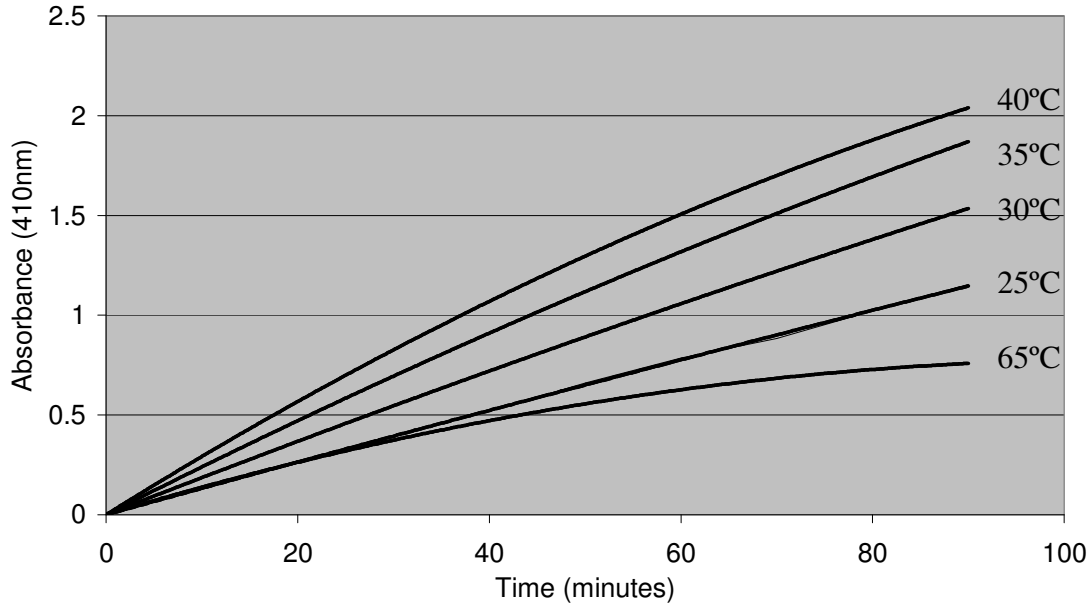

Figure 2.5: Average trial results of enzyme reactor model three using acid phosphatase.

This method again does not improve on the low number of data points collected or the cost of operation. A question not yet addressed was: Will reactions containing immobilized enzymes be sufficiently mixed? This was tested using penicillin amidase.

Enzyme Reactor Model 3 trials were performed using free and immobilized Penicillin Amidase, and the substrate NIPAB, purchased from Sigma Chemical Company.
4485µL O.1M Sodium Phosphate Buffer pH 7.4 and 500µL 1.5mM NIPABB were equilibrated to the desired temperature within the reaction vessel; the reaction was initiated by the addition of either 12.5µL of free or immobilized penicillin amidase (0.1mg/mL). 50µL of the reaction mix was removed at 10 minute intervals for a total of one hour, diluted 20 fold in buffer and the absorbance measured immediately at 380nm.

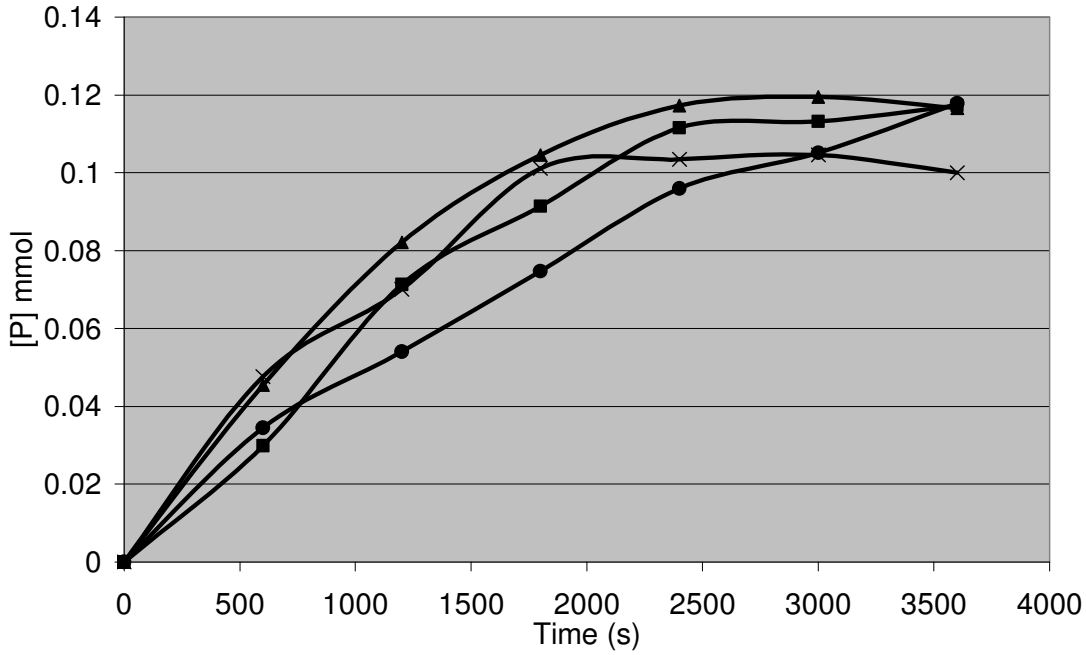

Figure 2.6: Average trial results of enzyme reactor model three using immobilized penicillin amidase. 25 °C (●); 35°C (■); 45°C (▲); 55°C (×).

This enzyme reactor failed dismally as the beads on which the enzyme was immobilized sunk to the bottom of the reaction vessel: as a result of poor mixing therefore, the reaction did not progress normally and could not be correctly monitored as shown from the average product concentration calculated from triplicate values in figure 2.6. Compounding the bad results obtained from these trials the water bath used broke down, the replacement did not have a shaker and was shaped in such a way that prevented the Cole-Parmer® Stir-Pak® heavy duty mixer head from being manoeuvred appropriately above it using the heavy duty stand required to support it. This enzyme reactor design was therefore rejected.

2.2.8 Stirred Tank Batch Reactor: Model Four

The instrumentation and method of operation of this enzyme reactor was based on an enzyme assay, however it used a 3.5mL stirred quartz cuvette and a much longer running time. The reactor was operated directly within a spectrophotometer allowing temperature to be simply controlled by a peltier, stirred by a magnetic stirring flea and the reaction to be followed directly and continuously allowing a much greater number of temperature points to be collected. This reactor was smaller scale, therefore more cost effective, allowed for more accurate temperature control, the level of stirring could be controlled and allowed for the more accurate collection of data points. The only shortcoming of this enzyme reactor was that for the entirety of the run the absorbance change had to remain within the accurate detection limits of the spectrophotometer, i.e., about 0.7. Enzyme reactor runs were operated according to section 2.1.3 with data points collected every second for a total run time of one hour. Figure 2.7 shows that the method of stirring used by enzyme reactor model 4 is sufficient to mix reactions containing immobilized enzymes as the reaction progress curves of average product concentration are smooth, reproducible and display the expected effects of temperature on enzyme activity.

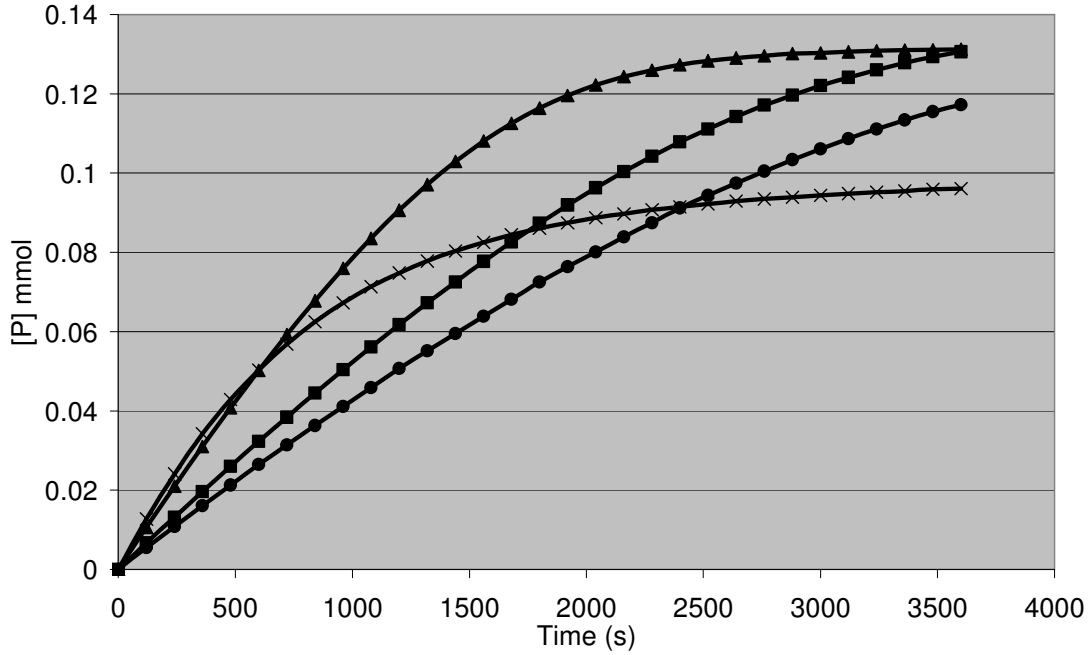

Figure 2.7: Average trial results of enzyme reactor model four using immobilized penicillin amidase. 25 °C (●); 35°C (■); 45°C (▲); 55°C (×).

2.2.9 Penicillin Amidase: Enzyme Reactor Procedure

Materials

Penicillin G Amidase (EC 3.5.1.11) (ammonium sulfate suspension and immobilized on Eupergit® C) from *Escherichia Coli* and NIPAB were purchased from Sigma-Aldrich (St Louis, USA). Phosphate buffer was made using reagent grade materials available through recognised chemical suppliers.

Reagents

O.1M Sodium Phosphate Buffer pH 7.4

1.5mM NIPAB substrate

0.01mg/mL free enzyme

25mg/mL immobilized enzyme

Reactor Technique

To a 3.5mL quartz cuvette 350µL 1.5mM NIPAB, 3140µL O.1M Sodium Phosphate Buffer pH 7.4 and a magnetic stirring flea were added and equilibrated to the desired temperature. The reaction was initiated by the addition of 10µL of either 0.01mg/mL free enzyme or 25mg/mL immobilized enzyme. The reaction was monitored at 380nm with a data point collected every second over the temperature range of 25-60ºC.

2.2.10 Alkaline Phosphatase: Enzyme Reactor Procedure

Materials

Alkaline Phosphatase (EC 3.1.3.1) (in 50% glycerol with 5mM $MgCl_2$ and 0.1mM $ZnCl_2$ and immobilized on acrylic beads in ammonia sulphate suspension) from calf intestinal mucosa and *p*-NPP from were purchased from Sigma-Aldrich. Diethanolamine buffer was made using reagent grade materials available through recognised chemical suppliers.

Reagents

1M Diethanolamine buffer pH 9.8 containing 0.5mM $MgCl_2$

0.05M *p*-NPP substrate

0.0015% free enzyme

0.0.125% immobilized enzyme (100% being solution in purchased bottle).

Reactor Technique

To a 3.5mL quartz cuvette 350µL 0.05M *p*-NPP, 3115µL 1M Diethanolamine buffer pH 9.8 containing 0.5mM $MgCl_2$ and a magnetic stirring flea were added and

equilibrated to the desired temperature. The reaction was initiated by the addition of either 15µL 0.0015% free enzyme or 35µL 0.0.125% immobilized enzyme. The reaction was monitored at 405nm with a data point collected every second over the temperature range of 25-60ºC.

2.2.11 Data Analysis

Construction of Experimental 3D Plots

The construction of 3D plots from experimental enzyme reactor data was done as outlined in section 2.1.4, however the large number of data points collected from enzyme reactor operation was reduced using Microsoft® Office Excel. By applying a data filter to the complete data set a data file containing every tenth data point was constructed allowing the construction of Experimental 3D plots from a spreadsheet of a more manageable size.

Determination of Parameters associated with the Equilibrium Model

Two sets of parameters were calculated for each form of both enzymes, one called the 3 minute parameters which were calculated from the first 3 minutes of unfiltered enzyme reactor data and one called the 1 hour parameters which were calculated from the filtered data of the entire data set, parameters were calculated according to section 2.1.4.2.

Calculation of Simulated Data

One hour of simulated data according to the Equilibrium Model was calculated from determined parameter values using MicroMath® Scientist® for Windows software (version 2.01, MicroMath Scientific Software). This was done by opening a ‘new

parameter set', inputting the calculated parameter values, clicking 'calculate' then inputting appropriate temperature (Kelvin) and time (seconds) values. Scientist software calculated simulated product concentration with time data that follows the Equilibrium Model according to the input parameter values. Simulated data was calculated at the temperatures used in the collection of experimental data, at ten second intervals for the length of the experimental enzyme reactor run. Simulated rate data was then determined from the simulated time courses of product formation. The resulting simulated reaction rate data was graphed and compared to the experimental data as per section 2.1.4.

Simulated initial rate data was determined only if the simulated 3D plot of activity/ time and temperature did not fit to the experimental 3D plot of activity/ time and temperature. Simulated initial rate data was determined by MicroMath® Scientist® software by applying calculated initial rate parameters to the initial rate equation of the Equilibrium Model (equation 2.2).

2.3 RNase A

As stated in section 1.9, RNase A is an unusual enzyme as it so readily renatures and as a result may not obey typical variations in activity with temperature and therefore may not follow predictions made by the Equilibrium Model. However deviations from hyperbolic kinetics have been published using the substrate C>p due to the catalytic properties of the enzyme being modified as a function of the sequential binding of C>p to different subsites of RNase A (Moussaoui et al., 1998).

Assay method

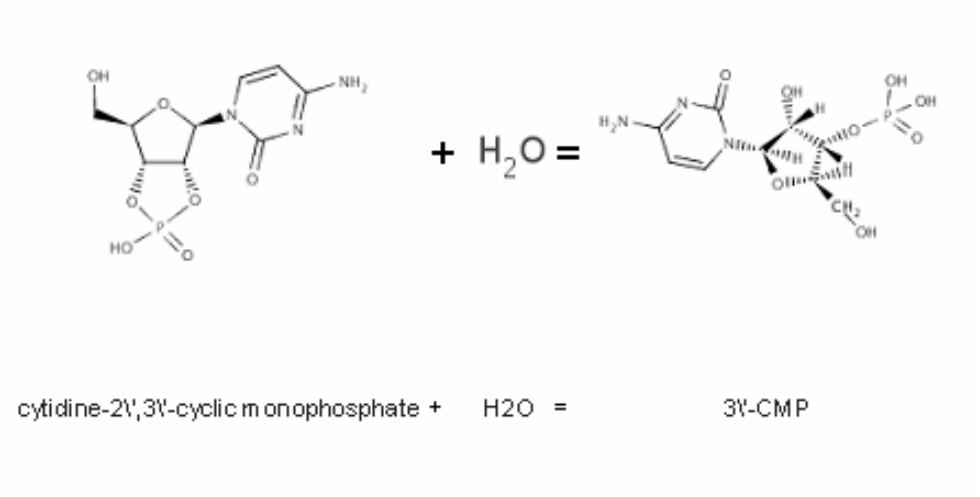

Figure 2.8: Hydrolysis reaction catalyzed by pancreatic ribonuclease (3.1.27.5) (http://www.brenda-enzymes.info)

Two methods were used to assay the activity of bovine pancreatic ribonuclease: one according to papers by (Crook et al., 1960; Blackburn, 1979; Benčina et al., 2007) and one according to papers by Fujii, Tanimizu and Moussaoui (Fuji et al., 2002; Moussaoui et al., 1998; Tanimizu et al., 2002), the difference being the buffers used and wavelength at which the reaction is monitored.

Materials

Ribonuclease A (E.C 3.1.27.5) from bovine pancreas and Cytidine 2':3'-cyclic monophosphate monosodium salt were purchased from Sigma-Aldrich. 50mM Tris-HCl pH 7.5 containing 2mM EDTA and 0.1M NaCl and 0.2M sodium acetate buffer pH 5.5 at 25°C were made using reagent grade materials available through recognised chemical suppliers.

Procedure

Reagents

62mM Cytidine 2':3'-cyclic monophosphate

50mM Tris- HCl pH 7.5 containing 2mM EDTA and 0.1M NaCl

0.2M sodium acetate buffer pH 5.5 @ 25°C

15mg/mL Ribonuclease A

Assay technique

To a 500µL quartz cuvette 440µL buffer (Tris- HCl or sodium acetate) and 50uL 62mM C>p were added and equilibrated to the desired temperature, the reaction was initiated by the addition of 10uL 15mg/mL enzyme. According to the assay method published by Crook, Blackburn and Bencina the buffer used was 50mM Tris- HCl pH 7.5 containing 2mM EDTA and 0.1M NaCl, the reaction was monitored at 288nm, under these conditions C>p has an extinction coefficient of 1308 $M^{-1}\bullet cm^{-1}$ and a K_M at 25°C of 0.62mM. The assay method published by Fujii, Tanimizu and Moussaoui uses 0.2M sodium acetate buffer pH 5.5, the reaction was monitored at 296nm. Under these conditions C>p has an extinction coefficient of 516.4 $M^{-1}\bullet cm^{-1}$ and a K_M at 25ºC of 0.62mM. The method published by Fujii, Tanimizu and Moussaoui was adopted due to poor results collected using the method published by Crock, Blackburn and Bencina. Assays were performed over the temperature range of 25-65ºC.

2.4 Ak. 1 Protease; Native and DTT Treated

Structural analyses have revealed the presence of a disulfide bond within the active-site cleft of native Ak. 1 protease, this bond has a dual role of maintaining substrate

binding cleft integrity and of increasing thermostability of the protease (Smith et al., 1998). The rationale for this work is that the molecular basis of the Equilibrium Model is suspected to be conformational changes at the active site (Daniel et al., 2008), so that cleavage of the active site disulfide bond may be a useful probe of the Equilibrium Model mechanism.

Dithiothreitol (DTT) is a very strong reducing agent and is frequently used to reduce disulfide bonds of proteins and more generally to prevent intramolecular and intermolecular disulfide bonds from forming between cystine residues of proteins (Cleland, 1964). DTT treated A.k 1 protease will therefore not have the disulfide bond within the active-site cleft present and is expected to have a substrate binding cleft of lower integrity and overall lower thermostability when compared to the native enzyme.

Assay method

Activity of native and DTT treated A.k 1 protease towards the synthetic pNA-linked peptide substrate suc-ala-ala-ala-pNA was analysed using the method of Toogood et al. (2000).

Materials

Ak. 1 protease was produced and purified from *Escherichia Coli* clone PB5517 by Toogood, et al., (1998) according to the methods of MacIver et al. and Peek et al. (MacIver et al., 1994; Peek et al., 1993). Suc-ala-ala-ala-pNA was purchased from Bachem (Bubendorf, Switzerland), 100mM HEPES/ NaOH buffer containing 5mM $CaCl_2$ pH 7.5 (at the appropriate temperature) and 100mM DTT were made using reagent grade materials available through recognised chemical suppliers.

Procedure

Reagents

100mM HEPES/ NaOH buffer containing 5mM $CaCl_2$, pH 7.5

22.5mM Suc-ala-ala-ala-pNA

100mM DTT

0.726mg/ml A.k 1 protease

Assay technique

Control and DTT treated protease were prepared by incubating 450µL 0.726mg/ml A.k 1 protease with either 50µL buffer or 50µL 100mM DTT for an hour at room temperature and then diluting 1 to 1 with buffer. In a 2mm path length quartz cuvette 395µL of 22.5mM Suc-ala-ala-ala-pNA was equilibrated to the desired temperature, the reaction was initiated by the addition of 5µL control or DTT treated A.k 1 protease, the reaction was monitored at 400nm for 3 minutes with a data point collected every second, over the temperature range of 40- 96°C. Under these conditions Suc-ala-ala-ala-pNA had a calculated extinction coefficient of 10976.9 $M^{-1} \bullet cm^{-1}$.

Chapter Three

The Implications of the Equilibrium Model for the Prediction of Enzyme Reactor Performance

---

Preface

This chapter deals with the collection and analysis of experimental enzyme reactor data to which simulated data calculated by the Equilibrium Model is fitted and compared. This paper is to be submitted to the journal "Enzyme and Microbial Technology".

Abstract

Enzyme reactors are used within the biotechnology industry for the production of desirable products of enzyme catalysis. The effects of temperature on enzyme activity makes enzyme reactor operation a very cost sensitive process, with the prediction of enzyme reactor operation being desirable for reactor optimisation.

Traditionally the effects of temperature on enzymes have been understood in terms of activation energy and thermal stability. The Equilibrium Model introduces a further two temperature dependant parameters which describe the temperature dependence of a rapidly reversible active-inactive enzyme transition. It has been developed to fully explain the effects of temperature on enzyme activity, simulations based on the Equilibrium Model have predicted unsuspected effects of temperature on enzyme reactor operation. The experimental work described here confirms these predictions, showing that the fastest reactor rates are not achieved at the highest operating temperature.

1. Introduction

Enzymes are required to be both flexible and stable molecules in order to function, with the delicate balance between enzyme flexibility and stability affected by variations in temperature [1-3]. This is because increases in temperature produces opposite affects on enzyme activity by simultaneously increasing reaction velocity [4] and inactivation rate [5,6]. Until recently the effects of temperature on enzyme activity was regarded as being a two-state system based on these two effects, and characterized by the Arrhenius activation energy of the catalytic reaction, $\Delta G^{\ddagger}_{cat}$, and the free energy of activation of the thermal denaturation process, $\Delta G^{\ddagger}_{inact}$ [7-9].

The enzyme temperature optima arising from these processes was at one time thought to be a characteristic of the enzyme, only to be later discredited as an ill- defined quality of limited value [10,11] due to temperature optimum being dependant on assay duration and arising from an unknown mixture of thermal stability and temperature coefficient [8,9]. More recently some enzymes have been observed to display lower activity at some point in their temperature profile at high temperatures that can be accounted for by irreversible denaturation [12-14], prompting a reappraisal of the two-state "Classical" system.

The Classical description of the effects of temperature on enzyme activity is described by the temperature dependence on enzyme reaction rate and thermal denaturation, defined by $\Delta G^{\ddagger}_{cat}$ and $\Delta G^{\ddagger}_{inact}$ respectively. This model proposes that in functional terms the enzyme exists in two species, the active form of the enzyme (E_{act}) and the thermally denatured state [8,9,15,16].

$$E_{act} \longrightarrow X$$

Figure 1C displays the simulated variation in reaction velocity with time and temperature calculated from the Classical Model, using experimental phenylalanine ammonia lyase data [7]. The simulated data in figure 1C displays an apparent temperature optima that decreases with increasing time, but at zero time (i.e. under initial rate conditions) no temperature optima exists [8]. The experimental data for phenylalanine ammonia lyase in figure 1A does not match the result expected from the Classical Model [7].

The recently developed and experimentally validated Equilibrium Model proposes that the enzyme exists in three species, one active enzyme form, one inactive enzyme form and one thermally denatured form [15,16]. The active form of the enzyme (E_{act}) is in reversible equilibrium with an inactive form (E_{inact}), which undergoes thermal denaturation to the thermally denatured state [15].

$$E_{act} \overset{K_{eq}}{\longleftrightarrow} E_{inact} \longrightarrow X$$

By assuming the reaction mechanism proposed by the Equilibrium Model a thermal buffer exists, through the equilibrium between E_{act} and E_{inact} , that protects the enzyme from thermal inactivation. The $E_{act,}$ E_{inact} equilibrium acts as a mechanism, separate from and additional to denaturation, by which enzyme activity decreases as the temperature is raised [15].

The Equilibrium Model is defined by four thermal parameters, $\Delta G^{\ddagger}_{cat}$, $\Delta G^{\ddagger}_{inact}$, ΔH_{eq} and T_{eq} [15,16]. ΔH_{eq} is the enthalpic change associated with the conversion of the active enzyme to the inactive form and T_{eq} is the temperature at which the concentration of the active and inactive forms of the enzyme are equal (K_{eq}= 1 and

ΔH_{eq}=0). K_{eq} is therefore a new temperature dependant property of the enzyme [15,16].

Figure 1B displays the variation in reaction velocity with time and temperature according to the Equilibrium Model, determined from experimental phenylalanine ammonia lyase data [7]. The simulated data presented in figure 1B fits the experimental data of phenylalanine ammonia lyase**,** presented in figure 1A [7]. Figure 1B shows an apparent temperature optima that decreases with increasing time during the assay. One major difference from the Classical Model is that here a temperature optima exists at zero time (i.e. under initial rate conditions), this enables a clear experimental distinction between the Classical and Equilibrium Models [8].

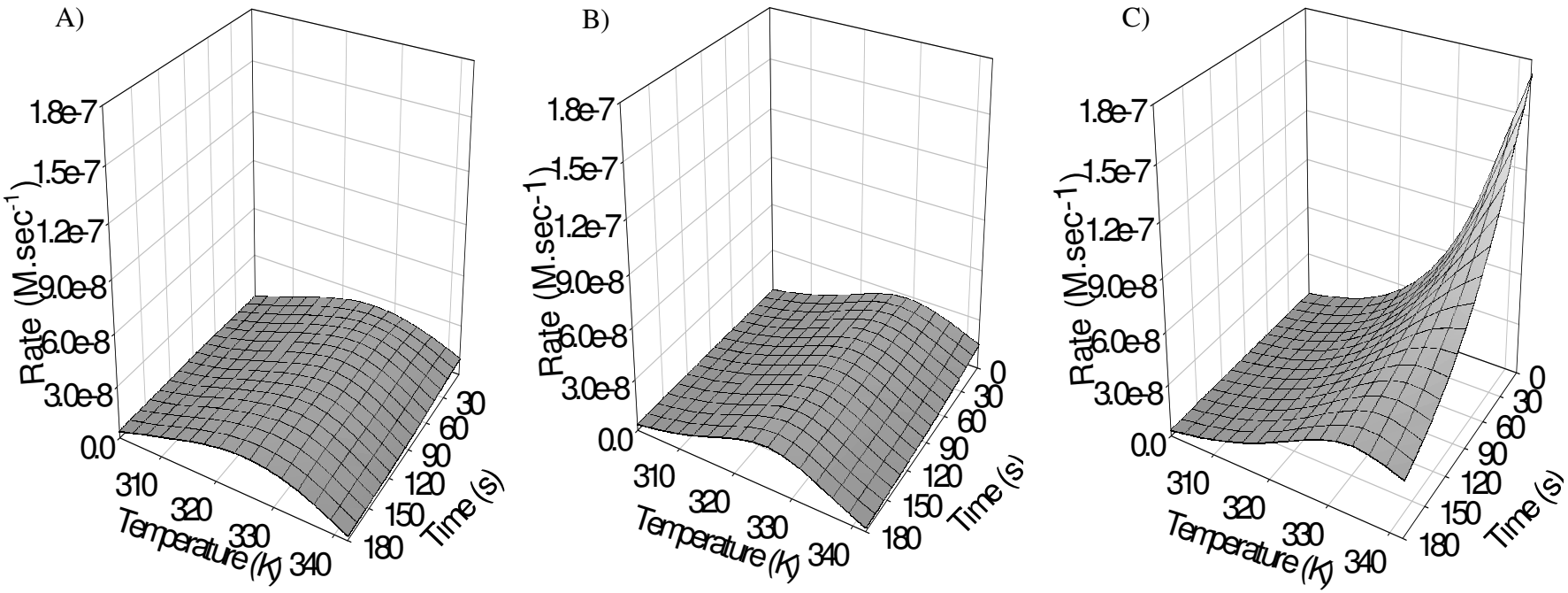

Figure 1: The temperature dependence of enzyme activity. The plots of rate (M.sec^{-1}) versus temperature (K) versus time (s) illustrate the effect of temperature on enzyme activity. A) Experimental phenylalanine ammonia lyase data. B) Simulated phenylalanine ammonia lyase data calculated by the Equilibrium Model. C) Simulated phenylalanine ammonia lyase data calculated by the Classical Model ($\Delta G^{\ddagger}_{cat}$ = 80 kJmol^{-1}, $\Delta G^{\ddagger}_{inact=}$ 97 kJmol^{-1}, T_{eq} = 330 K and $\Delta H^{\ddagger}_{eq}$ = 181 kJmol^{-1}) [7].

The way that enzymes respond to temperature is fundamental to many areas of biotechnology. A major biotechnological application of the Equilibrium Model is the prediction of enzyme reactor operation [17]. Since the Equilibrium Model is a more complete and accurate description of the effect of temperature on enzymes, its use should enable more accurate modeling of the effect of time and temperature upon enzyme reactor output. A theoretical treatment has already shown that results obtained using the Equilibrium Model are quite different from those obtained using the Classical Model [17].

In the following paper experimental data using a small scale enzyme reactor was collected and applied to the Equilibrium Model. Thermal parameters and simulated data according to the Equilibrium Model were calculated from the experimental data, 3D plots showing the variation of reaction rate with time and temperature of experimental and simulated data were constructed and comparisons made to determine how well the Equilibrium Model predicted enzyme reactor performance.

2. Materials and Methods

The methods used for the collection and processing of data for the Equilibrium Model were in general terms those described by Peterson et al [8].

2.1. Materials

Penicillin G Amidase (EC 3.5.1.11) (ammonium sulfate suspension and immobilized on Eupergit® C) from *Escherichia Coli* and Alkaline Phosphatase (EC 3.1.3.1) (50% glycerol with 5mM $MgCl_2$ and 0.1mM $ZnCl_2$ solution and immobilized on acrylic beads in ammonia sulphate suspension) from calf intestinal mucosa were purchased

from Sigma-Aldrich. The colorimetric substrates 6-nitro-3-phenylacetamido benzoic acid (NIPAB) and *p*-nitrophenyl phosphate (*p*-NPP) were purchased from Sigma-Aldrich. All other chemicals used were of analytical grade.

2.2. Enzyme Reactor Conditions

Enzyme reactor progress curves (absorbance versus time) were collected for each form of each enzyme, at each temperature in triplicate, with at least eight temperature points used and at least three temperature points above T_{eq} [8]. The reactions were repeated if the slope of the triplicates varied by more than 10%. Substrate concentrations were maintained at ten times K_M throughout the reaction, to ensure enzyme operation at V_{max}. To prevent loss of the enzyme onto walls of the cuvette all stock enzyme solutions contained 0.1% Triton X-100, a non-ionic detergent. pH was kept constant by a suitable buffer, adjusted to the appropriate pH of the assay temperature using a combination electrode.

Stirred, 3.5mL Quartz cuvettes were used in all experiments for their relatively quick temperature equilibration and their heat retaining capacity. At high reactor operation temperatures (above 60ºC) evaporation of cuvette contents and heat loss during circulation was minimised by fitting a cuvette cap and an insulation block around the cuvette holder.

Enzyme reactor reactions were initiated by the rapid addition of minimal amounts of chilled enzyme, so that enzyme addition had no significant effect on the temperature of the solution inside the cuvette.

2.3. Enzyme Reactor Operation

All enzyme reactor experiments were carried out directly within a spectrophotometer, with a data point collected every second for one hour.

Penicillin Amidase activity was measured by following the hydrolysis of NIPAB at 380nm (ε= 11600$M^{-1}\bullet cm^{-1}$) [18-21], over the temperature range of 25-60ºC. Reaction mixtures contained 3140µL sodium phosphate buffer pH 7.4, *I*=0.2M, 350µL 1.5mM NIPAB and 10µL of either 0.01mg/mL free enzyme or 25mg/mL immobilized enzyme.

Alkaline Phosphatase activity was measured by following the phenol released from *p*-NPP at 405nm (ε= 0.0182$M^{-1}\bullet cm^{-1}$) [22], over the temperature range of 25-60ºC. Reaction mixtures contained 3115µL 1M Diethanolamine buffer pH 9.8 containing 0.5mM $MgCl_2$, 350µL 0.05M *p*-NPP and either 15µL 0.0015% free enzyme or 35µL 0.0.125% immobilized enzyme [23,24].

As a control for possible temperature-induced non-enzymic catalysis of the reaction blank runs containing no enzyme were performed at each temperature.

2.4. Instrumentation

All enzyme activities were measured using a Thermospectronic™ Helios γ-spectrophotometer equipped with a Thermospectronic™ single cell peltier-effect cuvette holder. This system was networked to a computer installed with Vision32™ (Version 1.25, Unicam Ltd) software including the Vision Enhanced Rate Programme.

2.5. Temperature Control

The temperature of each enzyme reactor run was recorded directly using a Cole-Parmer Digi-Sense® thermocouple thermometer accurate to ± 0.1% of the reading and calibrated using a Cole-Parmer NIST (National Institute of Standards and Technology)-traceable high-resolution glass thermometer. The temperature probe was placed inside the cuvette adjacent to the light path during temperature equilibration before the initiation of the reaction and again immediately after completion of each enzyme reaction. Temperature gradients within the cuvette were checked for by taking temperature measurements at the top and bottom of the cuvette. Where the temperature measured before and after the reaction differed by more than 0.1°C, the reaction was repeated.

2.6. Protein Determination

Protein concentrations were determined by the Bradford Method using Bovine Serum Albumin (BSA) standards. A modified Bradford assay was used for the determination of immobilized enzyme concentration, due the binding of the Bradford reagent to both the protein and the immobilization support. The modified Bradford assay involved dissociation of the protein and standards by incubation with 1M NaOH overnight at room temperature, effectively removing the protein from the immobilization support and allowing the concentration of the dissociated protein to be determined.

2.7. Data Treatment

Construction of 3D Plots from Experimental Data

For each enzyme product concentration was calculated according to the Beer-Lambert Law from absorbance values and the rate of the reaction in terms of product formation then calculated. The entire data set containing a data point every second was then filtered using Microsoft® Office Excel to obtain a data set of a more manageable size, containing a data point at 10 second intervals. The filtered data set containing Time in seconds, Temperature in Kelvin and Rate in M^{-1}•second, was then input into SigmaPlot® 2001 for Windows™, Version 7.101, SPSS Inc where a Loess algorithm was used to smooth the data and construct the 3D plots of experimental rate data against time and temperature.

Determination of Parameters associated with the Equilibrium Model

Values for the parameters $\Delta G^{\ddagger}_{cat}$, $\Delta G^{\ddagger}_{inact}$, ΔHeq, Teq were determined using a stand-alone Matlab® [version 7.1.0.246 (R14) Service Pack 3; Mathworks] (*available on CD from R.M.D.), from a Microsoft® Office Excel file of experimental progress curves (product concentration against time). Initial parameter estimates of 80 kJ • mol^{-1} ($\Delta G\ddagger_{cat}$), 95 kJ • mol^{-1} ($\Delta G\ddagger_{inact}$), 100 kJ • mol^{-1} (ΔH_{eq}) and 320 K (T_{eq}) were input into the Matlab application, along with the concentration of protein in each assay (mol • l^{-1}).

Two sets of high resolution parameters were calculated for each form of both enzymes, one called the 3 minute parameters which were calculated from the first 3

(*available on request from Charles Lee (cklee@waikato.ac.nz) or Roy Daniel (r.daniel@waikato.ac.nz)).

minutes of unfiltered enzyme reactor data and one called the 1 hour parameters which were calculated from the filtered data of the entire data set.

Calculation of Simulated Data

One hour of simulated product formation with time and temperature data was calculated according to the Equilibrium Model from determined parameter values using MicroMath® Scientist® for Windows software (version 2.01, MicroMath Scientific Software). Simulated data was calculated at the temperatures used in the collection of experimental data, at ten second intervals for 1 hour, the length of the experimental enzyme reactor run. Simulated reaction rate data was determined from the simulated time courses of product formation. Simulated rate data was graphed in the same way as the experimental data using SigmaPlot® [16].

3. Results and Discussion

The overall dependence of enzyme catalysed reaction velocity on temperature with time can be described by the Equilibrium Model by the relationship,

$$rate = \frac{k_{cat} E_0 e^{-\frac{k_{inact} K_{eq} t}{1+K_{eq}}}}{1+K_{eq}}$$

Where:

$$k_{cat} = \frac{k_B T}{h} e^{-\frac{\Delta G^*_{cat}}{RT}} \quad k_{inact} = \frac{k_B T}{h} e^{-\frac{\Delta G^*_{inact}}{RT}} \quad K_{eq} = e^{\frac{\Delta H_{eq}}{R}\left(\frac{1}{T_{eq}} - \frac{1}{T}\right)}$$

k_{cat} is the enzymes catalytic constant, E_0 is the total concentration of the enzyme, k_{inact} is the enzymes thermal inactivation rate constant, K_{eq} is the equilibrium constant between active and reversibly inactive forms of the enzyme, t is time, k_B is Boltzmann's constant, h is Planck's constant, ΔG^*_{cat} is the free energy of activation of the catalytic reaction, ΔG^*_{inact} is the free energy of activation of the thermal denaturation process, T is the absolute temperature and R is the gas constant [9,16].

Errors

The standard deviation values output by the Matlab application refer to the fit of the data to the model. On the basis of the variation between the individual triplicate rates from which the parameters are derived for all the enzymes assayed so far, it has been found that the experimental errors in the determination of $\Delta G‡_{cat}$, $\Delta G‡_{inact}$, and T_{eq} are less than 0.5%, and less than 6% in the determination of ΔH_{eq} [8].

Eisenthal et al. [17] have shown that on theoretical grounds enzyme reactor operation obeying the Equilibrium Model display quite different, and under some circumstances quite counter intuitive, product formation curves with varying time and temperature, than that for the Classical Model, as shown in figure 2. It was observed from simulated data obeying the Equilibrium Model, that when T_{eq} exceeds the working temperature of the reactor (figure 2B), the catalysed reaction occurs faster as the temperature is raised, but also the more unstable the enzyme, as expected, and not so different from what would be expected from the Classical Model (Figure 2C). However, when the working temperature of the reactor exceeds T_{eq} (figure 2A) the opposite was seen, where the rate of the catalysed reaction decreases as the temperature is raised. Thus the Equilibrium Model could allow more accurate prediction of enzyme reactor performance over a wider range of temperatures. Figure 2C shows the time courses of product formation at various temperatures, as predicted by The Classical Model.

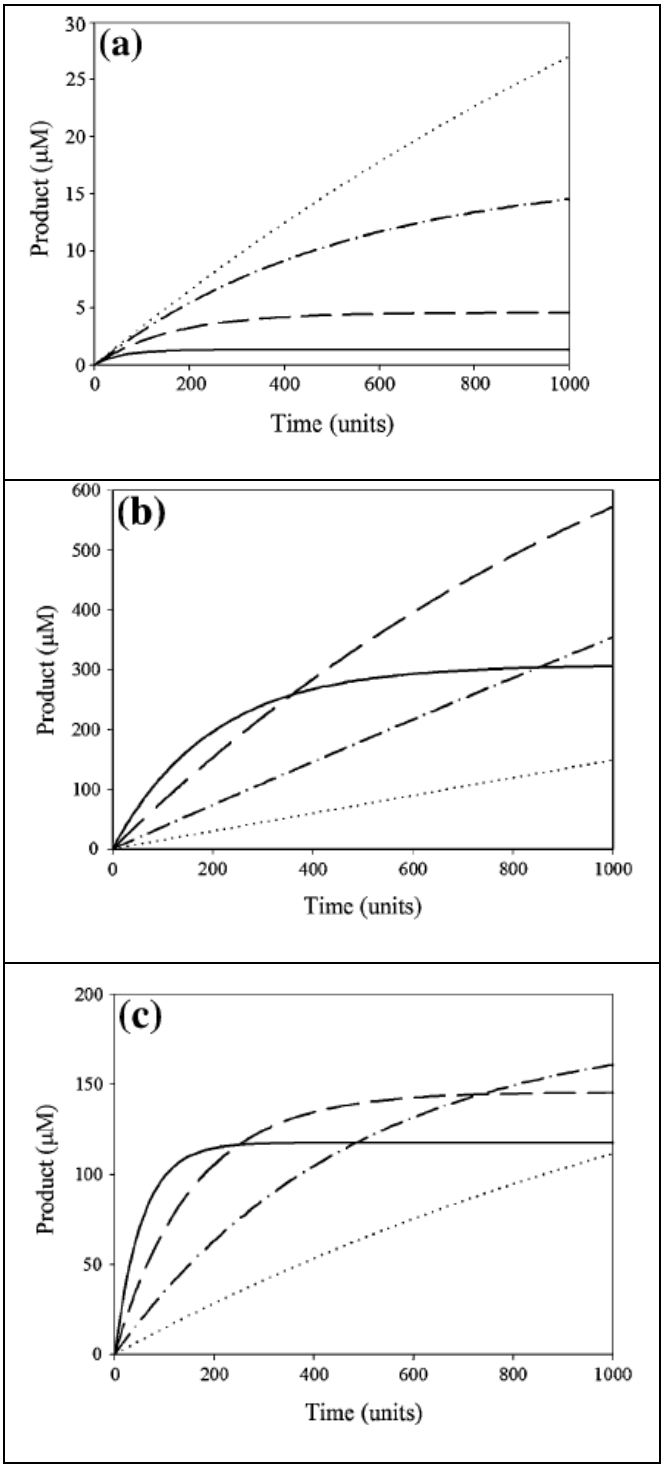

Figure 2: The effect of T_{eq} on time courses of product concentration simulated at various temperatures: 310 K (.....); 320 K (– · – · -); 330 K (– – –); 340 K (——). a) Equilibrium Model (T_{eq} = 300 K) b) Equilibrium Model (T_{eq} = 350 K) c) Classical Model (other parameter values: $\Delta G^{\ddagger}_{cat}$ = 75 kJ mol^{-1}, $\Delta G^{\ddagger}_{inact}$ = 95 kJ mol^{-1} $\Delta H^{\ddagger}_{eq}$ = 95 kJ mol^{-1}) [17].

3.1 Penicillin Amidase Results

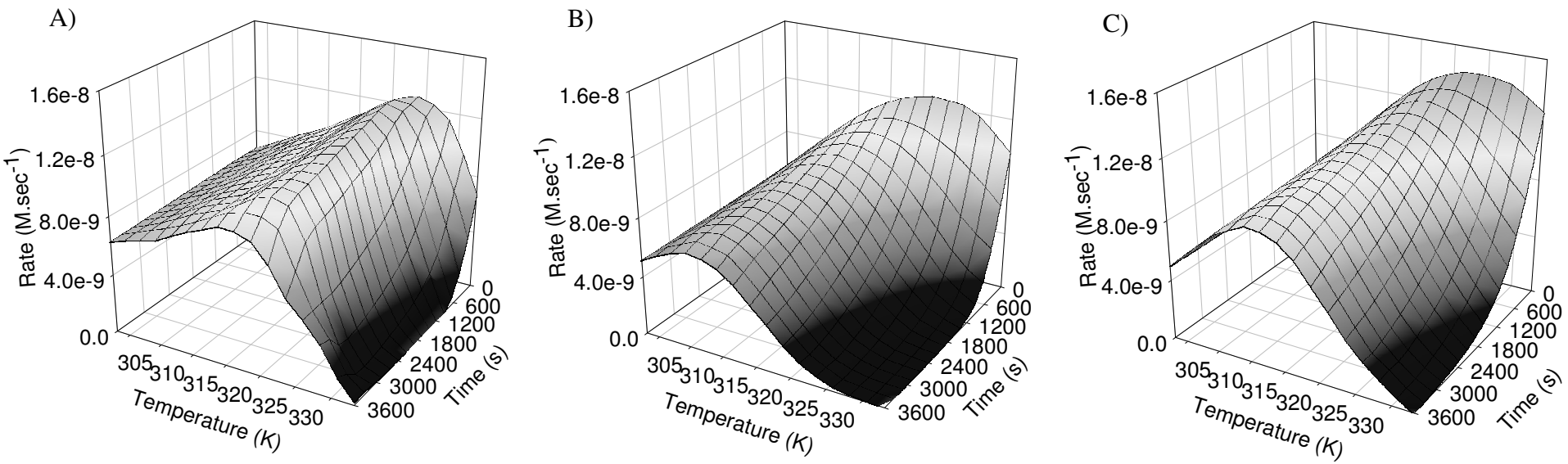

Figure 3: Free penicillin amidase enzyme reactor results. A) Experimental data B) Simulated data calculated from 3 minute parameters C) Simulated data calculated from 1 hour parameters.

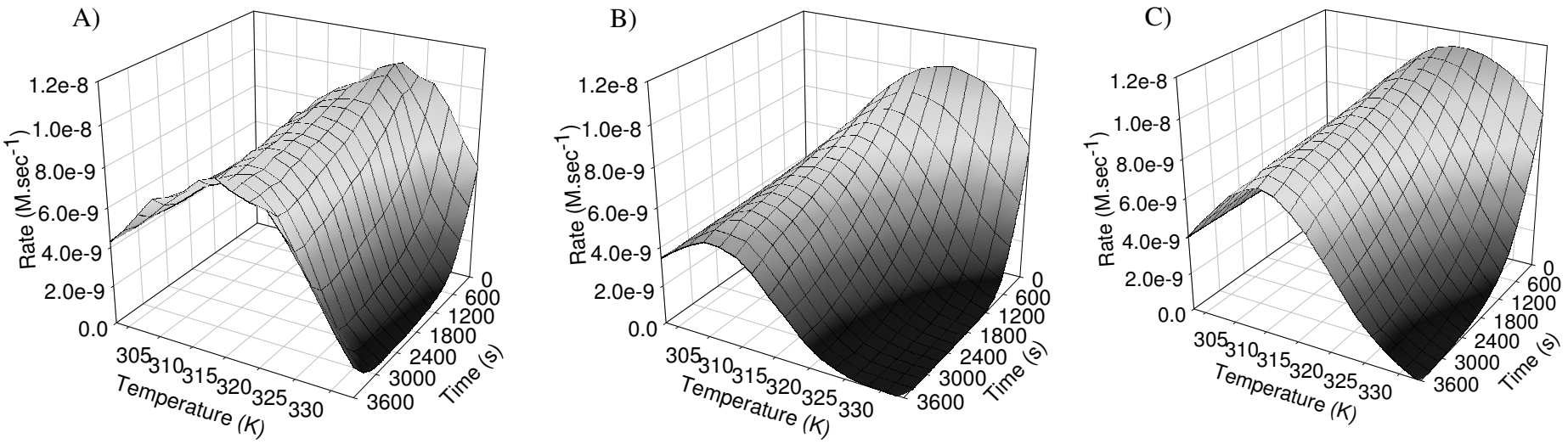

Figure 4: Immobilized penicillin amidase enzyme reactor results. A) Experimental data B) Simulated data calculated from 3 minute parameters C) Simulated data calculated from 1 hour parameters.

The experimental and simulated data of free penicillin amidase (figure 3A and B) display “tent” type graphs typical of the Equilibrium Model with a temperature optimum at time zero, Classical Model-like behaviour where no temperature optima at time zero exists is not seen. The overall shape and trends of the data simulated from parameters derived by fitting experimental data to the Equilibrium Model are a good fit to that of the experimental data, meaning that the Equilibrium Model has estimated well the effects of temperature on the activity of free penicillin amidase within the enzyme reactor. Thus, as expected, free penicillin amidase does follow the Equilibrium Model. The simulated data calculated from the one hour parameters predicts the rate of the catalytic reaction, the rate of denaturation and optimum enzyme activity better than data simulated from the three minute parameters, this data is therefore a better fit to the experimental. This is also seen with the immobilized enzyme in figure 4.

Immobilized penicillin amidase also follows the Equilibrium Model, with both the plots simulated from parameters derived by fitting experimental data to the Equilibrium Model being a good fit to the experimental data, as seen in Figure 4. The Equilibrium Model has estimated well the effects of temperature on the activity of immobilized penicillin amidase within the enzyme reactor. Data simulated from one hour parameters is a better fit to the experimental data than that from the 3 minute parameters. In particular, as might be expected the one hour plot gives a better fit in respect of longer term denaturation and optimum catalytic activity. Overall the shapes and trends of figures 4A, B and C are similar to each other.

Enzyme	Length of Experimental data used (s)	T_{eq} K	$\Delta G^{\ddagger}_{cat}$ kJ•mol^{-1}	$\Delta G^{\ddagger}_{inact}$ kJ•mol^{-1}	ΔH_{eq} kJ•mol^{-1}
Free Penicillin Amidase	180	309	71.4	97.4	86.9
Free Penicillin Amidase	3600	314	71.9	99.5	98.5
Immobilized Penicillin Amidase	180	309	78.1	97.8	109
Immobilized Penicillin Amidase	3600	310	78.1	100	108

Table 1: Thermodynamical parameters of penicillin amidase from *Escherichia Coli;* calculated by the Equilibrium Model from experimental data.

The thermodynamical parameters calculated for penicillin amidase show that the free and immobilized enzyme have similar T_{eq} values, with the exception of the T_{eq} calculated from 1 hour of free penicillin amidase experimental data being slightly higher. Immobilization raises $\Delta G^{\ddagger}_{cat}$, and there is more than one possible reason for this; the energy barrier of the catalytic reaction may be changed by immobilization, or immobilization may have caused some steric hindrance, the effect may also be due to the difficulties in quantifying the immobilized enzyme, which is known to effect $\Delta G^{\ddagger}_{cat}$ although not the other parameters [8]

Enzyme immobilization sometimes increases enzyme stability [25, 26], however any effect here is small and debatable, with similar $\Delta G^{\ddagger}_{inact}$ values of the free and immobilized enzyme with the largest differences being due to the difference in duration of the two data sets. The better fit of the simulated data from the 1 hour parameters to the experimental data is likely to be due to the slightly higher $\Delta G^{\ddagger}_{inact}$ values of the 1 hour parameters.

The slightly higher ΔHeq of the immobilized enzyme can be interpreted as the enathalpic change associated with the reversible active-inactive conversion of the enzyme being higher for the immobilized enzyme, with the catalytic activity of the immobilized enzyme being slightly more sensitive to temperature, however, it should be noted that the error values of ΔHeq are higher than for the other parameters, as previously stated [8].

To determine whether the simulated data obeying the Equilibrium Model followed the observations published by Eisenthal et al., product formation curves with varying time and temperature, such as those in figure 2, were constructed. To display the effect of T_{eq} on time courses of product concentration a set of two product formation curves with varying time and temperature were constructed from each batch of parameter values, one containing temperatures below T_{eq} and one containing temperatures above T_{eq}.

Similar graphs showing the variation in product formation with temperature and time were constructed from experimental data, two graphs were also constructed, one displaying the increase in experimental reaction rate with increasing temperature up to a maximum rate and one displaying the decrease in reaction rate with increasing temperature down from a maximum rate. According to simulated data of the Equilibrium Model and Eisenthal et al.'s observations T_{eq} should be a good predictor of maximal enzyme reactor performance.

Figure 5A shows that simulated product formation of free penicillin amidase calculated from the 1 hour parameters increases with increasing temperature up to the maximum rate observed at 313 K, the temperature point closest to T_{eq}. This behaviour was also seen with data simulated from the 3 minute parameters (Appendix A figure

1). Figure 5B shows that as the temperature is increased above T_{eq} the rate of the catalytic reaction does not increase; therefore the simulated data displays the same behaviour observed by Eisenthal et al.

The experimental data displays similar behaviour, where the rate of the catalysed reaction increases with increasing temperature up to a point (figure 6A), where further increases in temperature above this point do not result in increasing reaction rates, even under initial reaction conditions. This point is shown on figure 6 to be 323 K, with the actual maximum rate being between 318 and 323 K. Therefore the 1 hour parameters T_{eq} value of 314 K, is a good estimate of maximal enzyme reactor performance. The T_{eq} of 309 of the 3 minute parameters is not such a good estimation of maximal enzyme reactor rate, this was expected due to the smaller amount of experimental data from which the parameters were calculated, this data is shown in appendix A.

Free Penicillin Amidase Simulated Product Formation Curves.

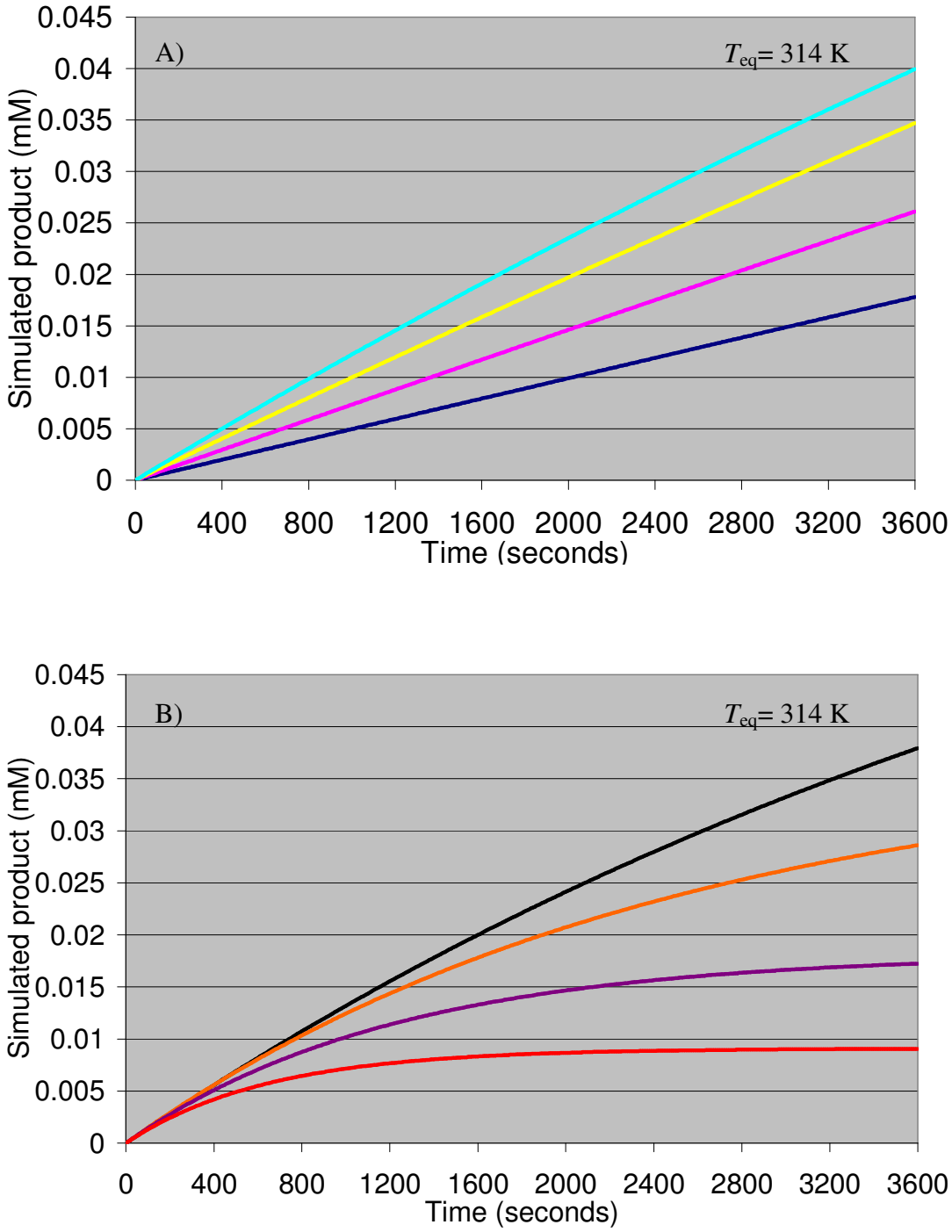

Figure 5: Free penicillin amidase simulated product formation, calculated from 1 hour parameters: 298 K (—); 303 K (—); 308 K (—); 313 K (—); 318 K (—); 323 K (—); 328 K (—); 333 K (—). A) T_{eq} exceeds reactor working temperature. B) Reactor working temperature exceeds T_{eq}.

Free Penicillin Amidase Experimental Product Formation Curves.

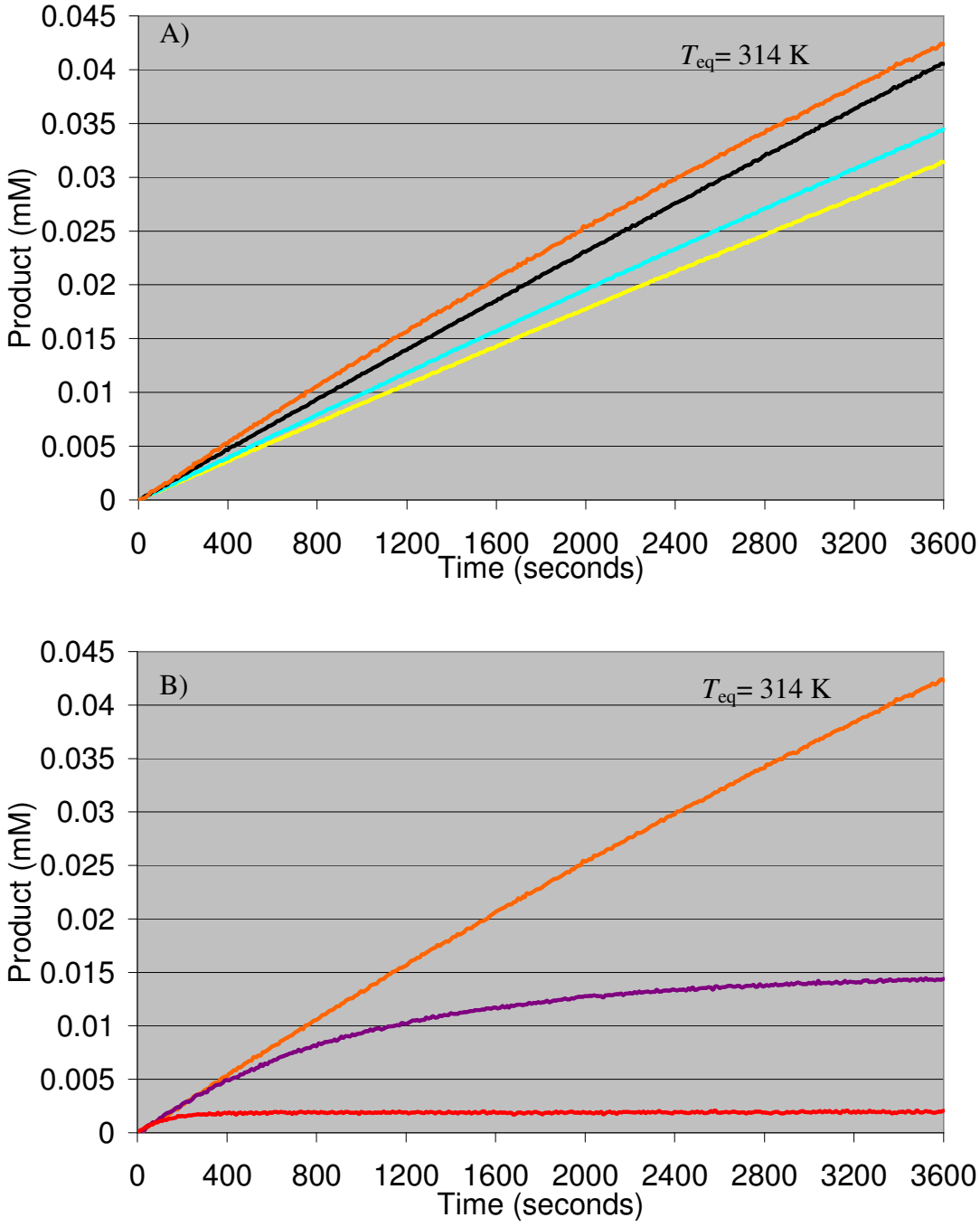

Figure 6: Free penicillin amidase experimental product formation: 308 K (—); 313 K (—); 318 K (—); 323 K (—); 328 K (—); 333 K (—). A) Increasing temperature causes increasing reaction rates B) Increasing temperature causes decreasing reaction rates.

The simulated and experimental data of immobilized penicillin amidase in Figures 7 and 8 display behaviour according to Eisenthal et al.'s predictions. Figure 7A shows that the simulated rate of product formation increases with increasing temperature up to a maximum rate, as the theoretical working temperature of the enzyme reactor is increased. The opposite of this is seen in figure 7B where the simulated rate of product formation decreases from a maximum rate with increasing temperature, as the theoretical working temperature of the enzyme reactor is increased. The maximum simulated rate observed is the temperature point closest to the calculated T_{eq} value of 308 K. Simulated product formation curves calculated from the 3 minute parameters are shown in appendix A figure 2.

This behaviour is also observed in the experimental data in figure 8, as the rate of product formation increases with increasing temperature up to a point (figure 8A), rates determined at temperatures above this point do not increase with increasing temperature, in fact they decrease as seen in figure 8B. The maximum rate observed from the experimental immobilized penicillin amidase enzyme reactor data is at 318 K.

318 K was also the temperature at which maximal product formation was experimentally observed for the one hour length of enzyme reactor operation for immobilized penicillin amidase, with the actual maximum point being between 318 and 323 Kelvin, as interpreted from figure 8. The T_{eq} value of 309 K is a good estimate of maximal enzyme reactor performance.

Immobilized Penicillin Amidase Simulated Product Formation Curves.

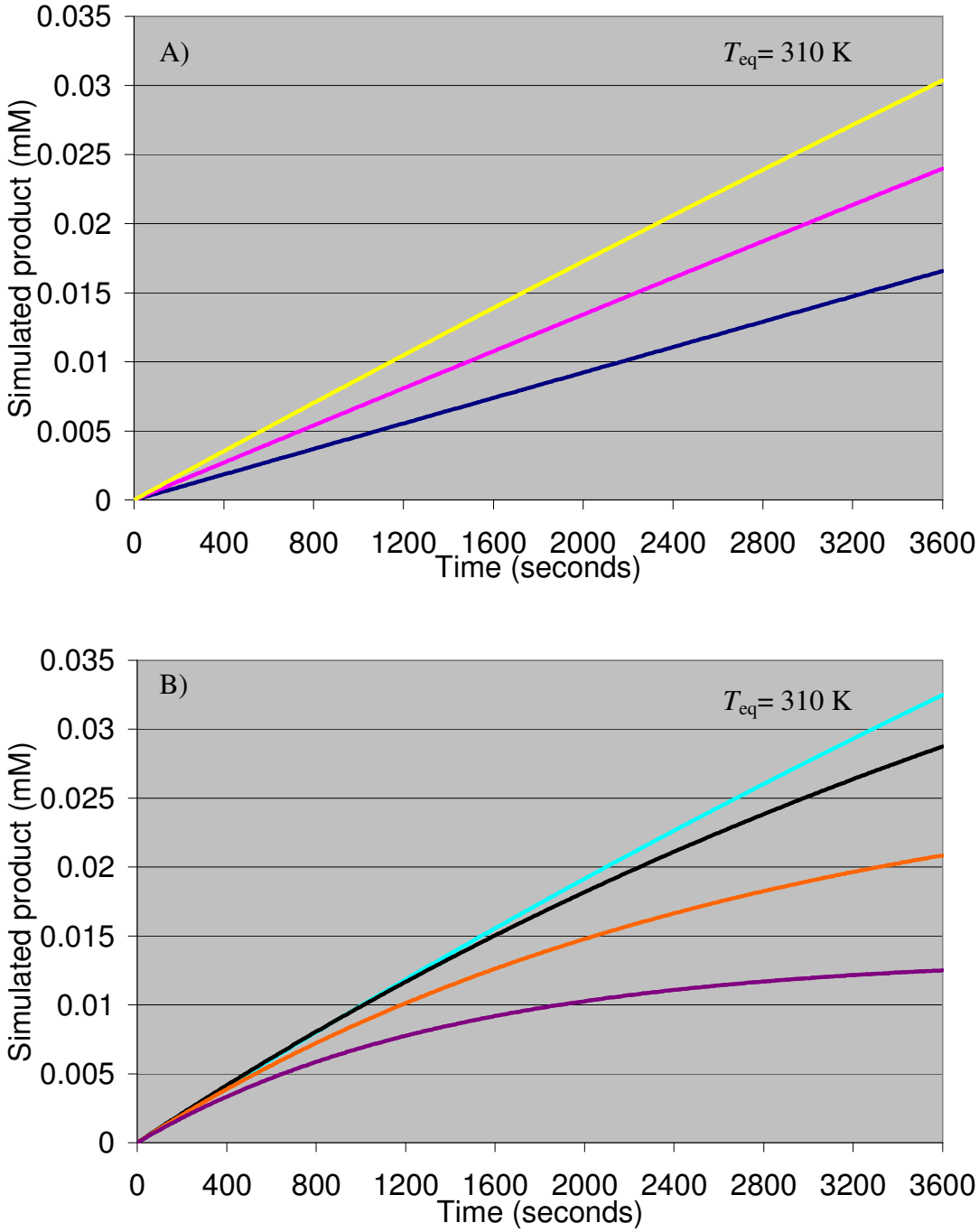

Figure 7: Immobilized penicillin amidase simulated product formation, calculated from 1 hour parameters: 298 K (—); 303 K (—); 308 K (—); 313 K (—); 318 K (—); 323 K (—); 328 K (—). A) T_{eq} exceeds reactor working temperature. B) Reactor working temperature exceeds T_{eq}.

Free Penicillin Amidase Experimental Product Formation Curves.

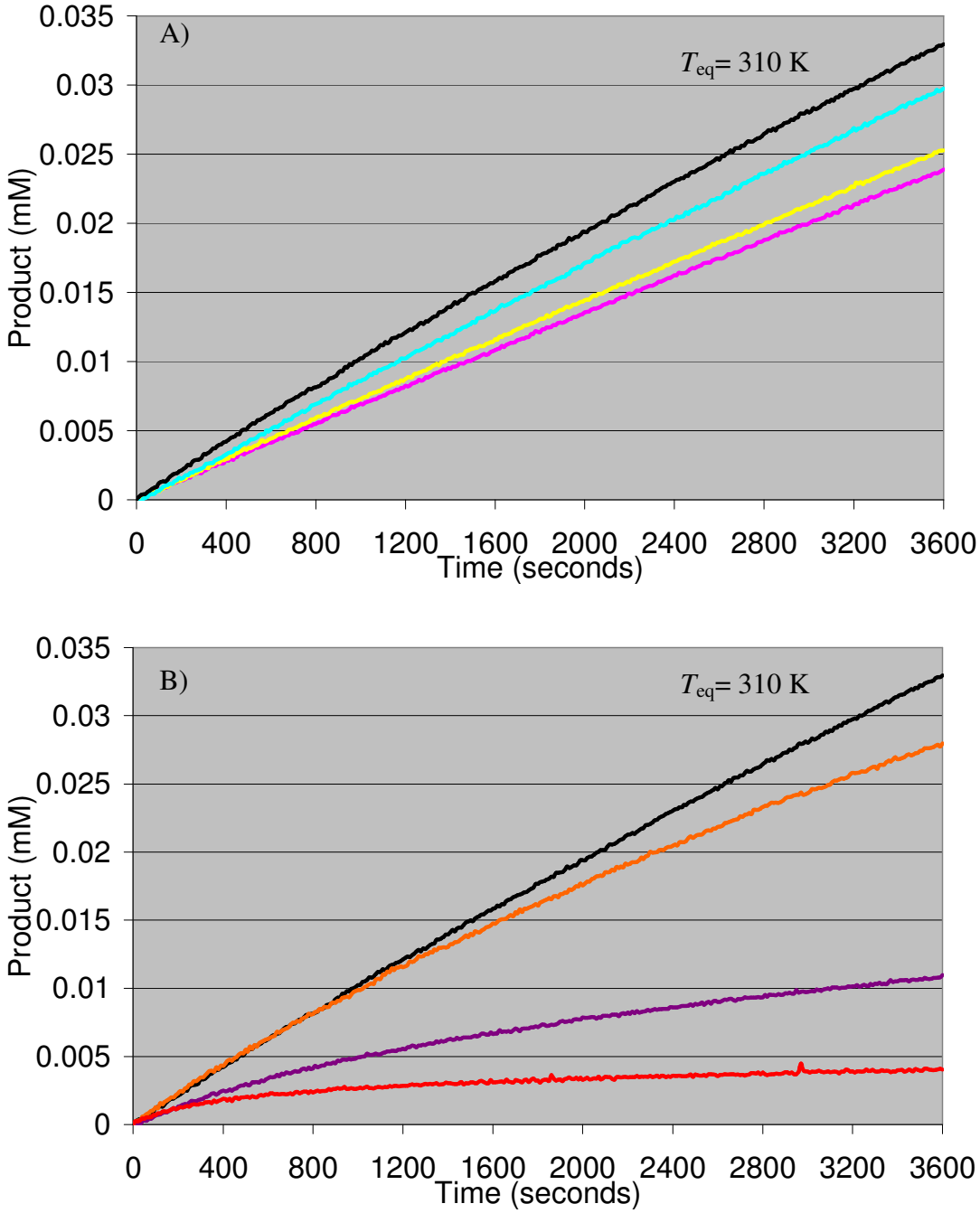

Figure 8: Immobilized penicillin amidase experimental product formation: 303 K (—); 308 K (—); 313 K (—); 318 K (—); 323 K (—); 328 K (—); 333 K (—). A) Increasing temperature causes increasing reaction rates B) Increasing temperature causes decreasing reaction rates.

3.2 Alkaline Phosphatase Results

The free and immobilized forms of alkaline phosphatase follow the Equilibrium Model as the experimental and simulated data of figures 9 and 10 display “tent” type graphs typical of the Equilibrium Model with a temperature optimum at time zero, Classical Model-like behaviour is not seen.

The overall shapes and trends of free alkaline phosphatase in figures 9A, B and C are similar, with both simulated plots giving a good fit to the experimental data. As seen for penicillin amidase, the simulated data calculated from the 1 hour parameters (figure 9C) is the best fit to the experimental data. Figure 9C predicts well the position of maximal enzyme activity and the rate of denaturation, less well predicted however is the rate of change of the catalytic reaction with temperatures below the optimum temperature.

The data for immobilized alkaline phosphatase also follows the Equilibrium Model, the Equilibrium Model has estimated well the effects of temperature on the activity of immobilized alkaline phosphatase within the enzyme reactor The simulated data calculated from the 3 minute parameters in figure 10B predicts well initial rates of the experimental data, but as expected does less well predicting the effects of temperature on enzyme activity for longer time courses. Simulated data calculated from 1 hour parameters does predict well the effects of temperature on the activity of immobilized alkaline phosphatase, with the rate of the upward and downward slopes of figures 10A and B being similar, however not well predicted is the rate of the reaction under initial conditions.

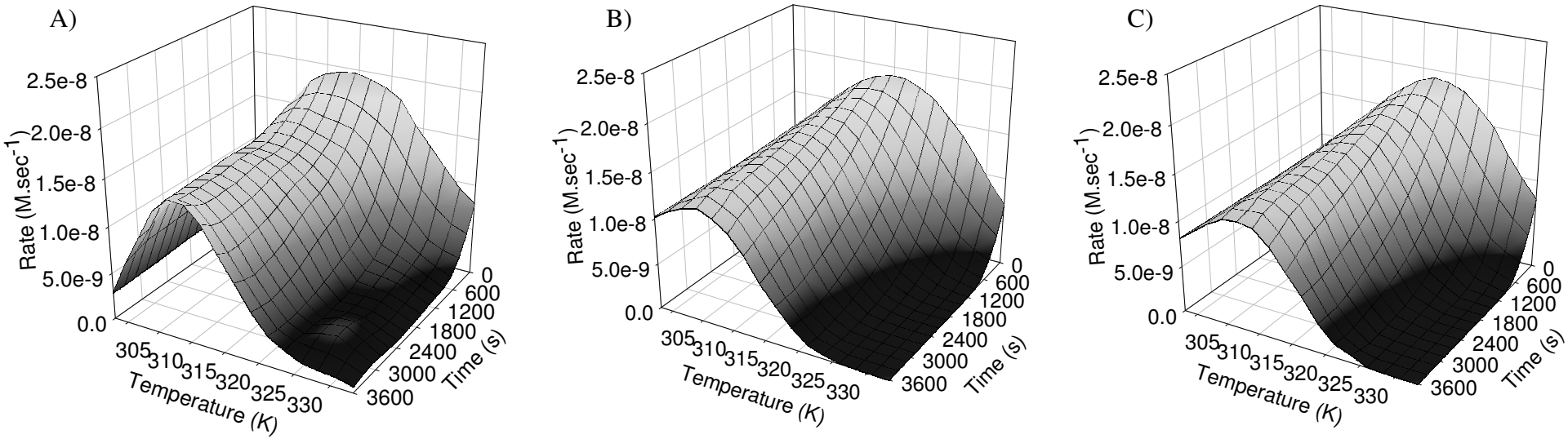

Figure 9: Free alkaline phosphatase enzyme reactor results. A) Experimental data B) Simulated data calculated from 3 minute parameters C) Simulated data calculated from 1 hour parameters.

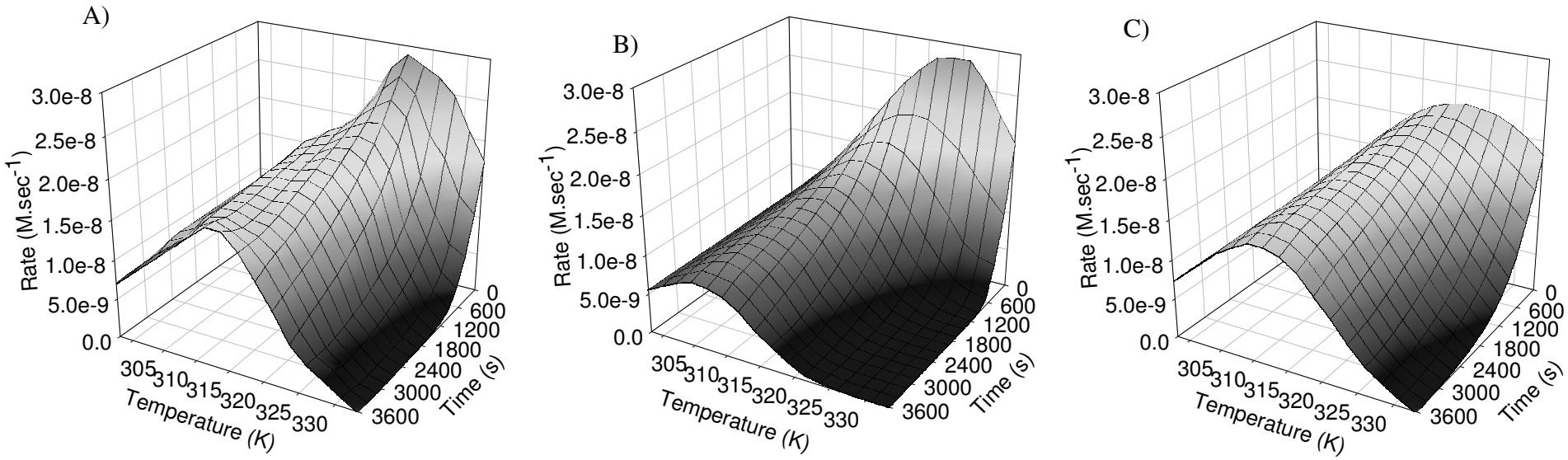

Figure 10: Immobilized alkaline phosphatase enzyme reactor results. A) Experimental data B) Simulated data calculated from 3 minute parameters C) Simulated data calculated from 1 hour parameters.

Enzyme	Length of Experimental data used (s)	T_{eq} K	$\Delta G^{\ddagger}_{cat}$ kJ•mol^{-1}	$\Delta G^{\ddagger}_{inact}$ kJ•mol^{-1}	ΔH_{eq} kJ•mol^{-1}
Free Alkaline Phosphatase	180	317	50.1	95.8	118.4
Free Alkaline Phosphatase	3600	320	50.8	95.9	143
Immobilized Alkaline Phosphatase	180	321	77.2	94.4	95.0
Immobilized Alkaline Phosphatase	3600	314	76.4	99.8	108

Table 2: Thermodynamical parameters of alkaline phosphatase from calf intestinal mucosa; calculated by the Equilibrium Model from experimental data.

The thermodynamical parameters calculated for alkaline phosphatase show that the free and immobilized enzyme have somewhat varying T_{eq} values. The immobilized penicillin amidase's 1 hour T_{eq} of 314 K implies a reduction in T_{eq} as a result of immobilization. The $\Delta G^{\ddagger}_{inact}$ values tend to show that the shorter time runs are predicting a lower enzyme stability than the longer runs (particularly for the immobilized enzyme where this effect is very marked), and that some enzyme stabilisation has occurred as a result of immobilization, which is not detected from 3 minutes of experimental data by the Equilibrium Model. As found for penicillin amidase, immobilization apparently raises the value of $\Delta G^{\ddagger}_{cat}$, possibly due to immobilization increasing the energy barrier of the catalytic or through steric hindrance as a result of immobilization. However, the effect may also be due to the difficulties in quantifying the immobilized enzyme, which is known to effect $\Delta G^{\ddagger}_{cat}$ although not the other parameters [8]. The larger ΔH_{eq} of the free enzyme may mean that the enathalpic change associated with the reversible conversion between the

active enzyme and its inactive state is higher for the free enzyme. However, it should be noted that the error values for ΔH_{eq} are systematically higher than for the other parameters due to the form of the Equilibrium Model equation where ΔH_{eq} appears as an exponential of an exponential [8,15,16].

The simulated product formation data of free alkaline phosphatase calculated from the 1 hour parameters in Figure 11A displays increasing reaction rates with increasing temperature. In accordance with predictions made by Eisenthal et al., the maximum rate is observed at the temperature closest to T_{eq}, the theoretical maximum reaction rate of the enzyme reactor containing free alkaline phosphatase is observed under initial conditions at 318 K, this is the temperature closest to the calculated T_{eq} values of 320 K for the 1 hour parameters and 317 K for the 3 minute parameters. Simulated product formation data calculated from the 3 minute parameters is shown in appendix A figure 3. Temperature points above the calculated T_{eq} values decrease in reaction rate with increasing temperature as shown in figure 11B. The simulations show that the temperature which yields maximum product of the enzyme reactor for the full length of the run is 308 and 313 K for the 1 hour parameters (308 K for the 3 minute parameters).

The experimental data of free alkaline phosphatase in figure 12 displays similar behaviour as observed with the simulated data. The rate of the catalysed reaction increases with increasing temperature and a maximum rate is observed at 318 Kelvin. Figure 12B shows that further increases in temperature do not result in increased reaction rates, even at initial conditions.

Like the simulated data the temperature which yields maximum product of the enzyme reactor is 308 Kelvin. The T_{eq} value of the 1 hour parameters of 320 Kelvin enables a good estimate of maximal enzyme reactor performance.

Free Alkaline Phosphatase Simulated Product Formation Curves.

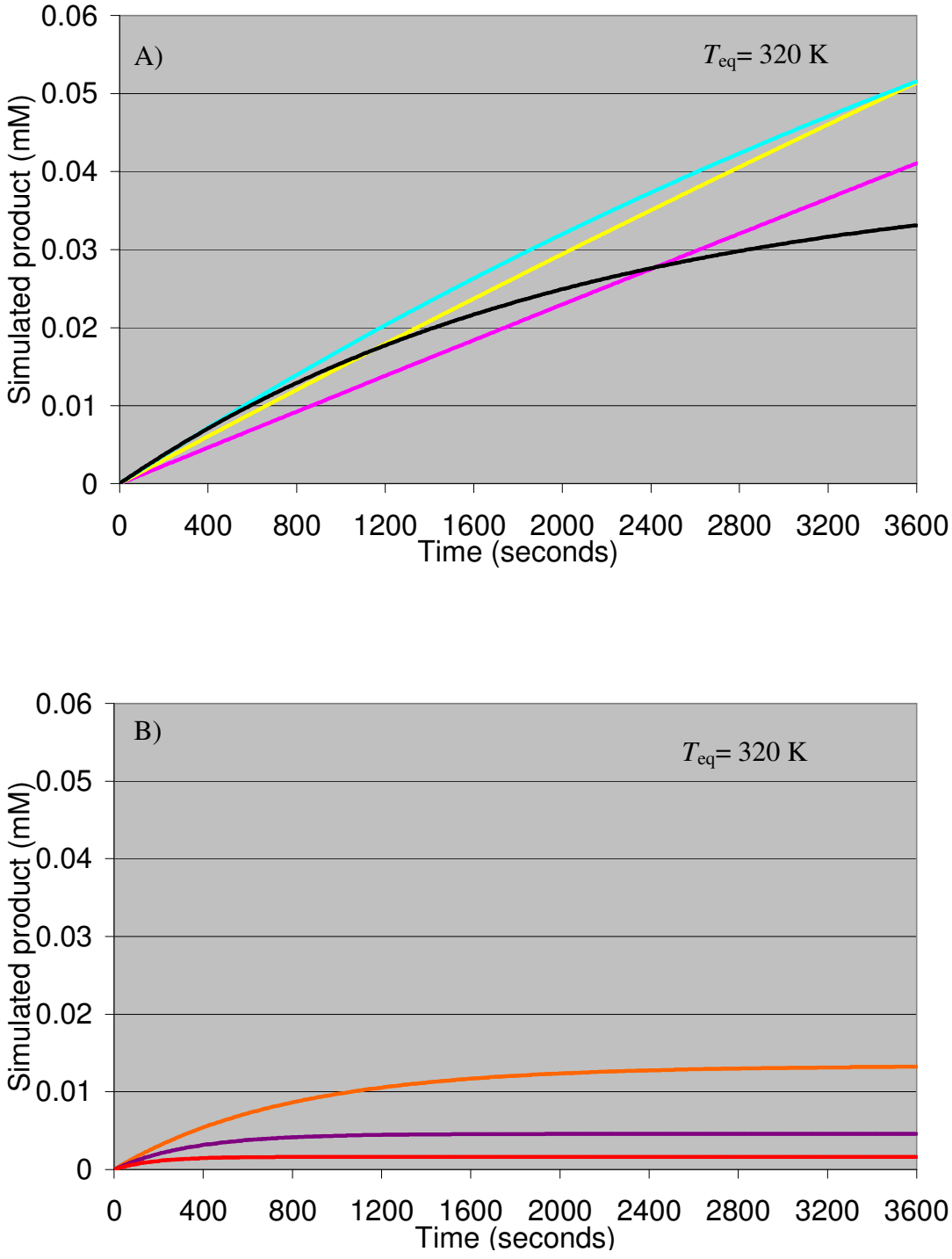

Figure 11: Free alkaline phosphatase simulated product formation, calculated from 1 hour parameters: 298 K (—); 303 K (—); 308 K (—); 313 K (—); 318 K (—); 323 K (—); 328 K (—); 333 K (—). A) T_{eq} exceeds reactor working temperature. B) Reactor working temperature exceeds T_{eq}.

Free Alkaline Phosphatase Experimental Product Formation Curves.

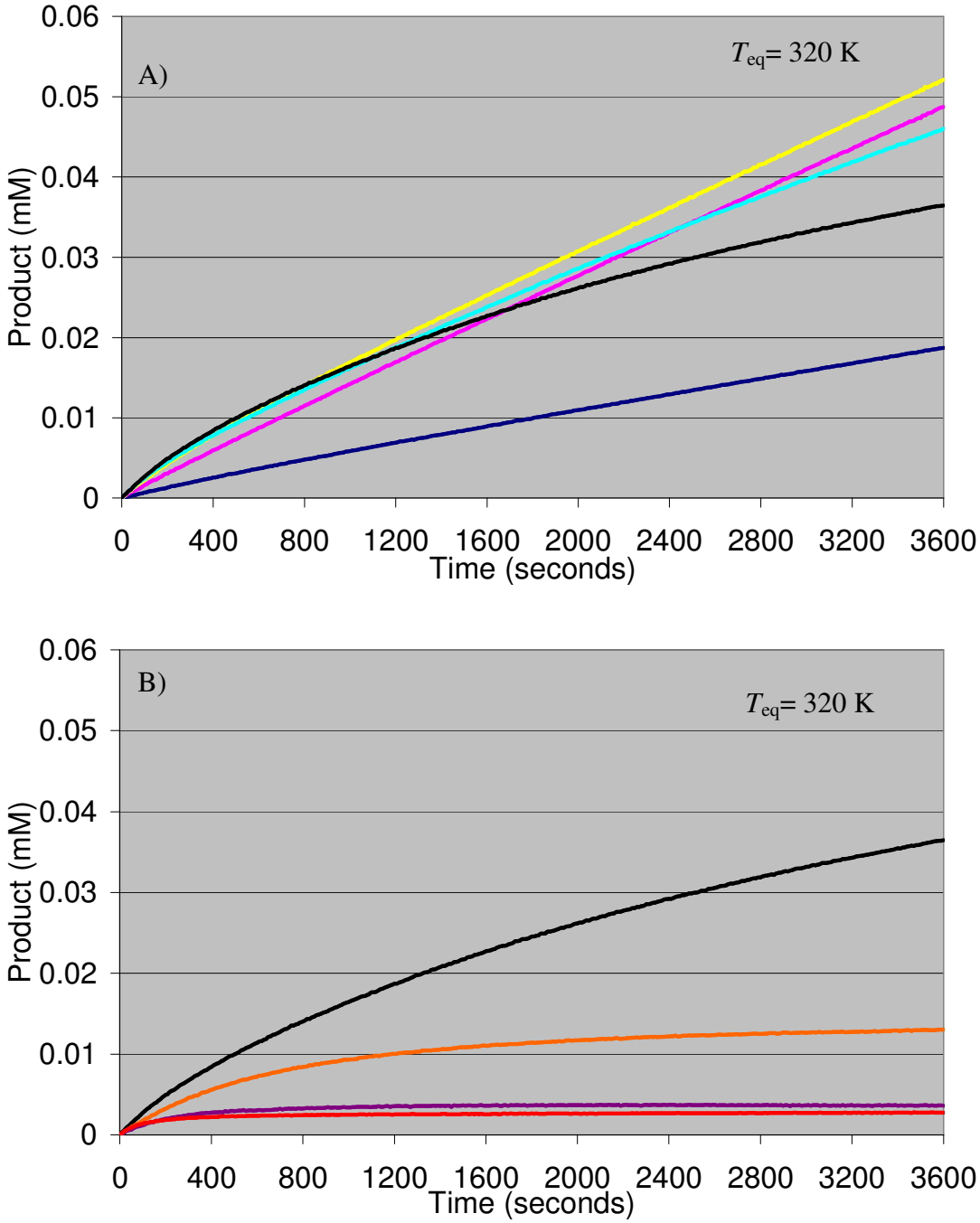

Figure 12: Free alkaline phosphatase experimental product formation: 298 K (—); 303 K (—); 308 K (—); 313 K (—); 318 K (—); 323 K (—); 328 K (—); 333 K (—). A) Increasing temperature causes increasing reaction rates B) Increasing temperature causes decreasing reaction rates.

Figures 13 and 14 illustrate that the both the simulated and experimental data of immobilized alkaline phosphatase display the enzyme reactor behaviour observed by Eisenthal et al. Figures 13A and 14A show that as the experimental and theoretical working temperature of the enzyme reactor is increased, the rate of the experimental and theoretical catalysed reaction increases up to a point where a maximum is seen. Figures 13B and 14B show that when the experimental and theoretical working temperature of the enzyme reactor is increased above the temperature where the maximum rate is observed the rate of the experimental and theoretical catalysed reaction does not increase with increasing temperature, it in fact decreases.

The maximum rate observed for the simulated data is predicted by the T_{eq} values of 314 K for the 1 hour parameters and 321 K for the 3 minute parameters (appendix A figure 3). Figure 14 shows that the maximum rate observed for the experimental immobilized alkaline phosphatase data is at 323 K.

The temperature which yields maximum product formation from the enzyme reactor is 313 K.

The T_{eq} of 321 K, of the 3 minute parameters is a good estimation of maximal performance of immobilized alkaline phophatase within the enzyme reactor as the actual maximum performance of the enzyme reactor occurs between the temperature points 318 and 323 K.

Immobilized Alkaline Phosphatse Simulated Product Formation Curves.

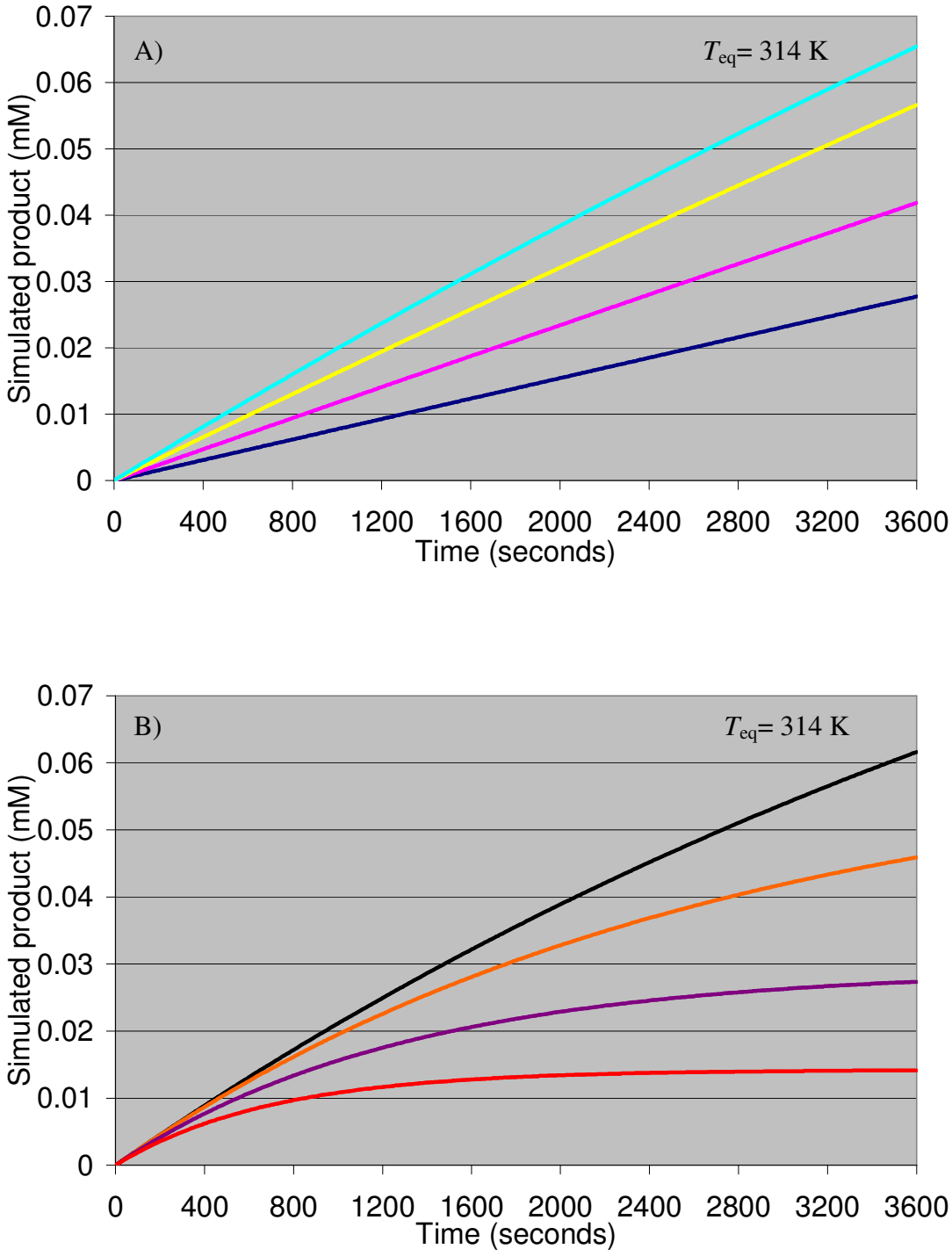

Figure 13: Immobilized alkaline phosphatase simulated product formation, calculated from 1 hour parameters: 298 K (—); 303 K (—); 308 K (—); 313 K (—); 318 K (—); 323 K (—); 328 K (—); 333 K (—). A) T_{eq} exceeds reactor working temperature. B) Reactor working temperature exceeds T_{eq}.

Immobilized Alkaline Phosphatase Experimental Product Formation Curves.

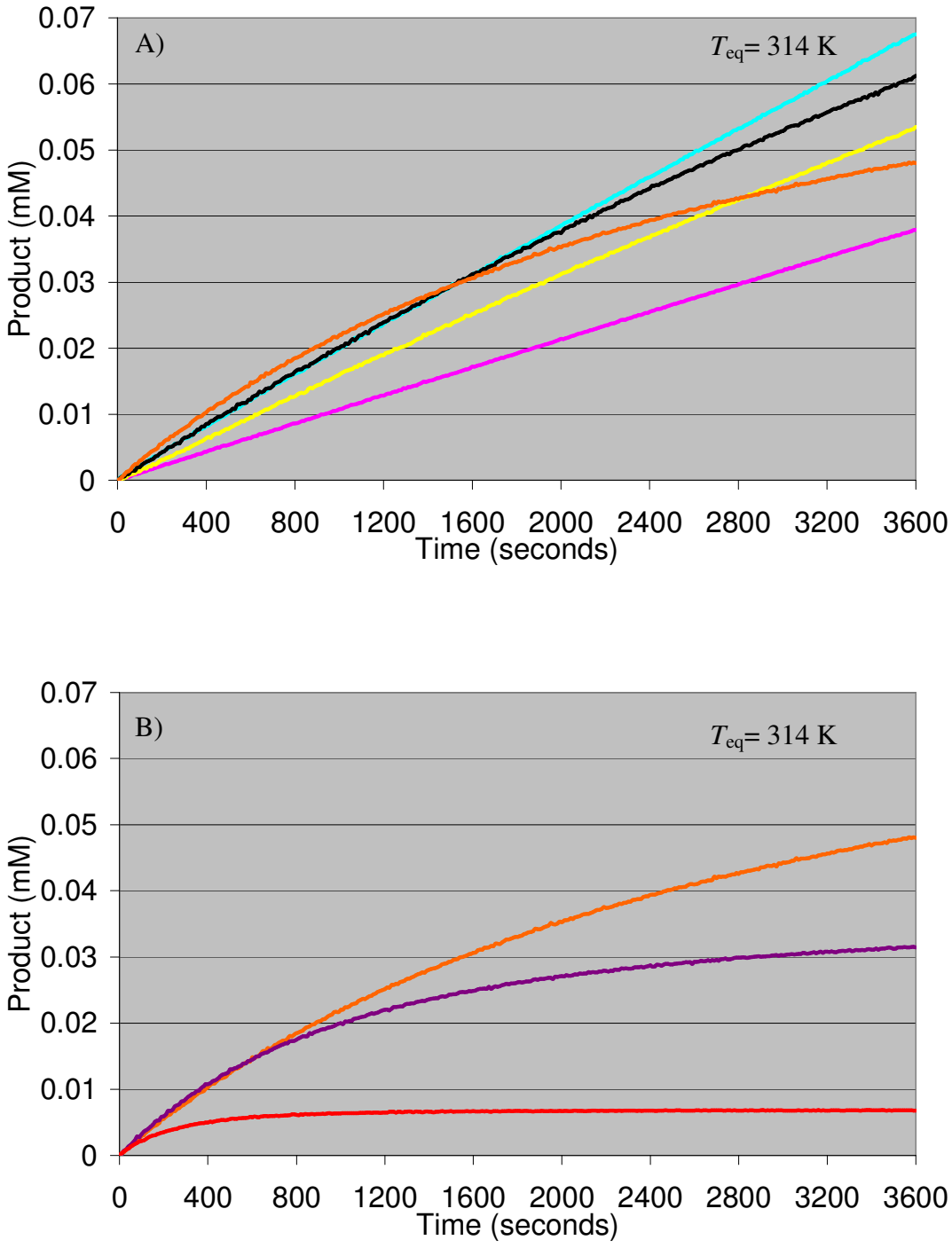

Figure 14: Immobilized alkaline phosphatase experimental product formation: 303 K (—); 308 K (—); 313 K (—); 318 K (—); 323 K (—); 328 K (—); 333 K (—). A) Increasing temperature causes increasing reaction rates B) Increasing temperature causes decreasing reaction rates over all time periods.

4. Conclusion

Intuition would predict that the higher the operating temperature of an enzyme reactor the faster the velocity of the catalytic reaction and the more unstable the enzyme. Predictions published by Eisenthal et al. in 2006 relating to enzyme reactor operating temperature, reaction rate and T_{eq} refute this. It was observed through simulated data that the higher the operating temperature the faster the reaction, but only up until the temperature of T_{eq}. When the operating temperature of the reactor exceeded T_{eq} the simulated data according to the Equilibrium Model displayed decreasing reaction rates with increasing temperature, even under initial reaction conditions. This suggested that the knowledge of T_{eq} would be useful in the prediction of enzyme reactor behaviour and operation.

The research presented here shows that the observations made by Eisenthal et al. are correct through both simulated data which obeys the Equilibrium Model and experimental enzyme reactor runs.

The Equilibrium Model has been shown to be a good predictor of enzyme reactor performance, experimental enzyme reactor data was collected using the enzymes Penicillin Amidase and Alkaline Phosphatase in both the free and immobilized forms and compared to simulated data calculated from either 3 minutes or 1 hour of experimental data by the Equilibrium Model. The experimental enzyme reactor data followed the Equilibrium Model as produced from both experimental and simulated data were 3D graphs of temperature, time and enzyme activity, typical of the Equilibrium Model, with “tent” type graphs and a temperature optimum at time zero. Classical Model-like behaviour where temperature optima at time zero does not exist were not observed. The comparison of experimental and simulated 3D graphs

revealed that the temperature of optimum enzyme activity after one hour was similar, making the Equilibrium Model a valuable tool in predicting optimal enzyme reactor operation. The simulated data calculated from 1 hour of experimental data produced 3D graphs that fitted to the experimental data better than simulated data calculated from 3 minutes of experimental data, as expected. The 1 hour parameters were therefore a more accurate description of the effects of temperature on enzyme activity within the enzyme reactor than the 3 minute parameters.

Enzyme	**3 minute Teq** **K**	**1 hour Teq** **K**	**Observed Experimental maximum rate** **K**	**Observed Experimental maximum product formation** **K**
Free penicillin amidase	309	314	323	323
Immobilized penicillin amidase	309	310	318	318
Free alklaline phosphatase	317	320	318	308
Immobilized alkaline phosphatese	321	314	328	313

Table 3: Comparison of T_{eq} to the temperatures of observed experimental maximum rate and observed experimental maximum product formation.

Overall values determined for T_{eq} were similar for the free and immobilized forms of both enzymes as shown in table 3, this was expected as T_{eq} is independent of thermal stability, with thermal stability expected to increase as a result of enzyme immobilization. The parameter values of penicillin amidase revealed little evidence of increased thermostability as a result of immobilization as $\Delta G^{\ddagger}_{inact}$ values were similar

for both the free and immobilized enzyme. Immobilized alkaline phosphatase however did show evidence of increased $\Delta G^{\ddagger}_{inact}$ as expected, suggesting slightly increased thermostability as a result of enzyme immobilization. Enzyme immobilization raised the $\Delta G^{\ddagger}_{cat}$ value, suggesting that the energy barrier of the catalytic reaction may be changed by immobilization, or immobilization may have caused some steric hindrance, as an alternative the change seen here could be resulting from difficulties in determining concentrations of the immobilized enzymes. ΔH_{eq} was also variable between both forms of both enzymes, possibly due to the larger error values associated with this parameter, as ΔH_{eq} appears as an exponential of an exponential on the equation of the Equilibrium Model.

Through product formation curves with varying time and temperature the behavior published by Eisenthal et al. was reproduced with simulated data calculated by the Equilibrium Model. This behaviour was also shown to be true for experimental enzyme reactor data, with increasing temperature causing increases in reaction rates up to a point, above which further increases in temperature do not result in the increased rate of the catalytic reaction, even under initial conditions. T_{eq} was shown to be useful in enzyme reactor operation prediction, with T_{eq} being a good estimation of maximal experimental enzyme reactor operation for both enzymes as shown in table 3.

5. References

[1] Fraunfelder, H., Petsko, G.A. and Tsernoglou, D. (1979) Temperature-dependant X-ray diffraction as a probe of protein structural dynamics. *Nature,* **280**, 558-563.

[2] Brooks, III, C.L., Karplus, M and Pettitt, B.M. (1988) *Proteins: A Theoretical Perspective of Dynamics, Structure and Thermodynamics,* John Wiley and Sons, New York.

[3] Gerstein, M., Lesk, A.M. and Chothia, C. (1994) Structural mechanisms for domain movements in proteins. *Biochemistry,* **33**, 6739-6749.

[4] Chang, R. (1994) In *Chemistry*, 5th Edition, McGraw-Hill, Inc., New York.

[5] Illanes, A. and Wilson, L. and Tomasello, G. (2000) Temperature optimization for reactor operation with chiti-immobilized lactase under modulated inactivation. *Enzyme and Microbial Technology,* **27,** 270-278.

[6] Engel, P.C. (1981) In *Outline studies in biology. Enzyme kinetics the steady state approach*, 2nd Edition, Chapman and Hall, London.

[7] Lee, C.K., Daniel, R.M., Shepherd, C., Saul, D., Cary, S.C., Danson, M.J., Eisenthal, R. and Peterson, M.E. (2007) Eurythermalism and the temperature

dependence of enzyme activity. *The Federation of American Societies for Experimental Biology Journal,* **21,** 1-8.

[8] Peterson, M.E., Daniel, R.M., Danson, M.J., Eisenthal, R. (2007) The dependence of enzyme activity on temperature: determination and validation of parameters. *Biochemical Journal,* **402,** 331-337.

[9] Daniel, R.M., Danson, M.J., Eisenthal, R., Lee, C.K. and Peterson, M.E. (2008) The effect of temperature on enzyme activity: new insights and their implications. *Extremophiles*, **12,** 51-59.

[10] Cornish-Bowden, A.J. (1995) In *Fundamentals of Enzyme Kinetics,* 2nd Edition, pp 193-197, Portland Press Ltd., London.

[11] Daniel, R.M. and Danson, M.J. (2001) Assaying activity and assessing thermostability of hyperthermophilic enzymes. *Methods in Enzymology,* **334,** 283-293.

[12] Thomas, T.M. and Scopes, R.K. (1998) The effects of temperature on the kinetics and stability of mesophilic and thermophilic 3-phosphoglycerate kinases. *Biochemical Journal,* **330**, 1087-1095.

[13] Gerike, U., Danson, M.J., Russell, N.J. and Hough, D.W. (1997) Sequencing and expression of the gene encoding a cold-active citrate synthase from an

Antarctic bacterium, strain DS2-3R. *European Journal of Biochemistry,* **248,** 49-57.

[14] Buchanan, C.L, Connaris, H., Danson, M.J., Reeve, C.D. and Hough, D.W. (1999) An extremely thermostable aldolase from *Sulfolobus solfactarius* with specificity for non-phosphorylated substrates. *Biochemical Journal,* **343,** 563-570.

[15] Daniel, R.M., Danson, M.J. and Eisenthal, R. (2001) The temperature optima of enzymes: a new perspective on an old phenomenon. *Trends in Biochemical Sciences,* **26,** (4), 223-225.

[16] Peterson, M.E., Eisenthal, R., Danson, M.J., Spence, A. and Daniel, R.M. (2004) A new intrinsic thermal parameter for enzymes reveals true temperature optima. *The Journal of Biological Chemistry,* **279,** (4), 20717-20722.

[17] Eisenthal, R., Peterson, M.E., Daniel, R.M. and Danson, M.J. (2006) The thermal behaviour of enzyme activity: implications for biotechnology. *Trends in Biotechnology,* **24,** 289-292.

[18] Galunsky, B., Schlothauer, R.C., Böckle, B. and Kasche, V. (1994)Direct spectrophotometric measurement of enzyme activity in heterogeneous systems with insoluble substrate or immobilized enzyme. *Analytical Biochemistry,* **221,** 213-214.

[19] Alkema, W.B.L., Vries, E.D., Floris, R. and Janssen, D. (2003) Kinetics of enzyme acylation and deacylation in the penicillin acylase- catalysed symthesis of β-lactam antibiotics. *European Journal of Biochemistry,* **270,** 3675-3683.

[20] Kasche, V., Haufler, U. and Riechmann, L. (1987) Equilibrium and kinetically controlled synthesis with enzymes: semisynthesis of penicillins and peptides. *Methods in Enzymology,* **136,** 280-292.

[21] Guncheva, M., Ivanov, I., Galunsky, B., Stambolieva, N. and Kaneti, J. (2004) Kinetic studies and molecular modelling attribute a crucial role in the specificity and stereoselectivity of penillin acylase to the pair ArgA145-ArgB263. *European Journal of Biochemistry,* **271,** 2272-2279.

[22] Hoylaerts, M.F, Manes, T and Millán, J.L. (1992) Molecular mechanism of uncompetitive inhibition of human placental and germ-cell alkaline phosphatase. *Biochemical Journal,* **286,** 23-30.

[23] Weissig, H., Schildge, A., Hoylaertis, M.F., Iqbal, M. and Milán, J.L. (1993) Cloning and expression of the bovine intestinal alkaline phosphatase gene: biochemical characterization of the recombinant enzyme. *Biochemical Journal,* **290,** 503-508.

[24] Fernley, H.N. (1971) In *The Enzymes,* Vol.4 (ed. Boyer, P.D.) 417-447, Academic Press, New York.

Chapter Four

RNase A Results and Discussion

RNase A was tested to determine whether an enzyme that renatured very readily would follow predictions made by the Equilibrium Model.

Much has been published documenting the usual catalytic features of native RNase A towards the substrate Cytidine 2':3'-cyclic monophosphate (C>p), with deviations from hyperbolic reaction kinetics seen at both low (Piccoli and D'Alessio, 1984) and high substrate concentrations (Walker et al., 1975; Walker et al., 1976). Piccoli and D'Alessio attributed the observed kinetic behaviour to changes in quaternary structure of RNase A. Walker et al. interpreted the deviation from hyperbolic kinetics by an allosteric model in which there is a substrate dependant change in the equilibrium between three pre-existing enzyme conformations, one being inactive. Moussaoui et al. proposed that the deviation from hyperbolic kinetics of RNasea A and C>p was due to the structure of subsites of RNase A, where the catalytic properties of the enzyme are modified as a function of the sequential binding of C>p to different subsites of decreasing affinity (Moussaoui et al., 1998), this proposed theory is now generally accepted.

Obtaining a temperature profile of RNase A activity was difficult due to the high price of C>p and complications encountered when using this substrate, including non-hyperbolic kinetics. As a result the concentration of C>p was not maintained at 10 times K_M at all temperature points used, since it was found that consistent results

were not achieved at high concentrations of C>p. Corrections were made to progress curves where the substrate concentration was not maintained at ten times K_M (according to section 2.1.4.5).

Trial assays according to the method published by Crook, Blackburn and Bencina (Crook et al., 1960; Blackburn, 1979; Benčina et al., 2007) performed at 25ºC with a substrate concentration of 6.2mM; ten times the published value at 25ºC (Benčina et al., 2007; Tanimuzi et al., 2002) resulted in very low absorbance changes and inconsistent results as shown by figure 4.1.

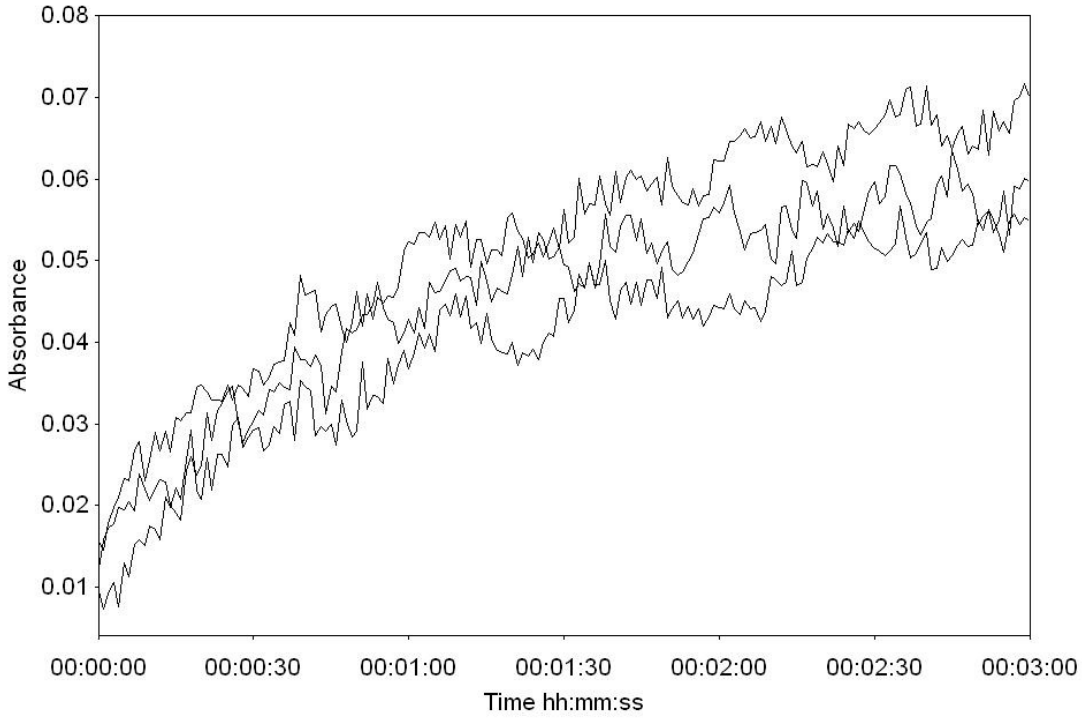

Figure 4.1: RNase A assay trial results performed at 25°C using the Rabin, Blackburn and Bencina method, with a substrate concentration of 6.2mM; ten times the Km at 25°C.

Crook, Blackburn and Bencina performed the assay at low substrate concentrations. To test the accuracy of the application of the published assay method trials were performed at a substrate concentration of 1.24mM, which is 2 times the published Km value at 25ºC and comparable to substrate concentrations used by Crook, Blackburn and Bencina. These trials obtained smooth, reproducible reaction progress curves as shown in figure 4.2, with a much larger absorbance change than that observed when the substrate concentration was at 10 times K_M.

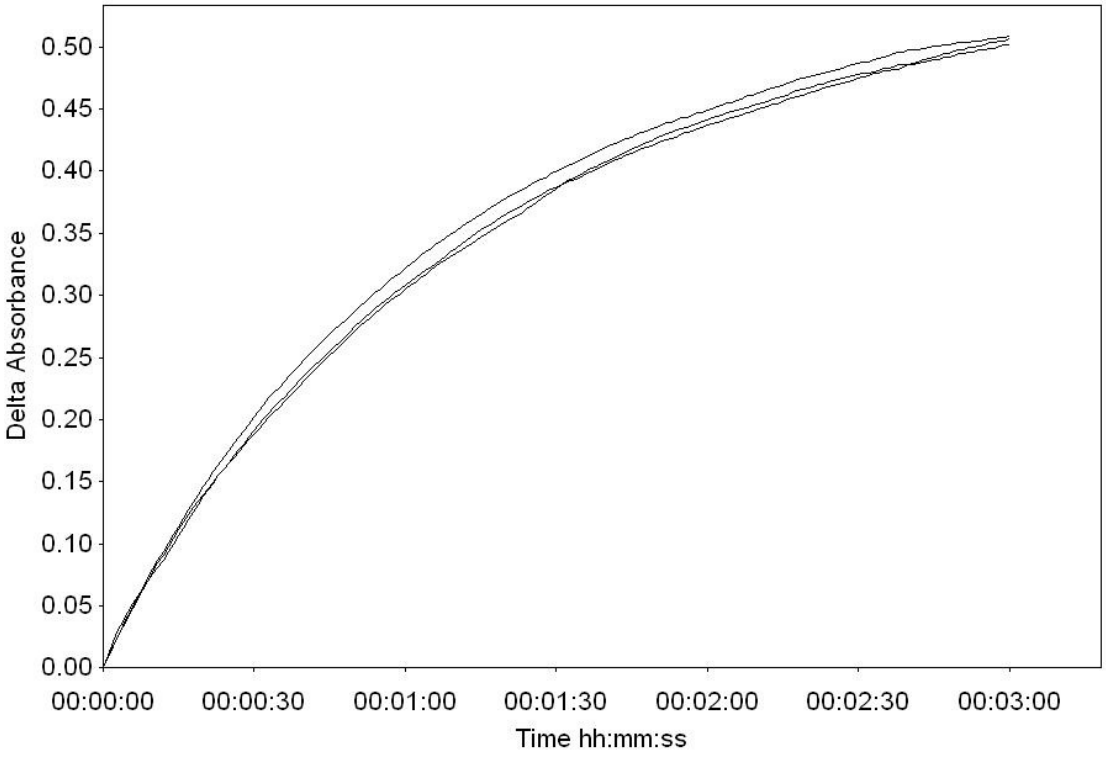

Figure 4.2: RNase A assay trial results performed at 25°C using the Rabin, Blackburn and Bencina method, with a substrate concentration of 1.24mM; two times the K_M at 25°C.

The assay method according to papers by Fujii, Tanimizu and Moussaoui (Fujii et al., 2002; Tanimizu et al., 2002; Moussaoui et al., 1998) was then trialled; this method used a different buffer of a lower pH and monitored the reaction at a slightly lower wavelength. Trial results with a substrate concentration of 6.2mM, shown in figure 4.3, obtained smooth and reproducible reaction progress curves, which were not achieved in the previously trailed assay method at this substrate concentration.

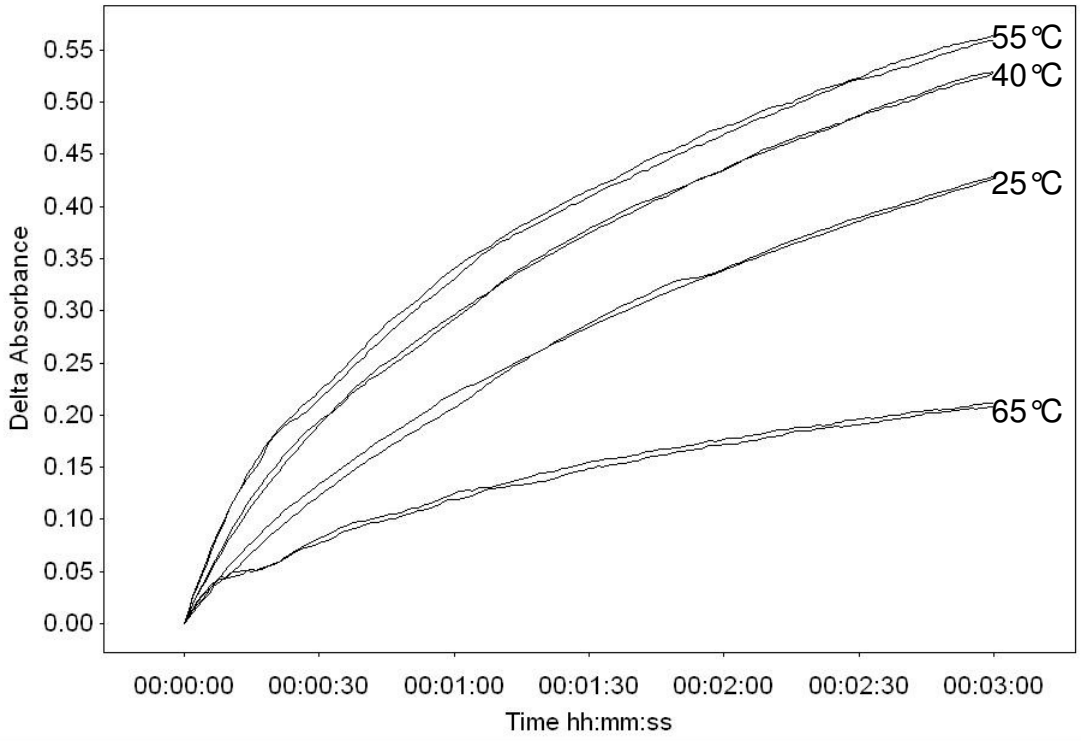

Figure 4.3: RNase A assay trial results performed using the Fujii, Tanimizu and Moussaoui method with a substrate concentration of 6.2mM; ten times the K_M at 25°C.

The assay method of Fujii, Tanimizu and Moussaoui was then used for the collection of data for application to the Equilibrium Model. 25ºC was the only temperature point at which substrate concentrations were maintained at ten times K_M, therefore the data collected at all other temperatures was subjected to a correction to compensate for deviations from operation of the enzyme at V_{max}. This assay method allowed the use of a higher substrate concentration than the method of Crook, Blackburn and Bencina, minimising the error introduced by the correction applied to the data.

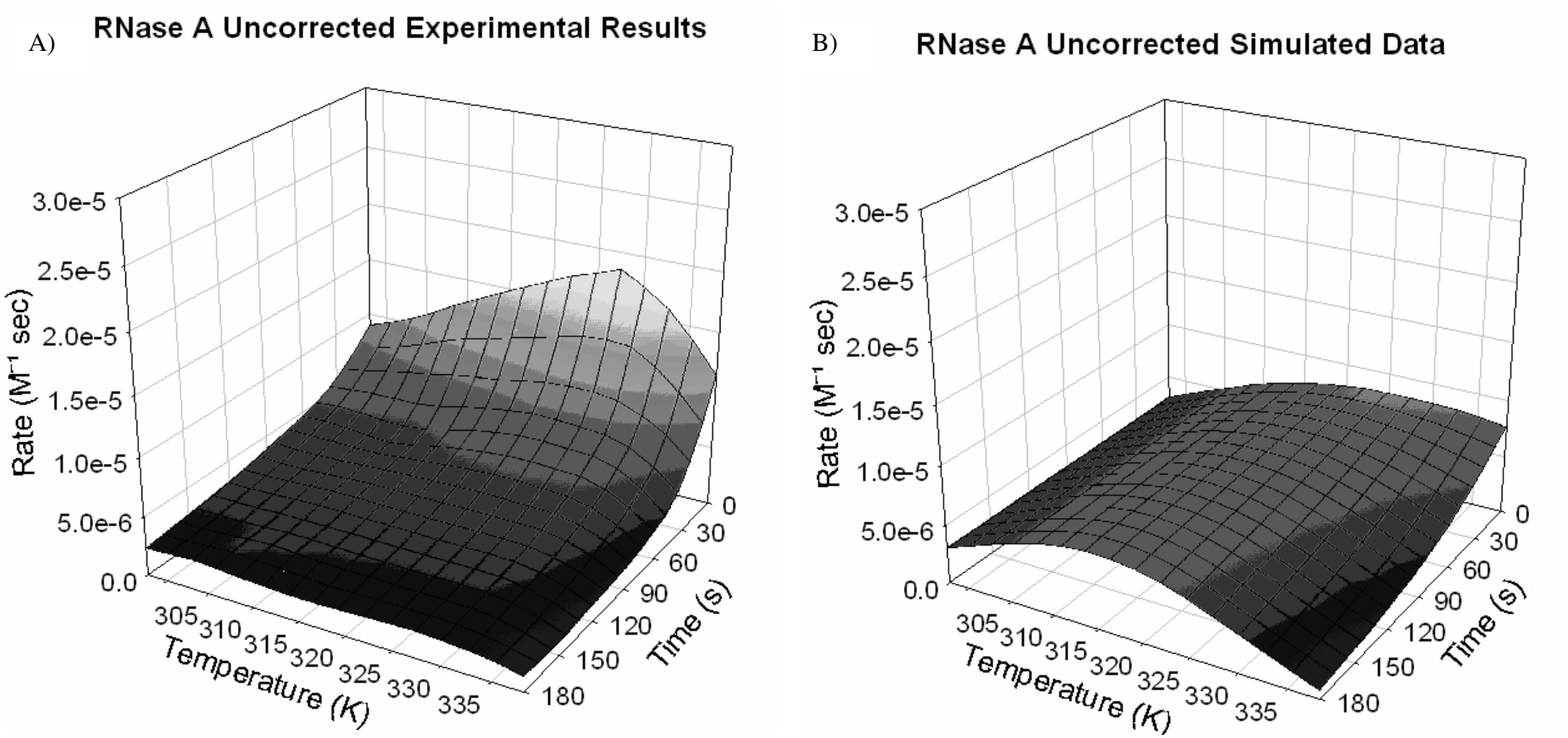

Figure 4.4: RNase A results with the K_M adjustment not made. A) Experimental data B) Simulated data.

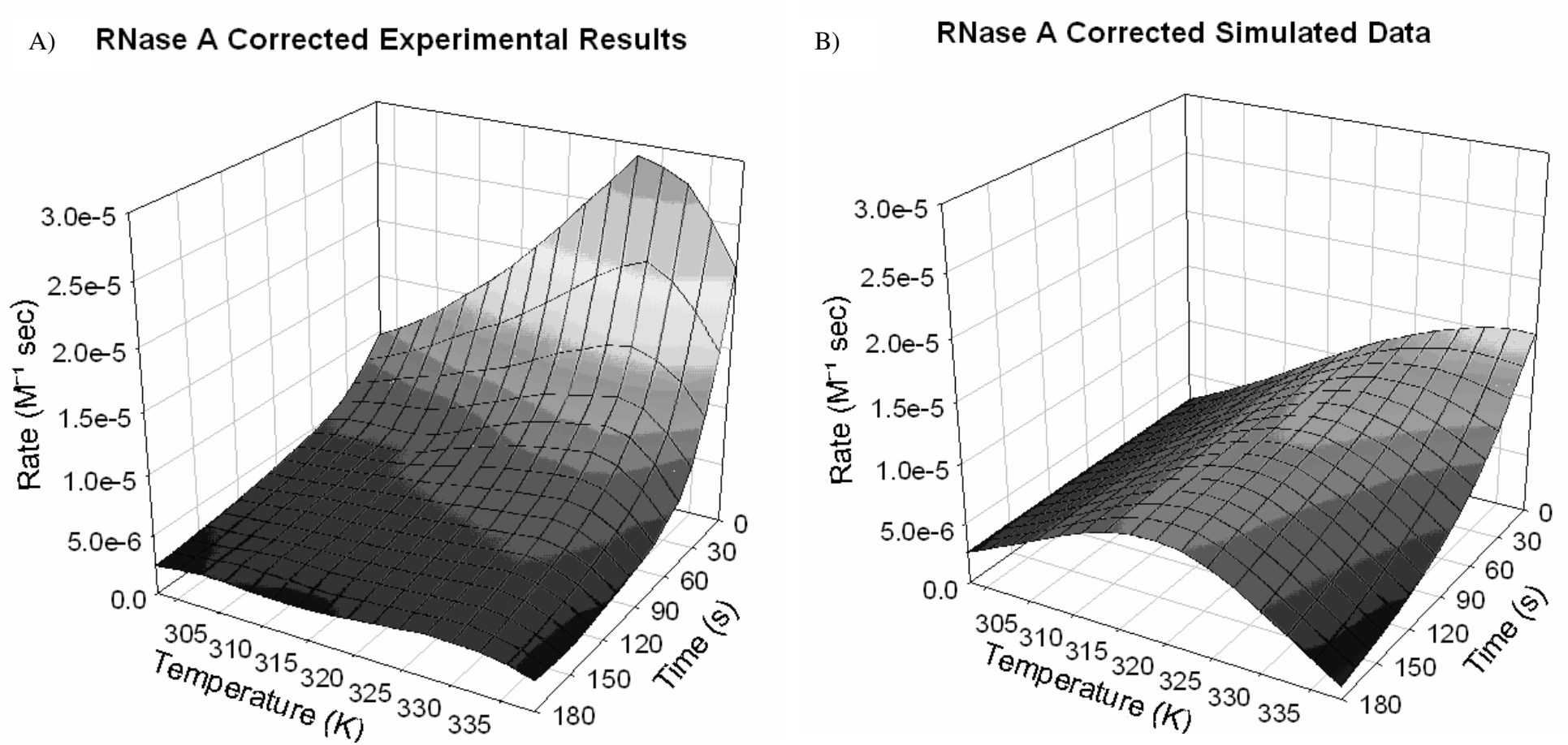

Figure 4.5: RNase A results with the K_M adjustments made. A) Experimental data B) Simulated data

The base assumption on which the Equilibrium Model rests is that measured rates represent the enzyme V_{max} for all temperatures concerned; this is not occurring in the uncorrected data. The data presented in figure 4.4 and the associated parameter values contain error due to the substrate concentration not being maintained at 10 times K_M at all temperature points and can therefore be disregarded.

The data presented in figure 4.5 has undergone an adjustment to compensate for deviations from V_{max}, using the Km values in table 4.2. The corrected experimental data in figure 4.5A does not display typical variations in reaction rate with time and temperature, with the typical “tent” type graph of the Equilibrium Model not seen. A temperature optimum at time zero is observed, however a clear temperature optimum is not observed for the entire duration of the experimental data. It appears that little catalytic activity is occurring at the longer duration end of the time scale of the experimental data, as reaction rates dramatically reduce to a near constant level at about 2.5^{-6} M^{-1} second.

The simulated data in figure 4.5B does not take into account the binding of the substrate to subsites of the enzyme, therefore the Equilibrium Model "assumes" that the catalytic reaction will follow hyperbolic reaction kinetic and that the enzyme is operating at V_{max}. The simulated data in figure 4.5B therefore shows typical variations in reaction rate with time and temperature of the Equilibrium Model with a “tent” type graph and a temperature optimum observed at time zero and throughout the entire duration of the simulated data.

The experimental data does not follow the Equilibrium Model as the overall shapes and trends of the simulated data is not similar to that of the experimental data meaning that the Equilibrium Model has not estimated well the effects of temperature on the activity of RNase A.

Temperature (°C)	**K_M (mM)**
25	0.68
30	0.76
35	1.01
40	1.43
45	1.97
50	2.68
55	3.55
60	4.57
65	5.79

Table 4.2: K_M values calculated at different temperatures.

Zero time analysis as shown in figure 4.6 was then performed, with experimental initial rates also not being characteristics of the model. The data presented in 4.6A is determined from data that has not undergone a correction compensating for operation of the enzyme at conditions which are not V_{max}. The simulated data of Figure 4.6A and the associated parameter values are therefore erroneous and can be disregarded.

Figure 4.6B presents initial rate data that has undergone K_M adjustment; the Equilibrium Model, however still does not apply as the shape of the simulated data's initial rates does not fit to that of the experimental data, with the position of optimal initial rate and the rate of denaturation not being well predicted.

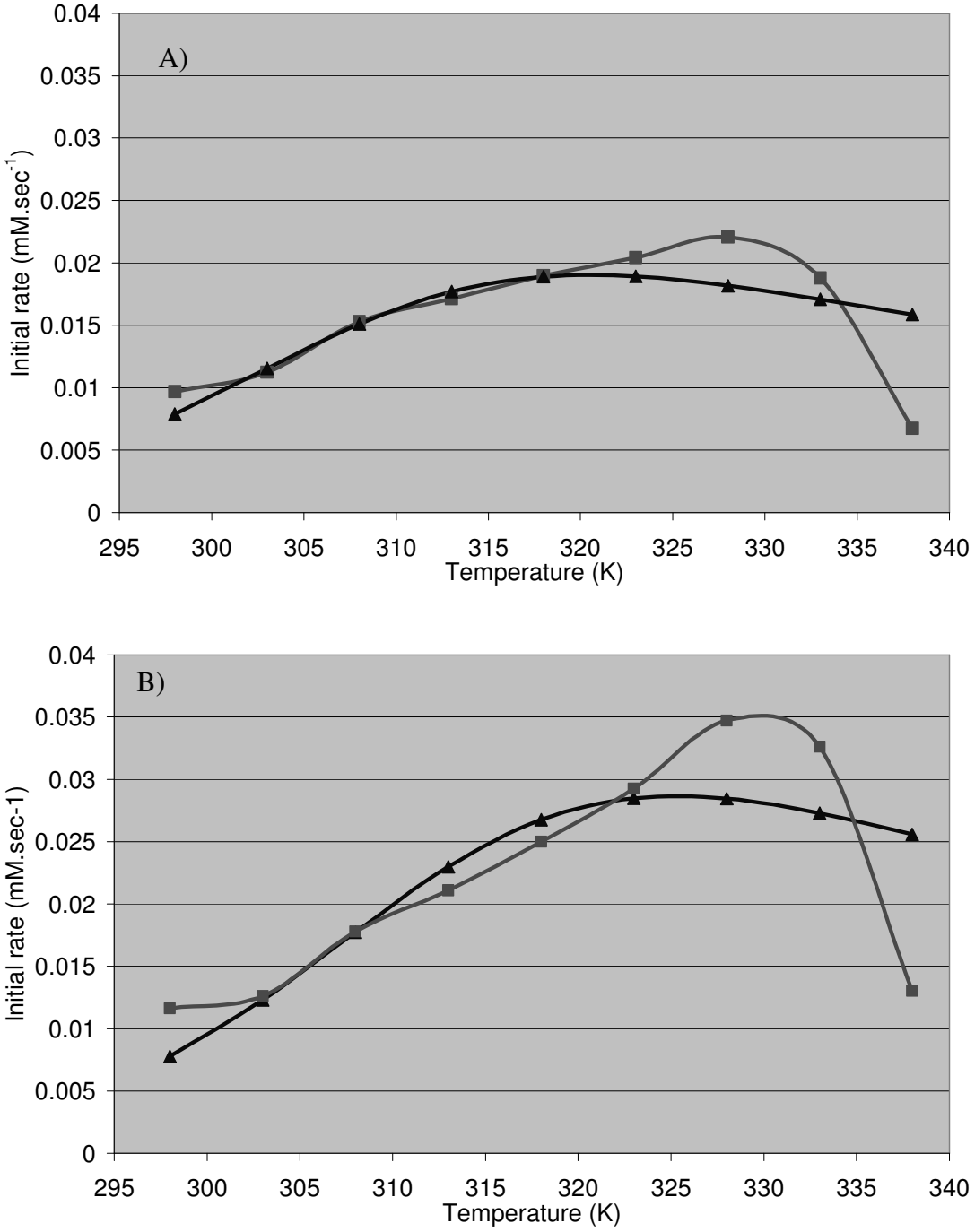

Figure 4.6: Initial rate analysis of RNase A activity. A) Uncorrected data. B) Corrected data. ▲ Simulated initial rates ■ Experimental initial rates.

Enzyme	Data	T_{eq} K	$\Delta G^{\ddagger}_{cat}$ kJ•mol⁻¹	$\Delta G^{\ddagger}_{inact}$ kJ•mol⁻¹	ΔH_{eq} kJ•mol⁻¹
RNase A	Uncorrected Progress curves	302	83.8	95.7	91.4
RNase A	Uncorrected Initial rates	308	82.7	*	103
RNase A	Corrected progress curves	307	84.4	95.5	82.8
RNase A	Corrected Initial rates	313	82.9	*	104

Table 4.1: Thermodynamical parameters of RNase A from bovine pancrease; calculated by the Equilibrium Model from experimental data.

From figure 4.5A it can be determined that the optimum temperature at time zero is in the range of 320- 330 K. A temperature difference between T_{eq} and the optimum temperature of more than 10°C has not been seen before (Lee et al., 2007). The difference between the T_{eq} of the corrected initial rates and the observed optimum temperature looks to be up to about 18°C, which compounds further that the experimental data does not fit to the Equilibrium Model. The initial parameter values were both increased and decreased within Matlab before a fit to the experimental initial rates was performed; this did not result in a better fit to the experimental data.

It was already known that the enzyme was not operating at V_{max} as this was not possible due to the large amount of substrate required; calculations carried out to compensate for this using the determined K_M values in table 4.2 showed that the experimental data did not follow the Equilibrium Model at both initial rates and for the duration of the assay. Checks were therefore performed to ensure that:

a) An enzyme catalysed reaction was occurring
b) Product inhibition was not occurring
c) A single enzyme was being assayed
d) The stock enzyme solution had not lost activity
e) The assay pH was constant

To test whether it was actually an enzyme catalysed reaction that was occurring control assays were performed using no enzyme and boiled enzyme at 25, 40 and 65ºC. Both controls resulted in no significant increases in absorbance, with any increase in absorbance being subtracted from the results of assays containing active RNase A.

Through literature searches no evidence of product inhibition of the reaction of bovine pancreatic RNase A with C>p was found.

It is common for some commercial preparations of RNase A to contain substantial RNase B content. So this was investigated, the preparation of RNase A used within this study was ≥85% pure (Sigma-Aldrich Specification Sheet, Ribonuclease A from bovine pancrease). Significant concentrations of RNase B may possibly have been present.

The activity of enzyme solutions were tested by performing assays using freshly prepared enzyme and enzyme that had been prepared and stored in the fridge for approximately a week. When comparing the results of these assays there was no difference between the fresh and week old enzyme.

The buffer used was 0.2M sodium acetate buffer pH 5.5, the pH was checked at different temperatures and was determined to be constant at 5.5 at the temperatures used.

Given the poor match between both the 2D (zero time) and 3D experimental plots and the simulated plots, the data was determined to not fit the Equilibrium Model well enough to allow the reliable generation of credible Equilibrium Model parameters.

This may be due to:

A] V_{max} not being achieved because of the effect of the enzymes subsites on catalytic activity, the known deviation from hyperbolic reaction kinetics, or for some other reason;

B] Inaccurate correction of rates using known values of the K_M at each temperature;

C] The enzyme not following the Equilibrium Model.

As things stand it is not possible to distinguish between these possibilities, although it seems quite likely that true V_{max} values have not been obtained. Additionally, since the experimental data does show the zero time optimum expected for an enzyme that obeys the model, the first two possibilities above seem the more likely explanations.

Chapter Five

A.k 1 Protease Results and Discussion

Structural analyses have revealed the presence of a disulfide bond within the active-site cleft of Ak. 1 protease. This bond has a dual role of maintaining substrate binding cleft integrity and of increasing thermostability of the protease (Smith et al., 1999; Toogood et al., 2000). Dithiothreitol (DTT) treatment to reduce disulfide bonds A.k 1 protease yields a substrate binding cleft of lower integrity and overall lower thermostability when compared to the native enzyme (Toogood et al., 2000).

Obtaining a temperature profile was difficult for A.k 1 as data must be collected from at least three temperature points above T_{eq} for accurate fitting of experimental data to the Equilibrium Model. As A.k 1 is a thermostable protease the highest temperature points used were at the upper limits of accurate data collection.

Native A.k 1 protease follows the Equilibrium Model, as simulated data fits very well to the experimental data as displayed in figure 5.1, with the experimental data of figure 5.1A and the simulated data of figure 5.1B displaying similar overall shapes and trends. The experimental and simulated data of the native enzyme display “tent” type graphs typical of the Equilibrium Model with a temperature optimum at time zero, Classical Model-like behaviour is not seen. The rate of the catalytic reaction of the experimental data in figure 5.1A has been estimated well by the simulated data in figure 5.1B, as has optimum enzyme activity as the peaks have similar heights and widths, also well predicted by the simulated data is the rate of thermal denaturation.

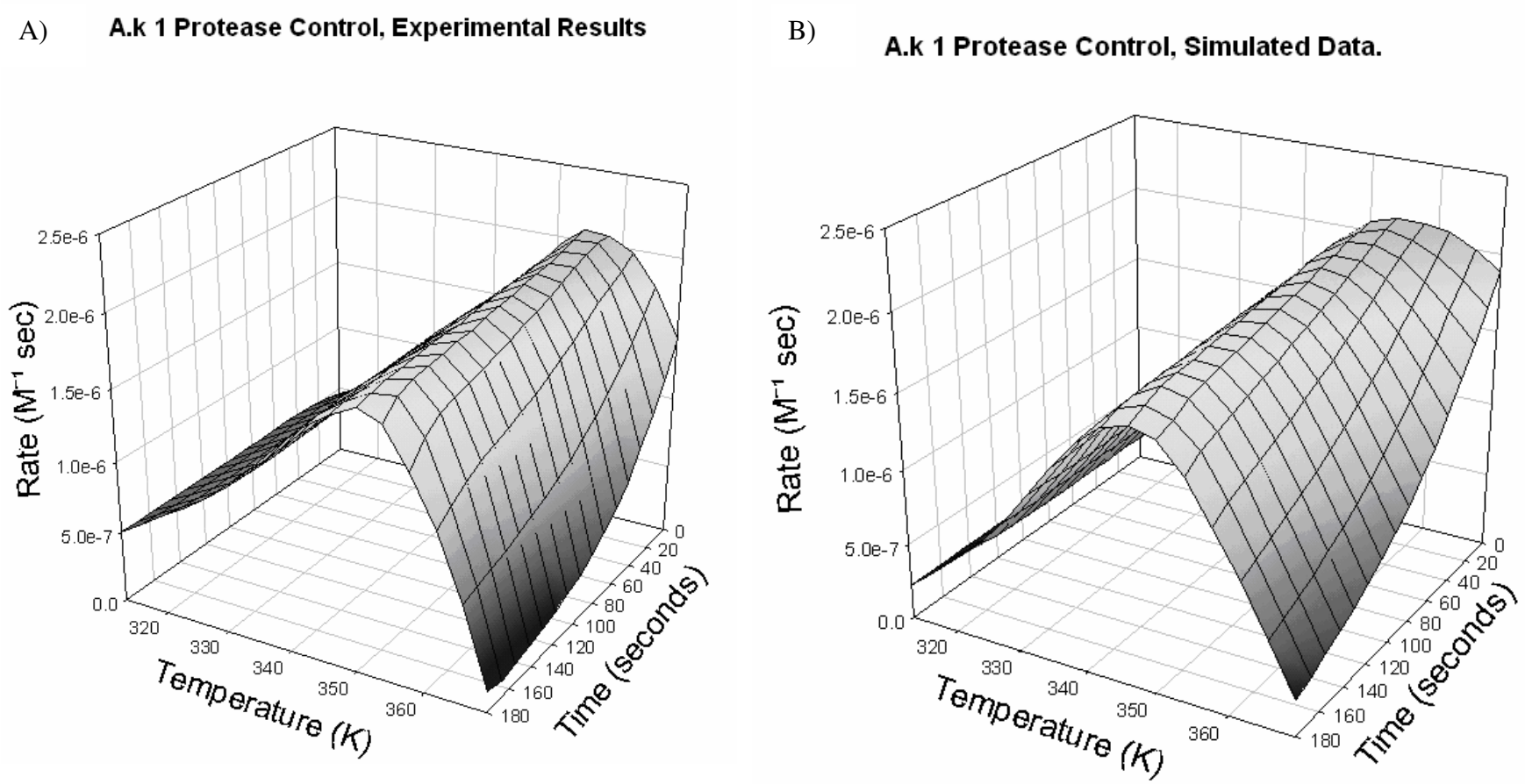

Figure 5.1: Native A.k 1 results. A) Experimental data. B) Simulated data.

A)

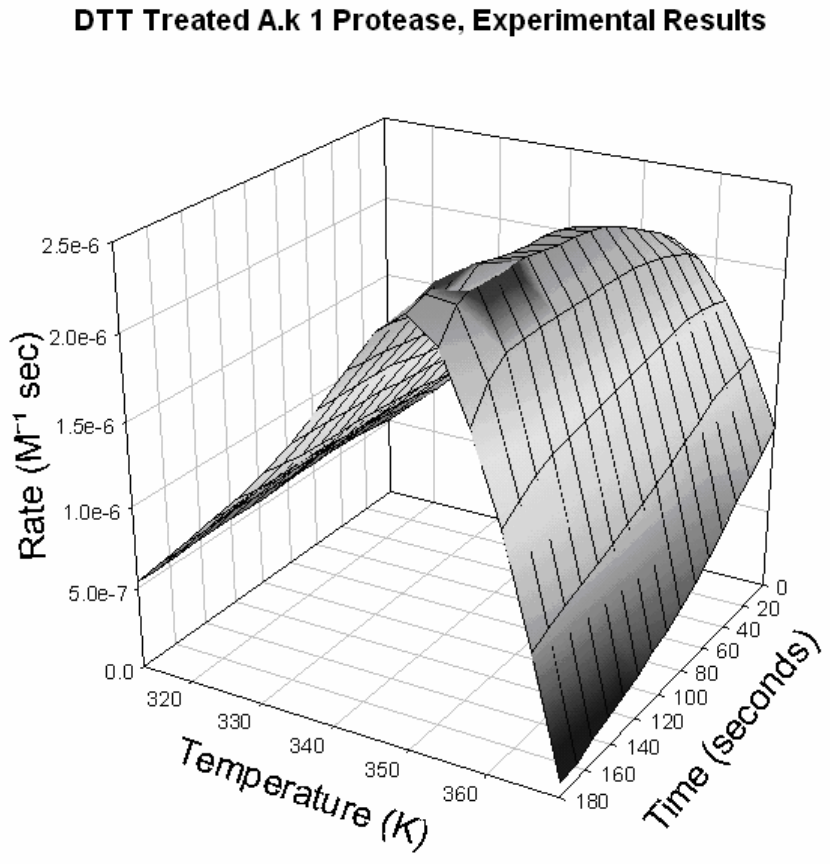

B)

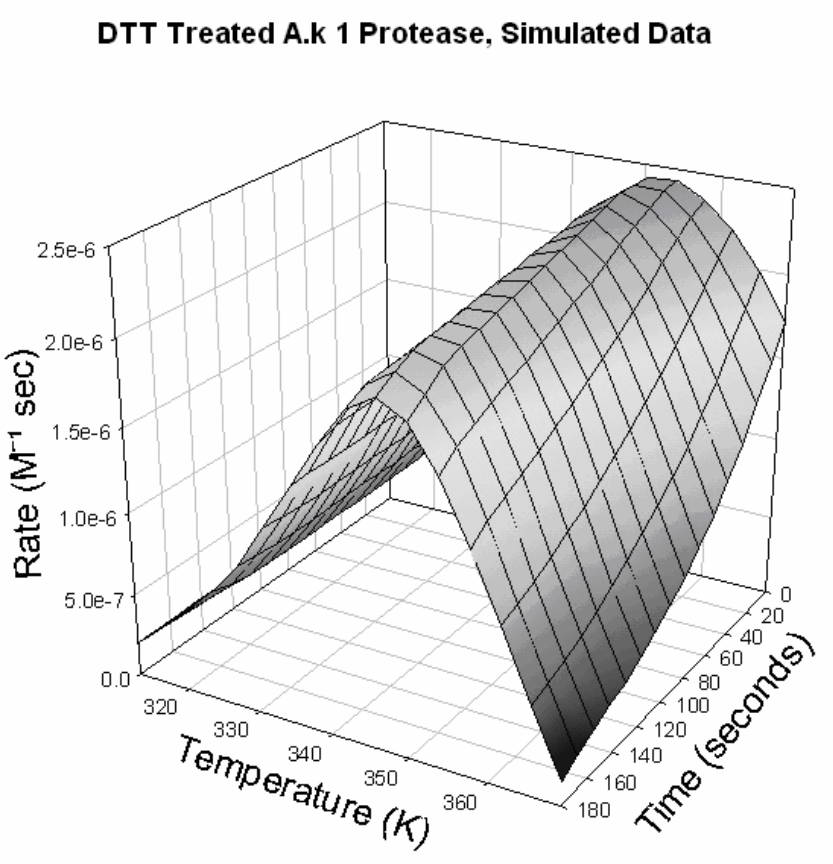

Figure 5.2: DTT treated A.k 1 results. A) Experimental data. B) Simulated data.

Figure 5.2 shows that DTT treated A.k 1 protease also follows the Equilibrium Model, with the overall shapes and trends of simulated and experimental DTT treated A.k1 protease, in figures 5.1A and B being similar. The rates of the catalytic reaction and of thermal denaturation have been well predicted by the Equilibrium Model, as the rates of the upward and downwards slopes are similar. Optimum activity of DTT treated A.k 1 protease has been well estimated by the Equilibrium Model, with peak height and width being very similar.

DTT treatment alters the fit of the enzyme to its thermal environment, this is reflected through differences between the experimental data in figures 5.1A and 5.2A and the calculated parameter values.

Enzyme	**Origin**	T_{eq} **K**	$\Delta G^{\ddagger}_{cat}$ **kJ•mol⁻¹**	$\Delta G^{\ddagger}_{inact}$ **kJ•mol⁻¹**	ΔH_{eq} **kJ•mol⁻¹**
A.k 1 native	Escherichia Coli clone PB5517	343	76.8	105	101
A.k1 DTT treated	Escherichia Coli clone PB5517	348	77.2	104	129

Table 5.1: Thermodynamical parameters of native and DTT treated A.k 1 calculated by the Equilibrium Model from experimental data.

The differences between the experimental 3D graphs infer that temperature affects the behaviour of the enzymes differently, although there is no significant change in the thermostability of the DTT treated enzyme. The increase in $\Delta G^{\ddagger}_{cat}$ of the DTT treated enzyme may possibly be due to a lowered specificity of the enzyme for its substrate,

as a result of the expected lower integrity of the substrate binding cleft. The only significant difference between the two forms of the enzyme is the higher T_{eq} and $\Delta H^{\ddagger}_{eq}$ values for the DTT treated enzyme, however as mentioned in chapter 3 the error of $\Delta H^{\ddagger}_{eq}$ is higher than for the other parameter values due to the nature of the Equilibrium Model equation (Peterson et al., 2007). On the basis of the variation between the individual triplicate rates from which the parameters are derived for all enzymes so far studied, it has been found that the experimental errors in the determination of $\Delta G^{\ddagger}_{cat}$, $\Delta G^{\ddagger}_{inact}$ and T_{eq} are less than 0.5%, and less than 6% in the determination of $\Delta H^{\ddagger}_{eq}$ (Peterson et al., 2007).

The T_{eq} finding supports the suggestion that the active- inactive enzyme transition arises from localised molecular changes at the enzymes active site; in this case through the reduction of the disulfide bond at A.k 1's active site. The changes in T_{eq} do not reflect changes in thermostability as T_{eq} is independent of thermostability. $\Delta G^{\ddagger}_{inact}$ describes the stability of the enzyme under reaction conditions, and we find here no significant change upon reduction of the disulphide bond. This is particularly interesting since it supports earlier findings that T_{eq} changes can occur independently of changes in stability.

The value of $\Delta H^{\ddagger}_{eq}$ was higher for the DTT treated enzyme, this suggests that the enathalpic change associated with conversion of the enzyme between its active and reversibly inactive forms is increased due to the effects of DTT treatment. The differences in $\Delta H^{\ddagger}_{eq}$ infer that there has been a change in the sensitivity of the enzymes's catalytic activity to temperature resulting from DTT treatment. Changes in $\Delta H^{\ddagger}_{eq}$ were expected with DTT treatment as the breakage of the disulfide bond within

the active site was expected to alter the active-inactive transition of the enzyme, and so is consistent with the observed change in T_{eq}.

Chapter Six

Final Discussion and Conclusions

The Equilibrium Model was developed to fully describe the effects of temperature on enzyme activity. Detailed studies on over 30 enzymes have shown that every enzyme studied displays behaviour predicted by the Equilibrium Model with "tent" type graphs describing the effect of time and temperature on enzyme activity, and a temperature optimum at time zero (Lee et al., 2007, Daniel et al., 2008).

Eisenthal et al. published rather counter intuitive observations made from simulated enzyme reactor data, calculated according to the Equilibrium Model. The simulated data showed that as the temperature is raised the rate of the reaction occurring within the enzyme reactor increases, as expected, but only up to the point of T_{eq}, where a maximum rate was observed. Unexpected, however, is that increases in temperature above T_{eq} did not result in further increases in reaction rate, instead the opposite was seen, where increases in temperature above T_{eq} resulted in decreases in reaction rates, even under initial conditions (Eisenthal et al., 2006).

Data presented has shown that the observations made by Eisenthal et al. are true for both of the enzymes tested, pencillin amidase and alkaline phosphatase, with increases in temperature above a certain point resulting in a decrease in reaction rates and not the expected increase. The experimental enzyme reactor data showed that T_{eq} was a good estimate of this maximum reaction rate observed. The knowledge of T_{eq}

and the application of the Equilibrium Model therefore is a valuable tool in the prediction of enzyme reactor behaviour and operation.

The operators of enzyme reactors will be mainly interested in the accurate prediction of maximal product yield from enzyme reactors, for the maximisation of output and therefore profit of reactor operation (eg. Giordano et al., 2006; Alkema et al., 2003). I recommend that the operators of enzyme reactors use simulated 3D temperature/ time/ activity plots, determined from simulated data calculated by the Equilibrium Model in the prediction of enzyme reactor performance. From such plots both enzyme reactor behaviour and maximal product yield can be predicted by the interpretation from the predicted maximal rate. I also recommend that the prediction of enzyme reactor performance be made from the full duration of the enzyme reactor run as this is more likely to give more accurate predictions; however this will require more input in terms of time, cost and work involved.

I have not dealt with large scale enzyme reactors, enzyme reactors are known to have variable results when scaled up, as a result of their variable nature. Therefore predictions determined from a small scale enzyme reactor may not accurately predict results from an enzyme reactor on a larger scale.

I also have not dealt with enzyme reactor types other than stirred tank batch reactors, however the data I have gathered suggests that the Equilibrium Model will apply to the prediction of other enzyme reactor types as essentially the same process is occurring but according to different methodology. However I suspect some variation in the prediction of reactor performance using different types of enzyme reactors, therefore I recommend that data used in the prediction of enzyme reactor

performance be collected from the type of enzyme reactor of which it is predicting performance.

The Equilibrium Model will not be able to predict all reactions carried out within enzyme reactors, as the reaction which is to be predicted must be operating under ideal conditions which is required for the application of experimental data to the Equilibrium Model (Peterson et al., 2004; Peterson et al., 2007).

RNase A is an unusual enzyme as it readily renatures from a denatured form, possibly giving this enzyme a unique temperature profile, the purpose of this experiment was to determine whether such an unusual enzyme followed predictions made by the Equilibrium Model. RNase A was experimentally shown to obtain a unique temperature profile with the colorimetric substrate C>p, predictions made according to the Equilibrium Model did not fit to the experimental data, therefore making the determined parameter values null and void. Complications were encountered when using this substrate at high concentrations with deviations from hyperbolic reaction kinetics encountered possibly due to the binding of the substrate to subsites on RNase A of varying affinities (Moussaoui et al., 1998). The concentration of the substrate C>p was not maintained at 10 times K_M at all temperatures used, the data was adjusted to correct for deviations from V_{max}, however the corrections applied could not elicit the ideal behaviour needed to obtain V_{max} data and without V_{max} data the Equilibrium Model does not apply.

As the data obtained from RNase A could not be applied to the Equilibrium Model, due to V_{max} data not being obtained I recommend that a different RNase assay be performed, using a different substrate, which does not bind to subsites of the enzyme.

This will have to be researched and investigated before the assay is performed. The application of an unusual enzyme to the Equilibrium Model is a nice test of the Equilibrium Model, as all enzymes tested have followed the Equilibrium Model. I recommend that an unusual enzyme or catalyst be pursued and its temperature dependence tested by the Equilibrium Model. If a suitable assay of RNase A can not be applied to the Equilibrium Model I recommend using a suitable assay of a catalytic antibody, a non- enzymic protein that has catalytic properties, a heavy metal catalyst or some other catalyst which is in someway unusual. However whatever catalyst is used will need a suitable spectroscopic assay which allows data of the performance at V_{max} to be obtained and therefore applied to the Equilibrium Model.

The active-inactive enzyme transition of the Equilibrium Model is proposed to arise from a conformational transition at or near the enzymes active site. A.k 1 protease is an enzyme which contains a disulfide bond within the active site cleft, which has suspected dual roles of maintaining substrate binding cleft integrity and of increasing thermostability of the enzyme (Smith et al., 1999; Toogood et al., 2000). A.k 1 protease was reduced and subsequently the disulfide bond broken by treatment with DTT. Both native and DTT treated A.k 1 protease were shown to follow the Equilibrium Model, with DTT treatment altering the fit of the enzyme to its thermal environment, through slight differences in the shape of the 3D temperature/ activity and time curves and in the calculated parameter values. No significant change in the thermostability of DTT treated A.k 1 protease was detected. The only significant difference detected between the native and DTT treated enzyme was the higher T_{eq} and $\Delta H^{\ddagger}_{eq}$ values of the DTT treated enzyme. The larger T_{eq} of the reduced enzyme supports the suggestion that the active- inactive enzyme transition arises from

localised molecular changes at the enzymes active site; in this case through the reduction of the disulfide bond at A.k 1's active site. Changes in $\Delta H^{\ddagger}_{eq}$ were expected with DTT treatment as the breakage of the disulfide bond within the active site was expected to alter the active-inactive transition of the enzyme, and so is consistent with the observed change in T_{eq}.

The disulfide bond was a nice, simple probe of the mechanism of the active- inactive enzyme transition of Equilibrium Model, and the results support already published results that suspect the mechanism being molecular changes at the enzymes active site. I do feel that more in depth analysis is required here to elucidate more precisely what the molecular changes are that result in conversion between the active and reversibly inactive forms of the enzyme. Active site mutations would be a better test of the Equilibrium Model mechanism than the disulfide bond cleavage of A.k 1 protease. By using active site mutations and associated structural analysis a more precise picture will be able to be obtained of the effects of active site modification and the resulting changes in the effects of temperature on the enzyme.

Appendix A

Simulated time courses of enzyme reactor product formation; calculated from 3 minute parameters

---

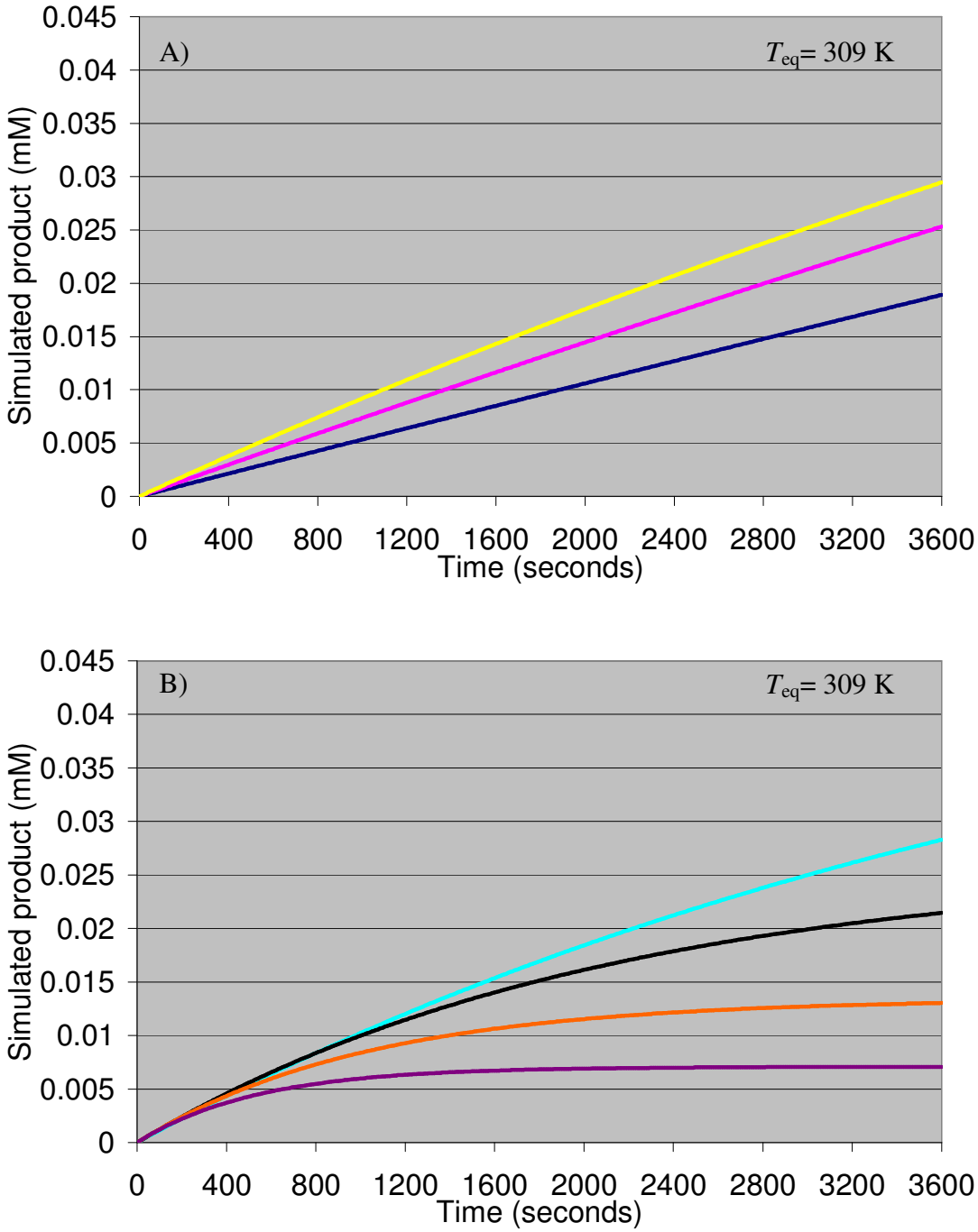

Figure 1: Free penicillin amidase simulated product formation, calculated from 3 minute parameters: 298 K (—); 303 K (—); 308 K (—); 313 K (—); 318 K (—); 323 K (—); 328 K (—). A) T_{eq} exceeds reactor working temperature. B) Reactor working temperature exceeds T_{eq}.

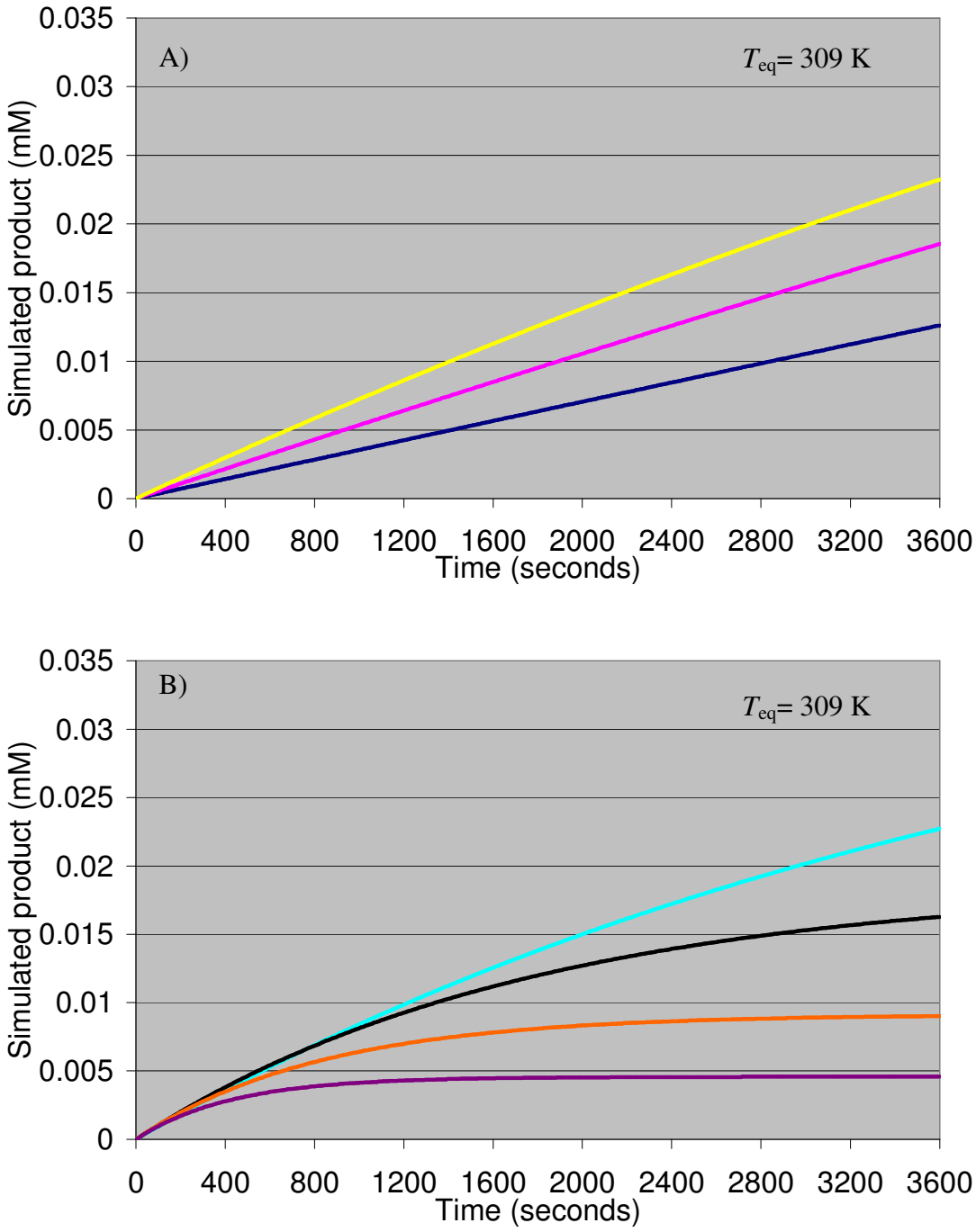

Figure 2: Immobilized penicillin amidase simulated product formation, calculated from 3 minute parameters: 298 K (—); 303 K (—); 308 K (—); 313 K (—); 318 K (—); 323 K (—); 328 K (—). A) T_{eq} exceeds reactor working temperature. B) Reactor working temperature exceeds T_{eq}.

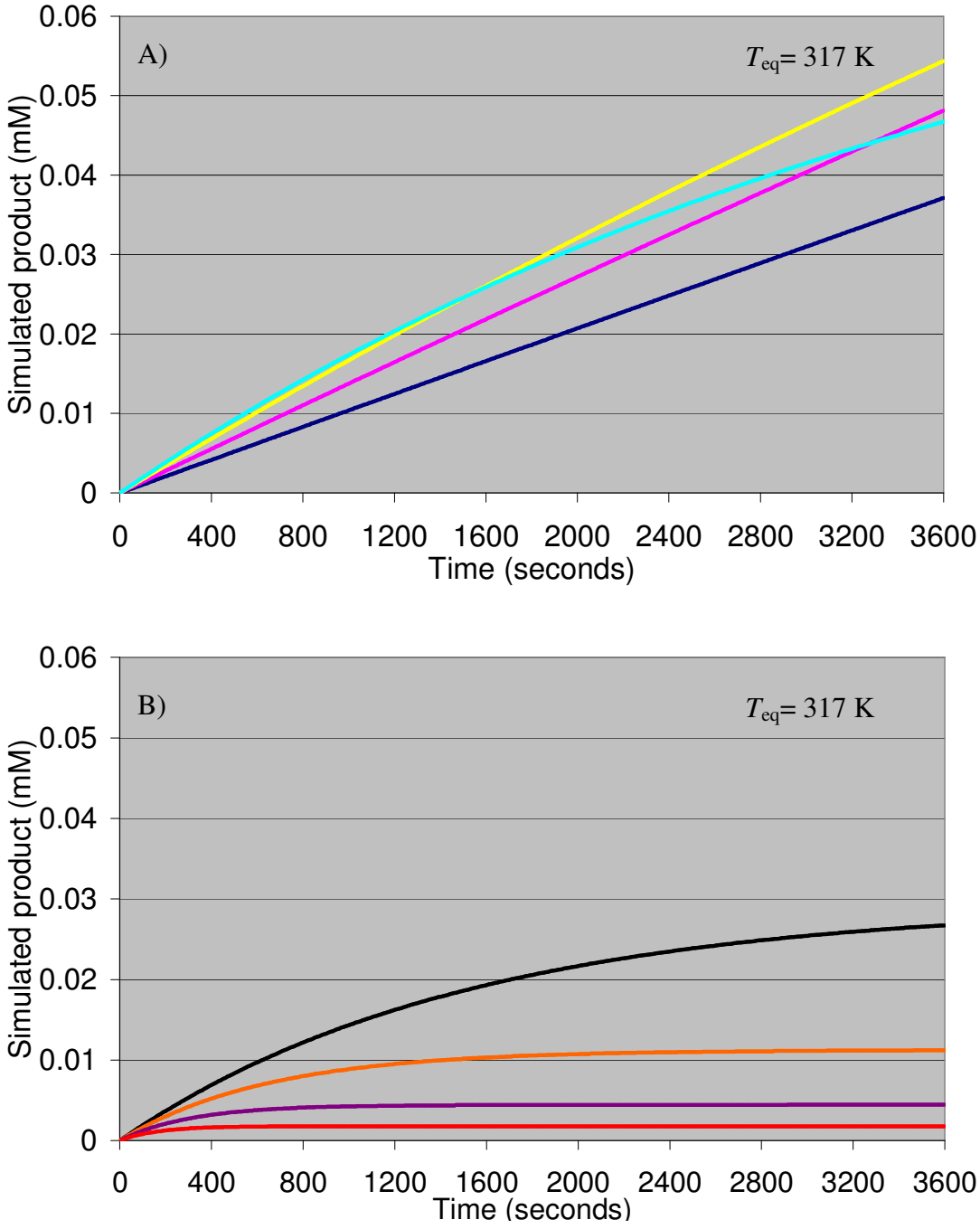

Figure 3: Free alkaline phosphatase simulated product formation, calculated from 3 minute parameters: 298 K (—); 303 K (—); 308 K (—); 313 K (—); 318 K (—); 323 K (—); 328 K (—); 333 K (—). A) T_{eq} exceeds reactor working temperature. B) Reactor working temperature exceeds T_{eq}.

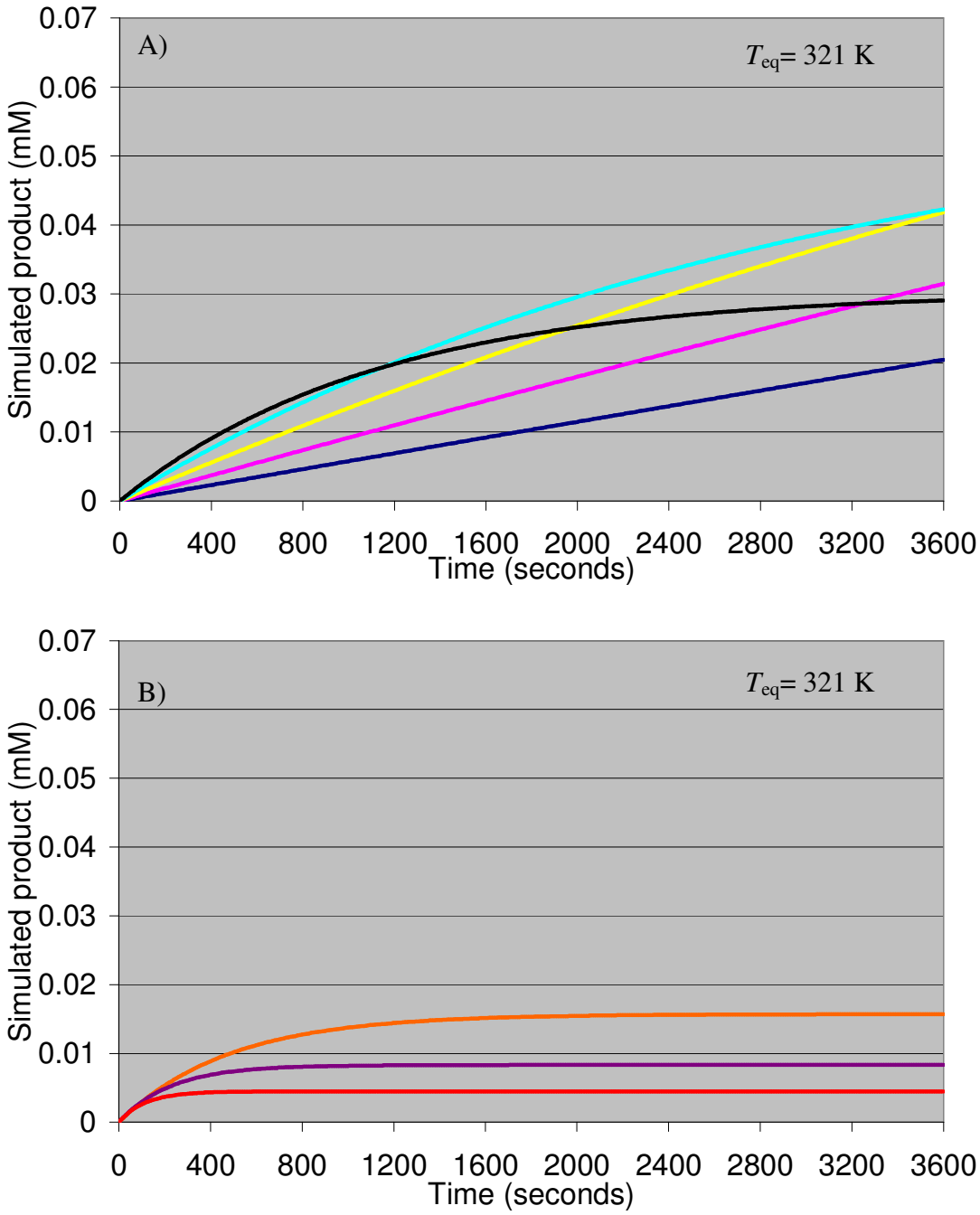

Figure 4: Immobilized alkaline phosphatase simulated product formation, calculated from 3 minute parameters: 298 K (—); 303 K (—); 308 K (—); 313 K (—); 318 K (—); 323 K (—); 328 K (—); 333 K (—). A) T_{eq} exceeds reactor working temperature. B) Reactor working temperature exceeds T_{eq}.

References

Abu-Reesh, I.M. (2005) Optimal design of continuously stirred membrane reactors in series using Michaelis-Menton kinetics with competitive product inhibition: theoretical analysis. *Desalination,* **180,** 119-132.

Alkema, W.B.L., Vries, E.D., Floris, R. and Janssen, D. (2003) Kinetics of enzyme acylation and deacylation in the penicillin acylase- catalysed symthesis of β-lactam antibiotics. *European Journal of Biochemistry,* **270,** 3675-3683.

Arrhenius, S. (1889) On the reaction velocity of the inversion of cane sugar by acids. *Zeitschrift für physikalische Chemie,* **4,** 226ff.

Bartholomew, S.R. and Tansey, J.T. (2006) Cost effective engineering of a small scale bioreactor. *Biotechnology and Bioengineering,* **96,** 401-407.

Benčina, M., Babič, J. and Podgornik, A. (2007) Preparation and characterisation of ribonuclease monolithic bioreactor. *Journal of Chromatography A,* **1144,** 135-142.

Benkovic, S.J. and Hammes-Schiffer, S. (2003) A perspective on enzyme catalysis. *Science,* **301,** 1196-1202.

Bickerstaff, G.F. (1997) In *Immobilization of Enzymes and Cells.* Humana Press, Totowa, New Jersey.

Blackburn, P. (1979) Ribonuclease Inhibitor from Human Placenta: Rapid Purification and Assay. *The Journal of Biological Chemistry,* **254,** (2), 12484-12487.

Blackburn P. and Moore, S. (1982) Pancreatic ribonuclease, *Enzymes,* **XV**, 317- 433.

Blanco, R.M. and Guisan, J.M. (1989) Stabilization of enzymes by multipoint covalent attachment to agarose aldehyde gels-borohydride reduction of trypsin agarose derivatives. *Enzyme and Microbial Technology,* **11,** 360-366.

Bradford, M. (1976) A rapid and sensitive method for the quantitation of microgram quantities of protein utilizing the principle of protein-dye binding. *Analytical Biochemistry,* **72,** 248-254.

BRENDA. The comprehensive enzyme information system, website (2008), viewed 28th February 2008, http://www.brenda-enzymes.info

Briedigkeit, L. and Frommel, C. (1989) Calcium ion binding by thermitase. *FEBS Letters,* **253,** (1,2), 83-87.

Brooks, III, C.L., Karplus, M and Pettitt, B.M. (1988) *Proteins: A Theoretical Perspective of Dynamics, Structure and Thermodynamics,* John Wiley and Sons, New York.

Buchanan, C.L, Connaris, H., Danson, M.J., Reeve, C.D. and Hough, D.W. (1999) An extremely thermostable aldolase from *Sulfolobus solfactarius* with specificity for non-phosphorylated substrates. *Biochemical Journal,* **343,** 563-570.

Chang, R. (1994) In *Chemistry*, 5th Edition, McGraw-Hill, Inc., New York.

Cleland, W.W. (1964) Dithiothreitol, a new protective reagent for SH groups. *Biochemistry,* **3,** 480-482.

Cornish-Bowden, A.J. (1972) Analysis of progress curves in enzyme kinetics. *Biochemical Journal,* **130,** 637-639.

Cornish-Bowden, A.J. (1995) In *Fundamentals of Enzyme Kinetics,* 2nd Edition, pp 193-197, Portland Press Ltd., London.

Creighton, T.E. (1993) Proteins: *Structures and molecular properties,* 2nd Edition, W.H Freeman and Co., New York.

Crook, E.M., Mathias, A.P. and Rabin, B.R. (1960) Spectrophotometric Assay of Bovine Pancreatic Ribonuclease by the use of Cytidine 2':3'-Phosphate. *The Biochemical Journal,* **74**, 234-238.

D'Alessio, G. and Riordan, J.F (1997) *Ribonucleases. structures and functions.* Academic Press, New York.

Daniel, R.M. and Cowan, D.A. (2000) Biomolecular stability and life at high temperatures. *Cellular and Molecular Sciences,* **57,** 250-264.

Daniel, R.M. and Danson, M.J. (2001) Assaying activity and assessing thermostability of hyperthermophilic enzymes. *Methods in Enzymology,* **334,** 283-293.

Daniel, R.M., Danson, M.J. and Eisenthal, R. (2001) The temperature optima of enzymes: a new perspective on an old phenomenon. *Trends in Biochemical Sciences,* **26,** (4), 223-225.

Daniel, R.M., Danson, M.J., Eisenthal, R., Lee, C.K. and Peterson, M.E. (2008) The effect of temperature on enzyme activity: new insights and their implications. *Extremophiles*, **12,** 51-59.

Daniel, R.M., Dunn, R.V., Finney, J.L., and Smith, J.C. (2003) The role of dynamics in enzyme activity. *Annual Reviews of Biophysics and Biomolecular Structure,* **32,** 69-92.

Dixon, M. and Webb, E.C. (1979) *Enzymes*, 3rd Edition, Longman Group Ltd., London.

Eisenthal, R., Peterson, M.E., Daniel, R.M. and Danson, M.J. (2006) The thermal behaviour of enzyme activity: implications for biotechnology. *Trends in Biotechnology,* **24,** 289-292.

Engel, P.C. (1981) In *Outline studies in biology. Enzyme kinetics the steady state approach*, 2nd Edition, Chapman and Hall, London.

Eyring, H. (1935) The activated complex in chemical reactions. *Journal of Chemical Physics,* **3,** 35-62.

Fernley, H.N. (1971) In *The Enzymes,* Vol.4 (ed. Boyer, P.D.) 417-447, Academic Press, New York.

Fraunfelder, H., Petsko, G.A. and Tsernoglou, D. (1979) Temperature-dependant X-ray diffraction as a probe of protein structural dynamics. *Nature,* **280**, 558-563.

Fujii, T., Hiroshi, U. and Hayashi, R. (2002) Significance of the four carboxyl terminal amino acid residues of bovine pancreatic ribonuclease A for structural folding. *Journal of Biochemistry,* **131,** (2), 193-200.

Galunsky, B., Schlothauer, R.C., Böckle, B. and Kasche, V. (1994)Direct spectrophotometric measurement of enzyme activity in heterogeneous systems with insoluble substrate or immobilized enzyme. *Analytical Biochemistry,* **221,** 213-214.

Garcia-Viloca, M., Gao, J., Karplus, M., and Truhlar, D.G. (2004) How enzymes work: Analysis by modern rate theory and computer simulations. *Science,* **303,** 186-195.

Garrett, R.H. and Grisham, C.M. (1999) In *Biochemistry,* 2nd Edition, Brooks/ Cole-Thompson, USA.

Gerhartz W. (1990) In *Enzymes in Industry: Production and Applications.* VCH, Germany.

Gerike, U., Danson, M.J., Russell, N.J. and Hough, D.W. (1997) Sequencing and expression of the gene encoding a cold-active citrate synthase from an Antarctic bacterium, strain DS2-3R. *European Journal of Biochemistry,* **248,** 49-57.

Gerstein, M., Lesk, A.M. and Chothia, C. (1994) Structural mechanisms for domain movements in proteins. *Biochemistry,* **33**, 6739-6749.

Giordano, R.C., Ribeiro, M.P.A and Giordano, R.L.C. (2006) Kinetics of β-lactam antibiotics synthesis by penicillin G acylase (PGA) from the viewpoint of industrial enzymatic reactor optimization. *Biotechnology Advances,* **24,** 27-41.

Guncheva, M., Ivanov, I., Galunsky, B., Stambolieva, N. and Kaneti, J. (2004) Kinetic studies and molecular modelling attribute a crucial role in the specificity and stereoselectivity of penillin acylase to the pair ArgA145-ArgB263. *European Journal of Biochemistry,* **271,** 2272-2279.

Hollander, V.P. (1971) In *The Enzymes,* Vol. 4 (ed. Boyer, P.D.) 417-447, Academic Press, New York.

Hoylaerts, M.F, Manes, T and Millán, J.L. (1992) Molecular mechanism of uncompetitive inhibition of human placental and germ-cell alkaline phosphatase. *Biochemical Journal,* **286,** 23-30.

Illanes, A. and Wilson, L. (2003) Enzyme reactor design under thermal inactivation. *Critical Reviews in Biotechnology,* **23,** (1), 61-93.

Illanes, A. and Wilson, L. and Tomasello, G. (2000) Temperature optimization for reactor operation with chiti-immobilized lactase under modulated inactivation. *Enzyme and Microbial Technology,* **27,** 270-278.

John, R.A. (1992) In *Enzyme Assays, a Practical Approach* (ed. Eisenthal, R. and Danson, M.J.), Oxford University Press, Oxford, UK.

Kasche, V., Haufler, U. and Riechmann, L. (1987) Equilibrium and kinetically controlled synthesis with enzymes: semisynthesis of penicillins and peptides. *Methods in Enzymology,* **136,** 280-292.

Kittel, C. and Kroemer, H. (1980) In *Thermal Physics,* 2nd Edition, Freeman and Co., New York.

Koshland, D.E. (1958) Application of a theory of enzyme specificity to protein synthesis. *Proceedings of the National Academy of Sciences of the USA,* **44,** 98-105.

Kraut, J. (1988) How do enzymes work? *Science,* **242,** 533-540.

Laidler, K.L. and Peterman, B.F. (1979) Temperature effects in enzyme kinetics. *Methods in Enzymology,* **63,** 234-257.

Lee, C.K., Daniel, R.M., Shepherd, C., Saul, D., Cary, S.C., Danson, M.J., Eisenthal, R. and Peterson, M.E. (2007) Eurythermalism and the temperature dependence of enzyme activity. *The Federation of American Societies for Experimental Biology Journal,* **21,** 1-8.

London Southbank University, Faculty of Engineering, Science and the Built Environment, website (2005), viewed 8th May 2008, http://www.lsbu.ac.uk/biology/enztech/reactors.html

MacIver, B., McHale, R.H., saul, D.J. and Bergquist, P.L. (1994) Cloning and sequencing of a serine proteinase gene from thermophilic *Bacillus* species and its expression in *Escherichia coli. Applied and Environmental Microbiology,* **60,** 3981-3988.

Matthews, B.W. (1993) Structureal and genetic analysis of protein stability. *Annual Review of Biochemistry,* **62,** 139-160.

Moussaoui, M. Nogués, M.V., Guasch, A., Barman, T., Travers, F. and Cuchillo, C. (1998) The subsites structure of bovine pancreatic ribonuclease A accounts for the abnormal kinetic behavior with cytidine 2',3'-cyclic phosphate. *The Journal of Biological Chemistry,* **273,** (40), 25565-25572.

Mozhaev, V.V. (1993) Mechanism-based strategies for protein thermostabilization. *Trends in Biotechnology,* **11,** 88-95.

Palmer, T. (1981) *Understanding Enzymes.* Ellis Horwood Ltd., Chichester.

Peek, K., Veitch, D.P., Prescott, M., Daniel., R.M., MacIver, B. and Bergquist, P.L. (1993). Some characteristics of a protease from a thermophilic *Bacillus* sp. expressed in *Escherichia Coli:* comparison with the native enzyme and its processing in *E. coli* and *in vitro*. *Applied and Environmental Microbiology,* **59,** 1168-1175.

Peterson, M.E., Daniel, R.M., Danson, M.J., Eisenthal, R. (2007) The dependence of enzyme activity on temperature: determination and validation of parameters. *Biochemical Journal,* **402,** 331-337.

Peterson, M.E., Eisenthal, R., Danson, M.J., Spence, A. and Daniel, R.M. (2004) A new intrinsic thermal parameter for enzymes reveals true temperature optima. *The Journal of Biological Chemistry,* **279,** (4), 20717-20722.

Piccoli, R. and D'Alessio, G. (1984) Relationships between nonhyperbolic kinetics and dimeric structure in ribonucleases. *Journal of Biological Chemistry,* **259,** (2), 693-695.

Raines, R.T. (1998) Ribonuclease A. *Chemical Reviews,* **98,** 1045-1065.

Sapan, C.V., Lundblad, R.L. and Price, N.C. (1999) Colorimetric protein assay techniques. *Biotechnology and Applied Biochemistry,* **29,** 99-108.

Sigma- Aldrich (2008) Specification Sheet, Ribonuclease A from bovine pancrease. Sigma- Aldrich.

Smith, C.A., Toogood, H.S., Baker, H.M., Daniel, R.M. and Baker, E.N. (1999) Calcium-mediated thermostability in the subtilisin superfamily: the crystal structure of *Bacillus* Ak.1 protease at 1.78Å resolution. *Journal of Molecular Biology,* **294,** 1027-1040.

Tanimizu, N., Ueno. H. and Hayashi, R. (2002) Replacement of his119 of bovine pancreatic ribonuclease A with acidic amino acid residues for the modification of activity and stability. *Journal of Bioscience and Bioengineering,* **94,** (1), 39-44.

Thomas, T.M. and Scopes, R.K. (1998) The effects of temperature on the kinetics and stability of mesophilic and thermophilic 3-phosphoglycerate kinases. *Biochemical Journal,* **330**, 1087-1095.

Toogood, H.S., Smith, C.A., Baker, E.N. and Daniel, R.M. (2000) Purification and characterisation of Ak.1 protease, a thermostable subtilisin with a disulfide bond in the substrate-binding cleft. *Biochemical Journal,* **350,** 321-328.

Torres, R., Pessela, B., Fuentes, M., Munilla, R., Mateo, C., Fernández-Lafuente, R. and Guisán, J.M. (2005) Stabilization of enzymes by multipoint attachment via

reversible immobilization on phenylboronic activated supports. *Journal of Biotechnology,* **120,** 396-401.

Van Langen, L., Janssen, M.H.A., Oosthoek, N.H.P., Pereira, S.R.M., Svedas, V.K., van Rantwijk, F. and Sheldon, R.A. (2002) Active site titration as a tool for the evaluation of immobilization procedures of penicillin acylase. *Biotechnology and Bioengineering,* **79,** (2), 224-228.

Walker, E., Ralston, G.B. and Darvey, I.G. (1975) An allosteric model for ribonuclease. *Biochemical Journal,* **147,** (3), 425-433.

Walker, E., Ralston, G.B. and Darvey, I.G. (1976) Further evidence for an allosteric model for ribonuclease. *Biochemical Journal,* **153,** (2), 329-337.

Walmsley, A. (1996) In *Enzymology: Labfax,* Chapter 5, Bios Scientific Publishers Ltd., Dublin.

Weissig, H., Schildge, A., Hoylaertis, M.F., Iqbal, M. and Milán, J.L. (1993) Cloning and expression of the bovine intestinal alkaline phosphatase gene: biochemical characterization of the recombinant enzyme. *Biochemical Journal,* **290,** 503-508.

Wells, J.A., and Estell, D.A. (1988) Subtilisin- an enzyme designed to be engineered. *Trends in Biochemical Sciences,* **13,** 291-297.

Yankeelov, J.A. and Koshland, D.E. (1965) Evidence for conformational changes induced by substrates of phosphoglucomutase. *Journal of Biological Chemistry,* **240,** 1593- 1602.